

# Management of harmful animal activities on levees: Fact finding fieldwork in the Living Lab Hedwige-Prosperpolder



Photo: Mischa Keijser



Adaptation  
to climate  
change

# Management of harmful animal activities on levees: Fact finding fieldwork in the Living Lab Hedwige-Prosperpolder

**Authors:**

Vana Tsimopoulou, André Koelewijn

**Project team:**

Robert Lanzafame, Stephan Rikkert, Ammar Aljer, Sarah Nguyen, Marios Karaoulis, Johannes Idsinga, Annette Kieftenburg

**Reviewers:**

Griet De Backer, Faye Lynch

## Table of contents

<b>INTERREG Polder2C's project</b>	<b>6</b>
Flood Defence	6
Emergency Response	6
Knowledge Infrastructure	6
Field Station	6
<b>1 Introduction</b>	<b>7</b>
1.1 Context and objectives	7
1.2 Methodology	8
<b>2 Exploratory fieldwork in 2020-21</b>	<b>10</b>
2.1 Introduction	10
2.2 Visual inspections	10
2.2.1 Larger holes at Doelpolder (March 11, 2020)	10
2.2.2 Larger holes at Doelpolder (June 8, 2020)	11
2.2.3 Bare spots from sheep at Prosperpolder (June 8, 2020)	11
2.2.4 Animal burrows at Doelpolder (September 1, 2020)	12
2.2.5 Foxhole at Hedwigepolder (September 16, 2020)	13
2.2.6 Larger holes at Prosperpolder (October 27, 2020)	13
2.2.7 Mole burrows at tree test site Prosperpolder (February 17-18, 2021)	14
2.2.8 Mole burrows at temporary repair site at Prosperpolder (March 30-31, 2021)	15
2.2.9 Mole and mice burrows at Hedwige- and Prosperpolders (June 2021)	16
2.3 Inspection camera	16
2.3.1 Doelpolder (September 1, 2020)	16
2.3.2 Prosperpolder (September 16, 2020)	17
2.4 Electrical Resistivity Tomography	17
2.4.1 Larger holes at Doelpolder (September 1, 2020)	17
2.4.2 Foxhole at Hedwigepolder (September 16, 2020)	19
2.4.3 Foxhole at Prosperpolder (October 27, 2020)	20
2.5 Simple excavation of larger holes at Doelpolder (March 11, 2020)	22
2.6 Grouting and excavation at Prosperpolder (June/July 2021)	23
2.7 Concluding remarks	23
<b>3 Preparation for 2021-22</b>	<b>24</b>
3.1 Initial hypotheses and possible testing approaches	24
3.2 Literature findings in topics of interest	26
3.2.1 Techniques for early detection and monitoring of animal burrows	26
3.2.1.1 Electrical Resistivity Tomography	27
3.2.2 Failure of levee segments damaged by animals.	29
3.2.2.1 Historical levee failures attributed to animal activity	29
3.2.2.2 Modelling failure processes	30
3.2.3 Preventive and corrective physical countermeasures	31
3.3 Questionnaire survey	32
3.4 Overview of knowledge gaps	33
3.5 Action plan for 2021-22	34

3.6	Concluding remarks	35
<b>4</b>	<b>Survey of small burrows Hedwigepolder (8 September 2021)</b>	<b>36</b>
4.1	Context and objectives	36
4.2	Location and levee geometry	36
4.3	Work method	37
4.4	Execution and results	39
4.4.1	Mapping	40
4.4.2	Imaging with Ground Penetrating Radar	44
4.4.3	Smoke test	47
4.5	Concluding remarks	48
4.5.1	Types, geometry and spatial distribution of burrows	48
4.5.2	Burrows detection process	48
4.5.3	App2C vs Paper mapping	49
4.5.4	Feasibility of non-destructive characterisation techniques (GPR and smoke test)	49
4.5.5	Selection of sections for testing against overflow	49
<b>5</b>	<b>First survey of small burrows Prosperpolder (24 September 2021)</b>	<b>51</b>
5.1	Context and objectives	51
5.2	Location and levee geometry	51
5.3	Work method	53
5.4	Execution and results	53
5.5	Concluding remarks	56
5.5.1	Selection of location for further animal burrows testing	56
5.5.2	Comparison to results of the survey in the Hedwigepolder levee	57
<b>6</b>	<b>Second survey of small burrows Prosperpolder (6 – 7 October 2021)</b>	<b>58</b>
6.1	Context and objectives	58
6.2	Location and levee geometry	58
6.3	Work method	58
6.4	Execution and results	59
6.5	The equipment that was used is listed in Table 6.2.	59
6.5.1	Paper mapping	60
6.5.2	Imaging with Ground Penetrating Radar	61
6.5.3	Smoke test	64
6.6	EPDM influence on the density of burrows	65
6.7	Concluding remarks	66
6.7.1	Smoke test	66
6.7.2	Ground Penetrating Radar	67
6.7.3	Spatial distribution and geometry of burrows	67
<b>7</b>	<b>Grouting experiments on the Prosperpolder levee (October 2021 &amp; February 2022)</b>	<b>68</b>
7.1	Context and objectives	68
7.2	Location and levee geometry	68
7.3	Work method	68
7.4	Execution and results	69

7.4.1	Initial excavations	69
7.4.2	Second experiment session (8 <sup>th</sup> and 9 <sup>th</sup> of February 2022)	69
7.4.3	RTK-GPS scans	70
7.4.4	LiDAR scans	73
7.5	Concluding remarks	74
<b>8</b>	<b>Overflow experiments on section with animal burrows (Nov-Dec 2021)</b>	<b>75</b>
8.1	Context and objectives	75
8.2	Locations and levee geometry	76
8.3	Activities in section with mole burrows (N-OF09)	77
8.3.1	Preparatory work	77
8.3.2	GPR scanning	78
8.3.3	ERT monitoring	81
8.3.4	Temporary protection with road plates	85
8.3.5	Smoke experiment	87
8.4	Observation of artificially created burrows in section N-OF03	87
8.5	Surface erosion patterns on reference section with mice burrows N-OF04	87
8.6	Concluding remarks	89
	<b>References</b>	<b>90</b>

## INTERREG Polder2C's project

The INTERREG Polder2C's is an international research project within the framework of the updated Sigmaplan for the river Schelde. The Hedwige-Prosperpolder will be transformed into tidal nature. Depoldering of Hedwige-Prosperpolder offers a unique testing ground, the Living Lab Hedwige-Prosperpolder, for flood defence and emergency response experts. In this environment current and innovative techniques, processes, methods and products can be tested for practical validation. Thirteen project partners, led by the Dutch Foundation of Applied Water Research (STOWA) and the Flemish Department of Mobility and Public Works (DMOW, Flanders Hydraulics Research), are working together. Together, they aim to improve the 2 Seas regions' capacity to adapt to the challenges caused by climate change.

### Flood Defence

The rising sea level is a serious threat to the countries in 2 Seas region. How strong are our current flood defences? What is the impact of environmental elements such as the weather, the presence of vegetation or man-made objects on our flood defences? To answer these questions numerous destructive field tests are carried out in the Living Lab to validate flood defence practices. The project entails in situ testing, guidance on levee maintenance and validation of flood defence infrastructure.

### Emergency Response

We aim to improve emergency response by developing the right tools for inspection of water defences, risk evaluation and solutions for flooding. If our water defences do not operate as designed, we must take the right measures to prevent flooding of valuable areas. The Hedwige-Prosperpolder Living Lab offers unique possibilities to exercise emergency management in the event of calamities under controlled but realistic circumstances. Activities that are part of the programme are levee surveillance and monitoring, emergency response exercises, breach initiation and the large European exercise.

### Knowledge Infrastructure

We aim to develop a knowledge infrastructure through which existing and new to be developed knowledge will become available and accessible. A necessary success factor for any initiative to improve knowledge is to have its outcomes integrated in practices of a wider community. Knowledge Infrastructure focuses therefore on the consolidation of knowledge acquired in the Living Lab with a variety of activities. Accessibility of data in a user-friendly manner, educational activities in the field and incorporation of knowledge in educational curricula are considered key elements.

### Field Station

How can we make sure that both experts in the field and the local public benefit from our project and the learnings about climate change, flood resilience, emergency response and the unique environment of the Hedwige-Prosperpolder? An important and unique way of reaching this goal is realising a Field Station at the project site. It will be used during and after the project for educational purposes, research and as a special meeting place for exclusive occasions.

# 1 Introduction

## 1.1 Context and objectives

Animal burrows create discontinuities on the body of earthen levees that under certain circumstances can threaten their structural integrity through hydraulic alteration and surface erosion, as shown in Figure 1.1 (Cobos Roa, 2015).

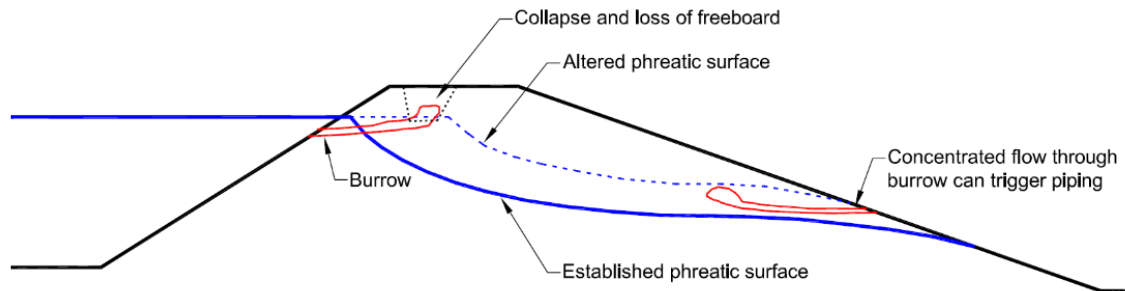


Figure 1.1. Effects of animal burrows in levees (Cobos Roa, 2015).

Although it is a virtually established fact that discontinuities can undermine the structural integrity of levees, there are limited studies that clarify when animal activity can be considered dangerous and which are the most effective approaches for dealing with it. Interaction with levee management agencies in the network of Polder2C's has shown that there is much tacit knowledge on the topic among levee guards in the Netherlands, Belgium, France and the UK, which has only been marginally reported so far. It is also of interest that the Dutch Government approved the inclusion of measures against harmful animal activity in flood defences more than a decade ago (Tweede Kamer 2010), but to this end, an integrated national management framework is still pending. This highlights the fact that formal knowledge on the topic is limited and fragmented.

In order to enable the development of a rational framework for dealing with animal activity on levees, a coordinated effort is required for the review and reporting of existing knowledge, identification of knowledge gaps and development of approaches to determine the level of risk incurred by various types of animal activities on levees and the effectiveness of reduction actions. This report presents activities that took place within Polder2C's and could support the development of such a rational framework.

After the first winter of experimentation in the Living Lab Hedwige-Prosperpolder, evidence was produced about possible adverse impact of animal- and vegetation-induced discontinuities on levees (Holscher & Zomer, 2021; Koelewijn et al. 2021). Overflow experiments at locations of anomalies caused by grazing sheep, trees and fox holes led to severe erosion of the structure within a considerably short time (see also Figure 1.2a). In June 2021 a mole burrow system was detected in a levee section that had been damaged during overflow experiments and where an emergency repair application with rock bags had been subsequently applied. In order to explore the geometry and extent of the system, the mole tunnels were grouted with fast drying concrete. Upon excavation of the concrete an extensive burrow system was revealed with exit points close to the toe and close to the crest of the section (see also b).

In preparation of the second winter of experimentation, a cross-work package team was created to identify knowledge gaps in the management of animal burrows on levees and suggest research activities that could potentially fill in identified gaps. This led to a longlist of possible activities, a number of which were eventually executed in the period September 2021 till February 2022. The final selection of activities was limited by the

contractor's work and other large-scale experiments and exercises. Priority was given to activities that had no conflicts with the abovementioned operations and for which there was available equipment and manpower within the involved organizations.



Figure 1.2. a) Foxhole on the Hedwige levee after overflow testing on 23 November 2020. Test conditions: discharge of 180 litres per second in a 2-metre-wide section for 1 hour and 13 minutes (Source: Koelewijn et al. 2020). b) Excavation of tunnel system created by mole activity, after filling it with fast hardening concrete (Source: Holscher & Zomer, 2021).

This report presents the work that was performed within Polder2C's on the management of harmful animal activity on levees in a chronological order. It starts with a description of observations in the first year of the project, and a subsequent study that led to the development of a knowledge agenda in the period February till June 2021. It continues with a description of activities that took place in a more coordinated manner in the second year of the project and it ends with a summary of key findings.

## 1.2 Methodology

The management of harmful animal activity on levees was not explicitly mentioned in the initial work plan of Polder2C's (see also Polder2C's Work Plan, 2019), but it is a topic whose importance was stressed soon after the Living Lab Hedwige-Prosperpolder activities were launched. Within the context of planned surveys, discontinuities on the levee were observed by visual inspections and other non-invasive techniques, while during overflow experiments remarkable damages occurred at sections with observed animal-induced discontinuities. These first observations led organically to the development of a more systematic approach of data collection that will ultimately allow to close knowledge gaps on this topic.

Triggered by the initial observations in the living lab, a literature review was performed to allow for an overview of current knowledge on the topic and existing knowledge gaps. Based on insights collected from literature and from interactions with levee management professionals in the network of Polder2C's, a questionnaire was designed to collect information about relevant practices within levee management authorities. The questionnaire was distributed to Dutch levee management authorities. Using the result of the literature study

and the collected responses in the questionnaire, and taking into account availability of resources, a plan of activities was developed for the second year of Polder2C's to address identified knowledge gaps (see also Figure 1.3).

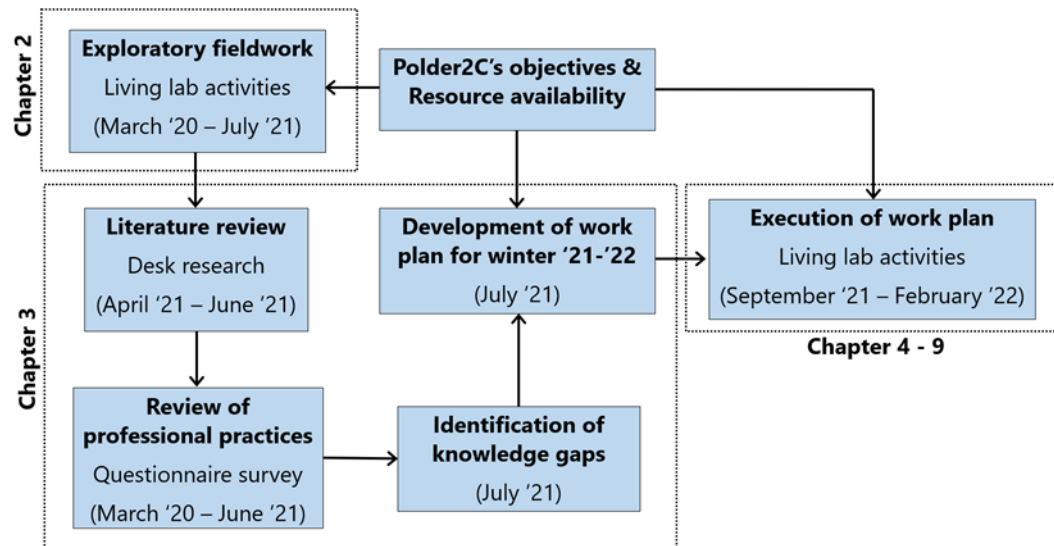


Figure 1.3. Work method illustrated in a flowchart.

It is important to note that many of the activities that were planned and executed in a systematic manner in the second year of Polder2C's were focused on the collection of datasets that can contribute to closing knowledge gaps in the longer run and not immediately. This is because all activities in the living lab lead to site-specific results that have to be compared and contrasted with results from other case studies in order to derive generic conclusions.

## 2 Exploratory fieldwork in 2020-21

### 2.1 Introduction

The characterization of animal burrows can be performed in various ways. The simplest approach is by visual inspection. This will only reveal the most superficial part, generally only above the water surface. Several inspections, with an increasing degree of thoroughness, are described in §2.2. Other techniques, revealing more information about the size, shape and extent of the burrows, are either non-destructive, leaving the burrows intact (§2.3 and 2.4), or destructive, causing additional damage to the levee (§2.5 and 2.6). Key findings are presented in §Error! Reference source not found..

### 2.2 Visual inspections

Visual inspections are the oldest form of levee inspection. With the help of measurement rods, dedicated forms, modern apps (like the App2C, developed within the Polder2C's project, #ref), detailed information concerning the condition of a levee can be obtained.

During the course of the project, several visual inspections were carried out in and near the Polder2C's field laboratory, as indicated in Figure 2.4. This figure only indicates the visual inspections related to animal burrows as described in this section. These inspections became more detailed as the awareness of the potential influence of animal burrows on flood risk grew.



Figure 2.4 Map showing the visual inspections carried out in the Hedwigepolder, Prosperpolder and Doelpolder in year 1 of Polder2C's.

#### 2.2.1 Larger holes at Doelpolder (March 11, 2020)

The levee along the Scheldt River continues beyond the Prosperpolder in South-East direction along the Doelpolder. In March 2020, many bare spots, some of them with animal burrows, were seen on this levee. In total, around 20 burrows of size that could be ascribed to rabbits or foxes were found, mostly on the landside slope of the levee, but some also on the waterside slope. These burrows appeared to be clustered in about five to seven groups (the number depending on the limits of some clusters). Examples are shown in Figure 2.5.

Follow-up investigations around this location are described in §2.3.1 (inspection camera), §2.4.1 (ERT) and §2.5 (simple excavation).



Figure 2.5. Various bare spots, some with animal burrows, on the landside slope of the levee along the Doelpolder (March 11, 2020).

### 2.2.2 Larger holes at Doelpolder (June 8, 2020)

A few months later, all animal burrows on both sides of the levee bordering the Doelpolder were covered by one or more truckloads of clay applied at each cluster and seemingly compacted by a crane's backhoe. The unmowed grass around these spots clearly showed the locations where the clay was applied (Figure 2.6).



Figure 2.6. Clay placed on top of all animal burrows (landside slope along the Doelpolder, June 8, 2020).

### 2.2.3 Bare spots from sheep at Prosperpolder (June 8, 2020)

Close to the landside toe of the Scheldt levee along the Prosperpolder, several bare spots were discovered. Not only the grass cover was missing, but at these parts the profile was also steeper. Examples are shown in Figure 2.7 and Figure 2.8. Presumably, these bare spots and small 'cliffs' were caused by sheep, grazing on this levee several times during the year. Along the toe of the levees in Belgium, also trees and small brushwoods are present, as can be seen in Figure 2.6 and Figure 2.8.



Figure 2.7. Bare spots in the grass cover caused by resting sheep at a steep part of the landside slope of the levee along the Prosperpolder (June 8, 2020).



Figure 2.8. Trees and bare spots in the grass cover caused by resting sheep at steep parts of the landside slope of the levee along the Prosperpolder (June 8, 2020).

One of the locations with a 'cliff' was tested in an overflow test (Depreiter et al. 2022b). At two locations with a tree, such tests were also carried out, and failure occurred from the mole burrows present around the trees (Depreiter et al. 2022b).

#### 2.2.4 Animal burrows at Doelpolder (September 1, 2020)

Several months later, the Scheldt levee along the Doelpolder was revisited to carry out an ERT survey (see §2.4.1). By then, the clay heaps were overgrown and new entrances to animal burrows were found in many of them. Some examples are shown in Figure 2.9 to Figure 2.11.



Figure 2.9. High vegetation on clay heap on top of an earlier animal burrow (landside slope along the Doelpolder, September 1, 2020).



Figure 2.10. Entrances to animal burrows in the clay heap of Figure 2.9.



Figure 2.11. Larger animal burrows on the landslide slope of the Scheldt levee along the Doelpolder.

#### 2.2.5 Foxhole at Hedwigepolder (September 16, 2020)

Two weeks later, on the occasion of the ERT measurements at the Hedwigepolder (§2.4.2), a foxhole was discovered near the landside toe of the Scheldt levee along the Prosperpolder, as shown in Figure 2.12. ERT measurements were carried out here on the 27<sup>th</sup> of October 2020 (§2.4.3).



Figure 2.12. Landside slope of Scheldt levee along the Prosperpolder, with an animal burrow in the foreground showing fox's excrements.

#### 2.2.6 Larger holes at Prosperpolder (October 27, 2020)

The next month, at a location near to the location shown in Figure 2.12, but much higher on the slope, close to the crest, new and fairly large holes were discovered, see Figure 2.13. The sand indicates that the hole extended into the sandy core of the levee, i.e. beyond the clay cover layer. The vegetation that already had

grown on top of the sand indicates that this must have happened rather soon after the exploration of the foxhole mentioned in §2.2.5 and §2.3.2.



Figure 2.13. Excavated sand close to the crest of the landside slope of the Scheldt levee along the Prosperpolder.

### 2.2.7 Mole burrows at tree test site Prosperpolder (February 17-18, 2021)

At the Living Lab Hedwige-Propserpolder, many large-scale overflow tests have been performed. Two of these aimed at determining the influence of a tree in the landside toe of a dike. At the first test, failure occurred after slightly more than an hour through mole burrows crossing the test flume. The second site, tested on February 17 – 18, 2021, was carefully inspected for the presence of mole burrows before the start of the test, and none were found.

Yet, after the first two hours of continuous flow, a burrow, presumably from a mole, was found quite close to the tree inside the 2 metre wide flume. During the next six hours of flow, some additional erosion occurred here. The introduction to failure did not become visible before 10 hours of flow, with some leakage at several metres away from the flume, see Figure 2.14 (left). Two hours of flow later, the first subsidence in the flume occurred (Figure 2.14, right). An hour of flow later, more sand was visible on the surface (Figure 2.15) and more subsidence occurred inside the flume, with a newly formed exit point inside the flume (Figure 2.16, left). Only two minutes of flow later, failure through the reactivated burrow occurred. The artificial burrows created after 12 hours of flow to speed up the process did not seem to have any significant influence on the failure. In fact, the part containing the artificial burrows failed last (Figure 2.16, right). A more extensive narrative is given by Koelewijn (2021).



Figure 2.14. Left: flow at a reactivated burrow outside the flume, right: depression inside the flume.



Figure 2.15. Sand deposits at reactivated burrow exit outside the flume.



Figure 2.16. Left: subsidence at reactivated burrow (upper), newly formed exit point (lower), right: flume during failure.

In conclusion, it seems that even old, buried and clogged animal burrows can be reactivated and attract erosive flow, and this cannot be mimicked adequately by an artificial 'burrow' of roughly the same size (but with smooth sides and not necessarily following an already weaker path).

#### 2.2.8 Mole burrows at temporary repair site at Prosperpolder (March 30-31, 2021)

At the end of March 2021, investigations were carried out at the Prosperpolder both to test various configurations of sand bags to withstand water (on the crest of the levee) and to test the resistance to erosion of rock bags placed on the levee after a previous failure of the cover layer during an overflow test. An overview of the test location, with the sand bags visible on the right and the rock bags visible on the left, is shown in Figure 2.17, left. From a hole in the grass cover, caused by a wooden peg driven through the cover layer at the time of the overflow test, connection was made to a mole burrow system that led down the slope, underneath the grass cover. At the intersection with the rock bogs, significant erosion of the sand core occurred, even at rather low flow rates, because of the lack of a proper filter between the sand core and the rock bags. During the new tests, parts of the mole burrow system collapsed, as visible in Figure 2.17, right.



Figure 2.17. Left: Overview of the test in progress, right: openings in the grass cover of the original flume upstream of the rock bags.

### 2.2.9 Mole and mice burrows at Hedwige- and Prosperpolders (June 2021)

After the discovery as described in the previous section was made, a more extensive plan was made, and carried out, to investigate animal burrows. This has been reported by Holscher & Zomer (2021).

### 2.3 Inspection camera

During the first year, the use of a simple, led-lighted camera at the end of a long line, connected to a USB-port of a laptop was explored in the field. The line was connected by tape to a long tension spring bought at a consumers' construction market (Figure 2.18, left). Operation is in practice by two people: one person inserting and guiding the camera into the burrow and one person checking the reception and recording of the video (Figure 2.18, right).



Figure 2.18. Assembly of the inspection camera and the tension spring, right: application on the levee.

#### 2.3.1 Doelpolder (September 1, 2020)

The system was first employed at the landside slope of the Scheldt levee along the Doelpolder, on the 1<sup>st</sup> of September 2020 (Figure 2.19). It appeared to be virtually impossible to determine the location and the orientation of the camera, including a detail like the direction of gravity (although often roots hanging down

in the burrow gave a useful indication). Moreover, it appeared impossible to steer the device into the desired direction, e.g. a different burrow than before at an underground intersection.



Figure 2.19. Screen during application of the camera in the Doelpolder

### 2.3.2 Prosperpolder (September 16, 2020)

Later, the system was also employed at the fox hole in the Prosperpolder. In spite of the experience gained and a better connection of the line to the spring, inserting and positioning the camera appeared to be troublesome. At some point, the line could be inserted for several meters – only to find out that the system got into a loop with multiple rounds right behind the entrance, as discovered from the occasional appearance of daylight when passing close to the entrance.

It was concluded that this system is not suitable for meaningful observations, due to the lack of orientation and steering possibilities.

## 2.4 Electrical Resistivity Tomography

*This section is written with input from Marios Karaoulis (Deltares).*

### 2.4.1 Larger holes at Doelpolder (September 1, 2020)

Some characteristics of this site are already given in §2.2.1, §2.2.2 and §2.2.4. For this first ERT survey of animal burrows, a location was chosen where two large holes were clearly visible at a location where earlier animal burrows were covered by clay. Presumably, the older burrows had been accessed again. First, two lines along the slope were measured after each other. Each of these lines had a 10 cm electrode spacing and 50 cm between the lines, as shown in Figure 2.20 and Figure 2.21. This spacing has initially been chosen to ensure sufficient resolution to enable detection of holes in the size of 5-10 cm, and larger.



Figure 2.20. Site at Doelpolder. Left: overview, right: data acquisition in progress.



Figure 2.21. Doelpolder, left: two rows of pins across two holes (connected underneath), right: view from below. An interpretation of the results is given in Figure 2.22. At the lower line, both holes are clearly visible. This corresponds with other observations in the field. At the upper line, a larger hole seems to be present at a depth of about 1 m. Near to the surface, no hole is detected. The blue parts indicate low resistivity, likely from (wet) clay.

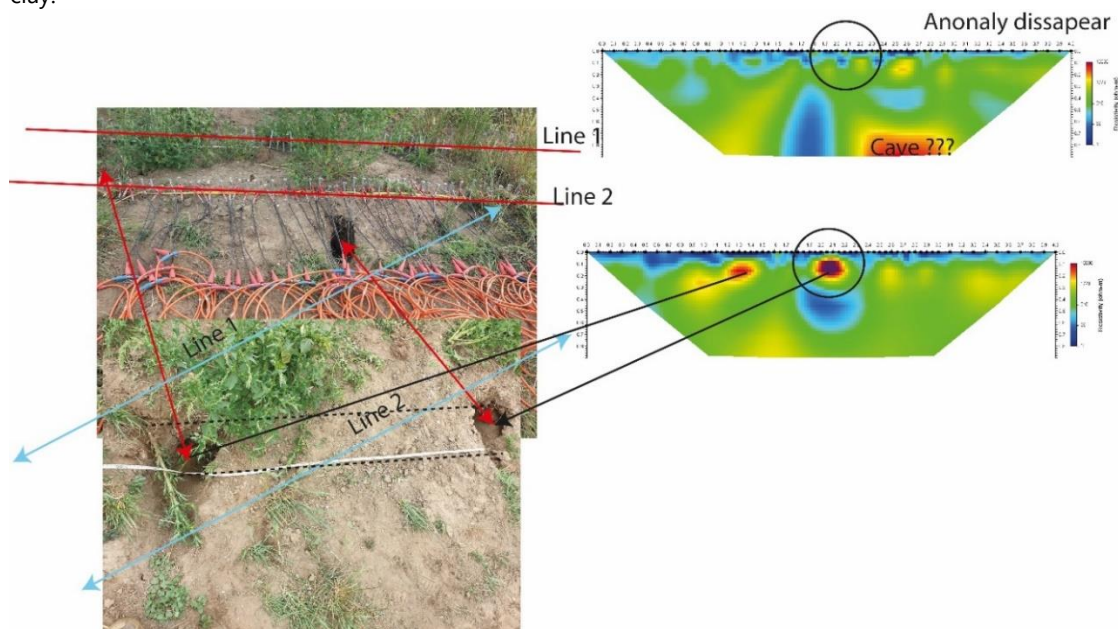


Figure 2.22. Doelpolder, interpretation of the high resistivity zones with respect to the locations of the animal burrows (note that on the left, two pictures taken from different angles are shown).

In addition, two lines were measured perpendicular to each other, with a much larger spacing: 50 cm between the electrodes. One line was laid out in the same direction of the previous two lines, extending in both directions beyond the limits of the previous lines, see Figure 2.23 (left). The other line was laid out across the levee, starting at the landside toe and ending on the waterside slope, across the crest, see Figure 2.23 (right). Unfortunately, no meaningful results were obtained. The presence of the asphalt layer on the crest, effectively reducing the number of electrodes connected to the soil, had a significant impact.



Figure 2.23. Doelpolder, lines with 50 cm spacing between electrodes. Left: lines crossing near the holes, right: line across the crest.

#### 2.4.2 Foxhole at Hedwigepolder (September 16, 2020)

The next series of ERT measurements was carried out at the location on the Scheldt levee along the Hedwigepolder where in the past years repeatedly a larger animal burrow with a fox was detected, near the staircase and the former summer house of the owner. Here, two perpendicular lines were applied, shown in Figure 2.24. The electrode spacing differed between the two lines: for the line parallel to the levee, a 10 cm spacing was applied, while for the line perpendicular to the levee, a 30 cm spacing was applied.



Figure 2.24. Hedwigepolder, left: measurements parallel to the levee, right: measurements across the levee.

Figure 2.25 shows a 3D representation of the results. The crest of the levee (here without an asphalt layer) is near the upper left corner. In red are the high resistivity zones, suggesting multiple burrows in this area; towards the crest, rather close to the surface. This was confirmed in the destructive overflow test N-OF05 (Depreiter et al., 2022a). The final data RMS error is 3.7% for the perpendicular line and 8.5% for the parallel line. In more common words: the accuracy of the result found across the levee was much higher than the accuracy of the result found along the levee. The reason for this difference is unknown. Yet, for both lines the accuracy is within the specialists' acceptance limits.

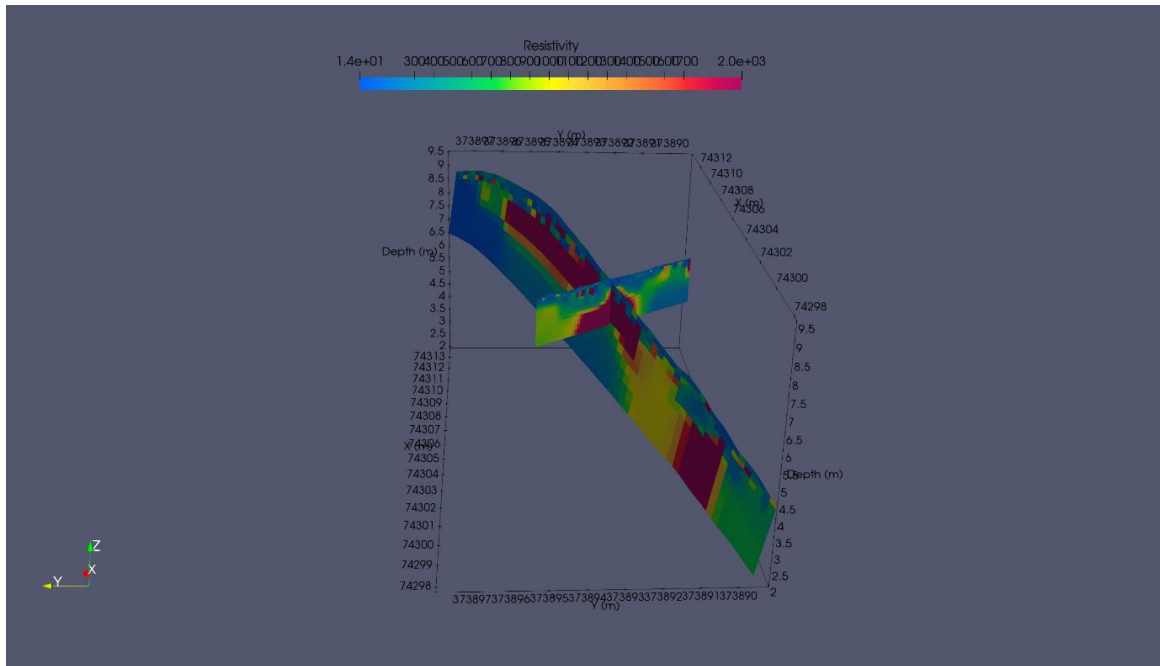


Figure 2.25. Hedwige polder, 3D representation of the results.

### 2.4.3 Foxhole at Prosperpolder (October 27, 2020)

The third series of ERT measurements was carried out at a foxhole close to the toe of the landside slope of the Scheldt levee of the Prosperpolder, near the radar tower (Figure 2.26 left). At this location, a full 3-dimensional configuration was utilized, with 9 parallel lines having 0.25 m electrode spacing along each line and 0.5 m interline spacing. The field situation during acquisition is shown in Figure 2.26 right.



Figure 2.26. Prosperpolder, left: location of the ERT measurements, right: overview of the acquisition site during the measurements.

The measuring protocol encompasses single cable measurements (i.e. pins used only from each cable separately) using a multi-gradient protocol (see Figure 2.27 left). Additionally, to get a better 3D measuring scheme, we utilized pins from 2 cables (i.e. some pins in cable 1, some pins in cable 2, Figure 2.27 right) using a bipole-bipole scheme. The measures between cables is repeated in pairs, with the following scheme. Since the combination of all possible cables and all possible interline cables leads to a large number of measures, we choose optimized protocols for cross-hole ERT measurements based on the Jacobian matrix method. Additionally, since the goal is to decrease the acquisition time to be able to capture time related changes, we further optimized the protocol to utilize measures that make the best use of the 8-channel system, with emphasis on changes on the model.

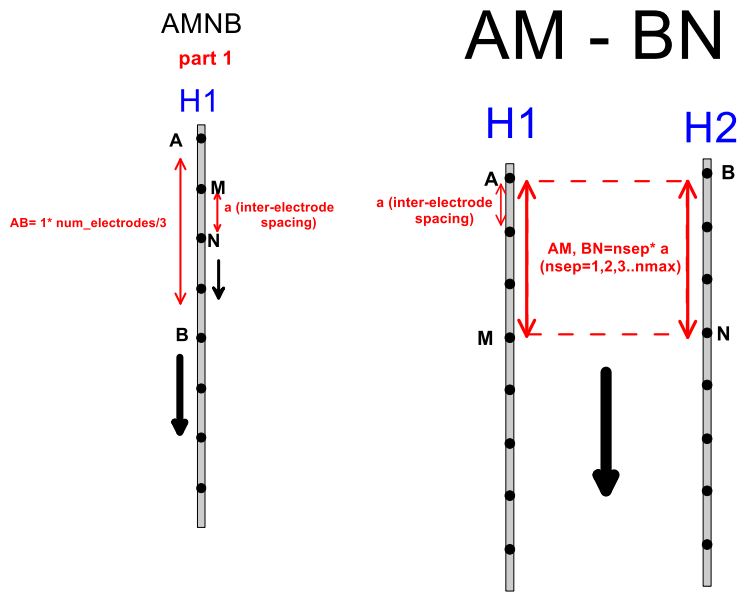


Figure 2.27 Multi-gradient single cable measurements (left) and measurements between the cables (right) for the 3D-configuration.

Some of the results are shown in Figure 2.28 and Figure 2.29. In the last figure, the subsurface animal burrow is clearly visible in the results.

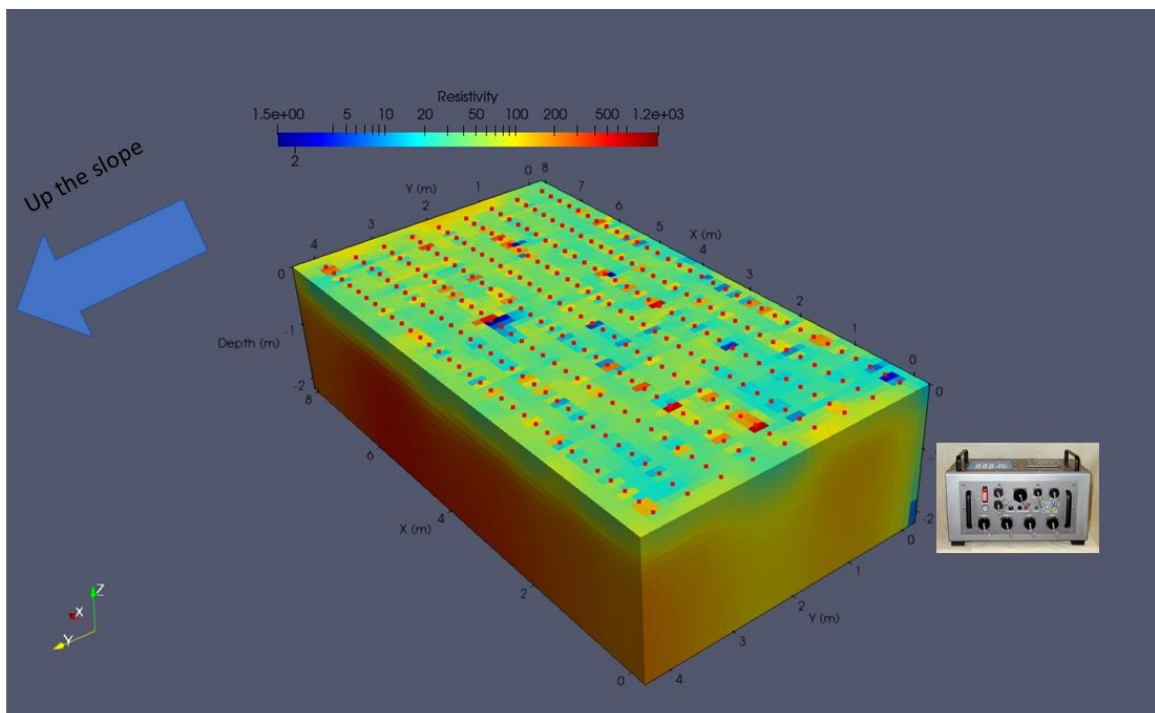


Figure 2.28 3D volume results.

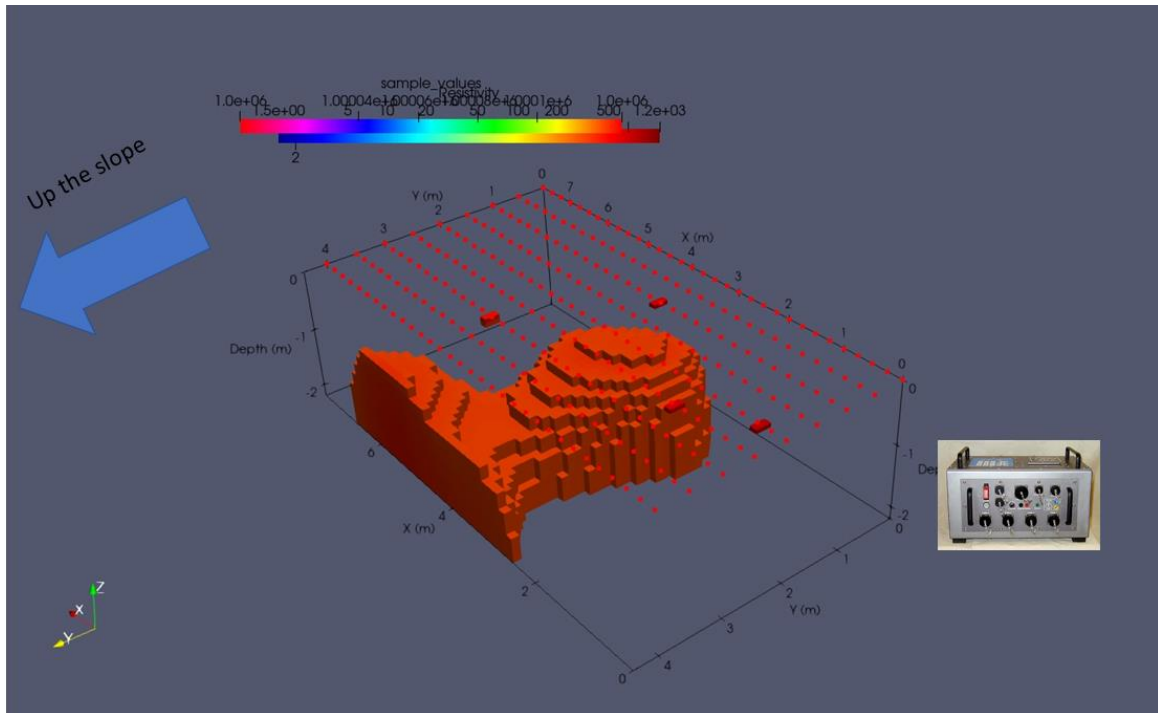


Figure 2.29 Iso-volume of the high-resistivity zone (the animal burrow location).

## 2.5 Simple excavation of larger holes at Doelpolder (March 11, 2020)

A common idea is that holes can simply be traced by excavating them from the opening. With a group of students of KU Leuven, this approach was adopted on the landside slope of the Scheldt levee along the Doelpolder, on 11 March 2020. Some pictures of this activity are shown in Figure 2.30 and Figure 2.31.



Figure 2.30. Overview of the animal burrow excavation alongside the Doelpolder.



Figure 2.31. Excavation of animal burrow in progress.

The main conclusion from this exercise was that it is rather difficult to keep track of the original excavation depth and to discern all, or at least any, branches in the burrow. The excavated material partly falls into the burrow, obscuring the view of the people excavating. Besides, proper mapping of the excavation on levee with a varying slope appeared to be more difficult than anticipated.

## 2.6 Grouting and excavation at Prosperpolder (June/July 2021)

Filling a selection of the discovered mole and vole burrows, and drought cracks, with a rather liquid fine cement grout was carried out after the extended visual inspections described in §2.2.9. Subsequently, the grouted volumes were excavated and described. This is reported by Holscher & Zomer (2021).

## 2.7 Concluding remarks

The key findings from the fieldwork in the first year are summarized as:

- The visual inspections remain too much at the surface, not giving much information about the depth, volume and interconnectivity of the burrows.
- The simple excavations and the simple camera are both, in different ways, unsuitable for detailed quantitative investigations, revealing size, orientation and extent of animal burrows.
- Grouting appeared to be a suitable, yet destructive and time-consuming method to gain more insight.
- ERT is not destructive, yet this method is time-consuming too, both in the field and in the post-processing phase.

Nevertheless, it appeared that the influence of animal burrows on flood safety could be significant, as was also illustrated by several large-scale overflow experiments that ended sooner than others, as it appeared because of the presence of animal burrows. Altogether, this was sufficient reason to extend and enlarge the research efforts on this theme, even though this was originally not foreseen in the Polder2C's research plan.

## 3 Preparation for 2021-22

### 3.1 Initial hypotheses and possible testing approaches

An integral rational approach to the management of harmful animal activity on levees requires a comprehensive consideration of solutions for dealing with the problem at hand. In order to acquire a complete picture of possible solutions to the problem and identify knowledge gaps that need to be filled for a successful evaluation of every solution, hypotheses for possible solutions were created using as a roadmap the safety chain concept (FEMA 2003; Dutch Ministry of the Interior 1993; Van Duin & Berghuijs 2007; Ten Brinke et al. 2014). According to this concept all risk reduction actions can be classified in five categories that represent five successive links in a safety chain; proaction, prevention, preparation, response and recovery. The original definition of these links for flood management and their adaptation to fit in the problem of managing harmful animal activity on levees is presented in Table 3.1.

Table 3.1. Definition of the successive links of a safety chain in flood management (Adapted from Ten Brinke et al. 2014).

Link	Original definition	Adapted definition
Proaction	Eliminating structural causes of accidents and disasters to prevent them from happening in the first place (e.g. by building restrictions in flood-prone areas).	Eliminating exposure to the risk of levee failures due to animal activity (e.g. by eco-engineering solutions for deterring animals from the levees).
Prevention	Taking measures beforehand that aim to prevent accidents and disasters, and limit the consequences in case such events do occur (e.g. by building dikes and storm surge barriers).	Taking measures that reduce the probability of levee failures due to animal activity (e.g. by using alternative materials for the cover layer that cannot be easily penetrated by animals or by improving levee monitoring for early repair of damages).
Preparation	Taking measures to ensure sufficient preparation to deal with accidents and disasters in case they happen (e.g. contingency planning)	Developing a plan for emergency repairs of burrows that can lead to a breach in anticipation of high water (e.g. with the use of sandbags and other easily portable materials).
Response	Actually dealing with accidents and disasters (e.g. response teams)	Training levee guards in the application of emergency repairs of burrows.
Recovery	All activities that lead to rapid recovery from the consequences of accidents and disasters, and ensuring that all those affected can return to 'normal' and recover their equilibrium.	n/a

The hypotheses that were developed for each one of the presented categories of possible solutions are listed below:

1. Proaction – measures that reduce exposure to the risk of levee failures due to animal activity
  - a. Design levees in a way that deters animal activity.
    - *Hypothesis:* different choice of materials or geometry can divert animal activity from the levee to another location.
  - b. Provide animals with an attractive alternative location in the proximity of the levee that can substitute a levee environment.
    - *Hypothesis:* eco-engineering interventions in the proximity of a levee can divert animal activity to another nearby location.
2. Prevention – measures that reduce the probability of a levee failure due to animal activity

- a. Early detection and monitoring of animal activity that can threaten the structural integrity of a levee.
  - *Hypothesis:* Electro-magnetic measurements is a feasible solution for early detection and monitoring of animal-induced anomalies in the body of a levee.
- b. Repair anomalies induced by animal activity.
  - *Hypothesis:* Harmful animal activity in the body of a levee can be repaired with grouting, cut and cover or cut-off wall applications (see also Figure 3.32).

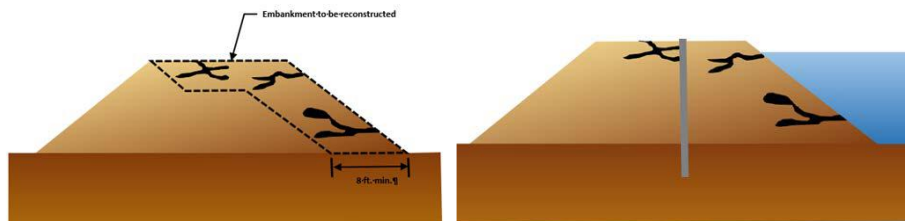


Figure 3.32. Illustration of 'cut and cover' (left) and 'cut-off wall' (right) techniques for animal burrow repairs (borrowed from: US Bureau of Reclamation 2017)

3. Preparation – measures that can be taken in advance to reduce impact when a levee fails due to animal activity
  - a. Apply temporary measures on animal-induced anomalies (in anticipation of levee overload) that can reduce or delay catastrophic damages during a flood emergency.
 

*Hypothesis:* Compositions of sandbags and other easily applicable materials can delay erosion of a section with animal-induced anomalies.
4. Repression – measures that can be applied quickly during a flood emergency
  - a. Apply temporary measures on animal-induced anomalies (after levee overload has started) that can reduce or delay catastrophic damages during a flood emergency.
 

*Hypothesis:* Damping sandbags during overflow or overtopping can delay erosion of a section with animal-induced anomalies.

Taking into account the availability of resources, possibilities and limitations of the living lab as experienced in the first year of Polder2C's, for every hypothesis a preliminary testing approach was developed (Table 3.2. Overview of testing approaches per hypothesis). This provided an overview of possible topics that could be investigated further in the living lab.

Table 3.2. Overview of testing approaches per hypothesis

Hypothesis		Testing approach
1a	different choice of materials or geometry can divert animal activity from the levee to another location.	A literature review and interviews with levee managers can provide reported and unreported information about most common animal activity patterns on different types of levees. If applicable, a selection of solutions that seem to encourage/discourage animal activity could be applied as a repair in damaged levee sections in LLHPP and subsequently monitored to evaluate effect.
1b	eco-engineering interventions in the proximity of a levee can divert animal activity to another nearby location.	A literature review and consultations with ecology experts can lead to the identification and detailing of such interventions. Feasibility of such interventions could be tested in LLHPP.
2a	Electro-magnetic measurements is a feasible solution for early	Animal burrows can be measured in LLHPP with EM. The accuracy of the measurements could be verified by excavating the location, exposing the burrow and measuring its dimensions with other conventional means.

	detection and monitoring of animal-induced anomalies in the body of a levee.	It would also be beneficial to explore whether EM measuring can be used to monitor geometry of animal burrows during overflow, overtopping and wave impact tests. Such measurements could provide interesting information about the erosion development in time.
2b	Harmful animal activity in the body of a levee can be repaired with grouting, cut and cover or cut-off wall applications.	Based on a literature study and interviews with levee managers and contractors, the three repair solutions can be further detailed and applied in LLHPP. In case there are not enough sections where all solutions can be applied at least once, artificial burrows can be applied to locations where the levee will have been breached by breaching experiments. The breached sections can be rebuilt and their artificial burrows can be repaired and subsequently tested against overflow/overtopping/wave impact.
3a	Compositions of sandbags and other easily applicable materials can delay erosion of a section with animal-induced anomalies.	Temporary repairs, similar to the ones that have been applied on Davy's damage and Patrik's cliff but of a smaller scale can be designed and applied on sections with animal burrows before testing. The sections can be tested afterwards.
4a	Damping sandbags during overflow or overtopping can delay erosion of a section with animal-induced anomalies.	This can be tried out during overflow/overtopping/wave impact of any section that contains an animal burrow.

### 3.2 Literature findings in topics of interest

Using as a roadmap the concept of the safety chain four topics of interest were identified for further studying:

1. Techniques for early detection and monitoring of animal burrows.
2. Failure paths and failure probability of levee segments damaged by animals.
3. Preventive and corrective physical countermeasures against harmful animal activity
4. Eco-engineering approaches for deterrence of animals from levees.

#### 3.2.1 Techniques for early detection and monitoring of animal burrows

Techniques that have been used by levee management authorities in various countries so far for the detection of animal burrows and other animal-induced discontinuities are the following (Bayoumi & Megouid 2011; Heyer & Stamm 2019; CIRIA 2013; Klerk et al., 2021; Klerk, 2022; Van der Steen, 2018):

- Visual inspection,
- Gravity survey,
- Resistivity methods,
- Seismic reflection,
- Ground penetration radar (GPR)
- Boat sonar.

The ground penetrating radar has been reported in the past as the most reliable of the abovementioned techniques (Bayoumi & Megouid 2011), but this conclusion has been contradicted by results of later studies (see e.g. Heyer & Stamm 2019). This shows that collection of quantitative and qualitative data that allow comparative studies between known techniques will be of added value.

Taking into account the living lab context and the experimental possibilities that it offers, the team looked for studies related to application of the aforementioned techniques for the evaluation of physical countermeasures against animal activity on levees and for acquisition of data in the form of timeseries during the execution of large-scale levee stress tests. These topics seem to be underreported in international literature.

### 3.2.1.1 Electrical Resistivity Tomography

*This section is written with input from Marios Karaoulis (Deltares).*

Electrical properties of soils are related to the chemistry and mineralogy of the soil material, the structural properties of the porous medium (e.g., porosity, cementation, etc.), and the electrical properties of the fluids on the grains or in the pores of the soil. The electrical properties can provide indirect indications of the nature of soils. The Direct Current (DC) Electrical Resistivity Tomography (ERT) method is an active method aimed at imaging the resistivity (the resistance of a material to the flow of an electrical current) of the subsurface by determining the electric potential field induced by applying an electric potential to a soil using electrodes (Figure 3.33).

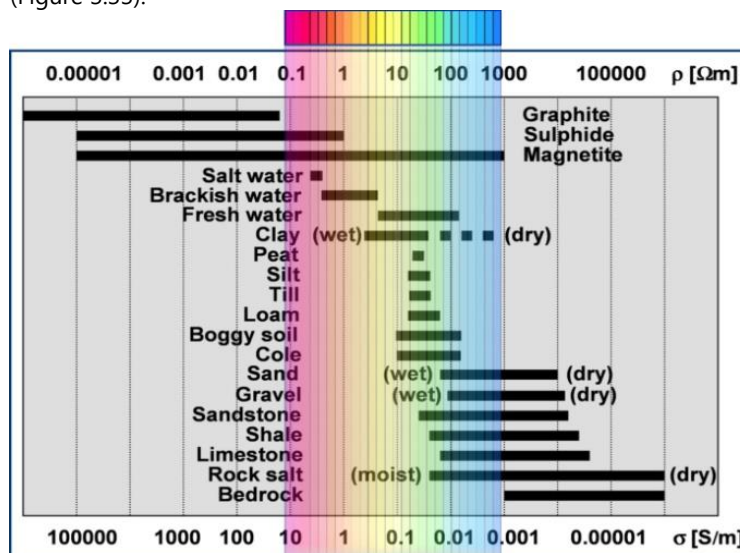


Figure 3.33. Typical electrical conductivities (resistivities) for various materials

When air-filled holes, such as animal burrows, are present in the ground, they will appear as resistive targets. Notice that even though air has infinite resistance, the current flows in 3D in the subsurface and thus the presence of a hole will increase the resistivity value in contrast to soil without holes. Thus, it will not reach an infinitely high value. The exact value depends on many parameters, mainly on the size, shape, and location (in 3D) of the hole. Holes will appear as resistive targets, with higher value than the surrounding. The proper way to address this issue, is to measure using a 3D setup. Yet, usually ERT data is collected by 2D arrays, because of time and budget constraints.

A typical acquisition system for Direct Current resistivity measurements comprises of a resistivity meter, an electric source (battery), cables with electrodes, a switching box and control and storage unit (computer). For each measurement, two current electrodes are used: one to inject the current into the subsurface and the other to retrieve the same amount of current from it. By convention, these electrodes are named A and B, respectively. The electric field is measured (at least) with two other electrodes (M and N) called the potential electrodes (Figure 3.34a). The way in which the current and potential electrodes are arranged on the Earth's surface is called an array. By changing the configurations of the array, the properties of subsurface are mapped (Figure 3.34b). Numerous electrode arrays have been designed and use several electrodes positions along a profile. Using switch boxes allows for a large number of measurements to be taken in a short time, resulting in the

capability for repeating measurements over longer time periods (time-lapse data) (c). These systems enable to collect data with high spatial resolution, allowing better and more reliable tomographic results. By applying multiple lines, a 3D image of the subsurface can be acquired (Figure 3.34d).

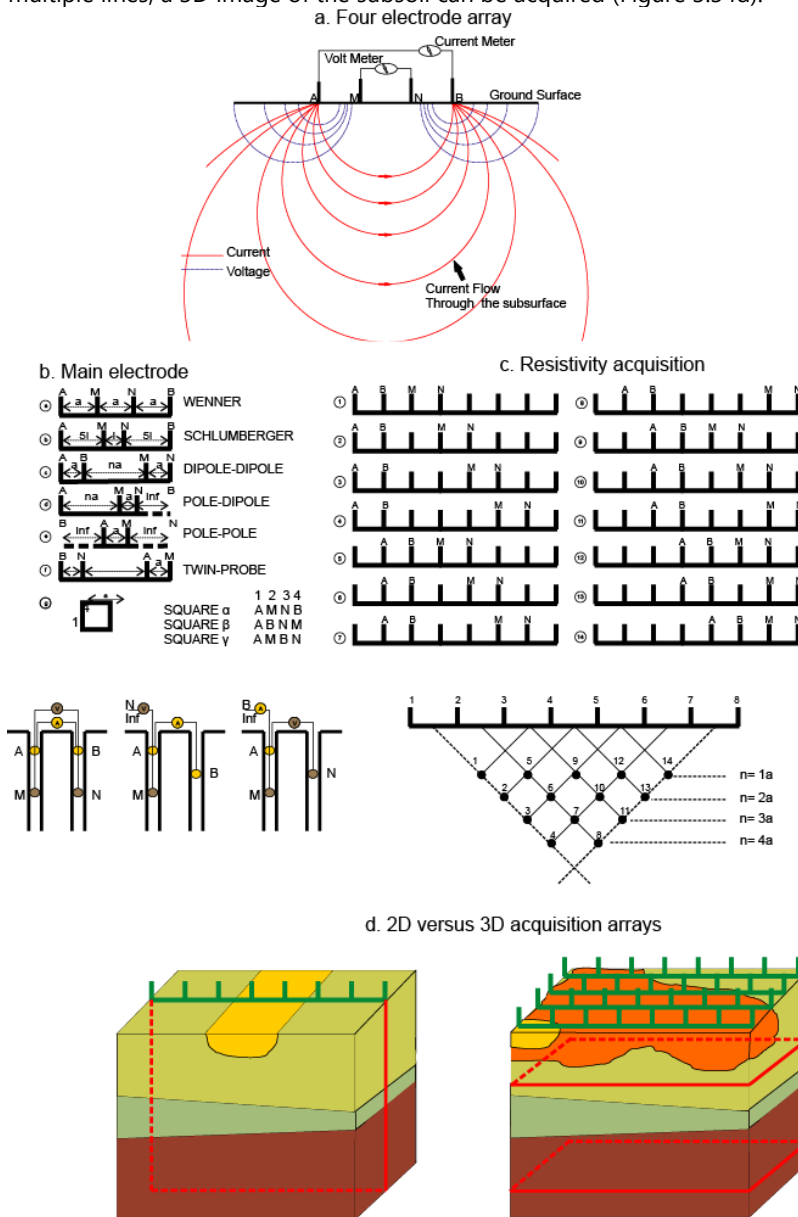


Figure 3.34. Principles of field resistivity measurements. a) sketch showing the main features, b) Classic electrode arrays for resistivity measurements, c) Construction of a so-called pseudo section, d) 2D- and 3D-acquisition arrays with possible variations.

ERT measurements typically require a lot of effort; with 2 people in the field, up to 300 m a day can be covered by two people. The technique requires cables on the surface and metal pins in the upper centimetres of the ground. The resolution and depth depend on the spacing between the electrodes: for a higher resolution, a smaller spacing is required. The more depth is to be covered, the longer the arrays need to be. Generally, burrows of around 20 cm can be detected in the upper 3-4 metres. At larger depths, 4-10 metres, burrows of 50 cm in size can be discerned. Tunnels or channels of only 10 cm diameter may be detected as well.

The collected data from actual field surveys are potential differences between the transmitting and receiving electrodes, and depend upon the distribution of the subsurface resistivity, which is the material property sought

for. Inversion aims to determine the subsurface resistivity configuration that gave rise to the measured data at the surface. This is a mathematical optimization procedure which uses the acquired data as input and prior knowledge (for example the depth to certain layers) to constrain the produced models.

The subsurface below the lines is first meshed into a grid. Inversion processing starts with an initial estimate of the subsurface resistivity configuration based on prior information. A geometrical factor, accounting for the electrode's topography and relative location is applied. The algorithm then proceeds with a forward calculation on this model to predict the potential differences that would arise if a survey were carried out over it.

At this stage, the actual field data are brought in and the inversion algorithm calculates the misfit between the actual data and the initial predicted mode. Depending on the desired misfit between the model and the measurements, additional iterations of this process will be performed (i.e. new configurations generated and tested), until a suitable model (satisfying the misfit criteria and inversion iteration numbers) is reached (cf. Figure 3.35). The mathematically acceptable model must then be assessed for its geological and geophysical plausibility.

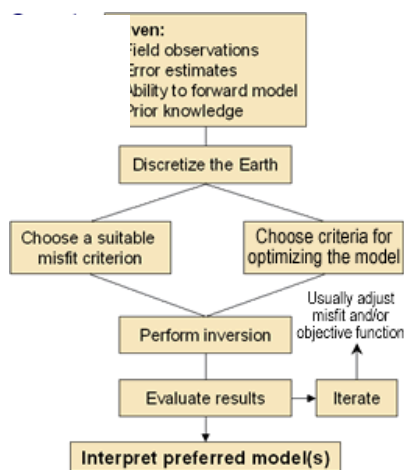


Figure 3.35. The data processing workflow.

Before starting with data processing, an evaluation of data quality is undertaken. At this stage, erroneous data, appearing as unreasonably high or low values, are filtered out. Erroneous data can result, for example, from electrical noise and improper electrode coupling to the ground. Filtering is performed on all lines to ensure optimal data quality.

A geophysical inversion is then conducted, e.g. using the Res2DINV software package (Loke, 2010), in order to assess the impact of different inversion options (such as the application of smoothing to regulate the sharpness of transitions between different layers) and to identify common features from these results in order to confidently interpret them.

### 3.2.2 Failure of levee segments damaged by animals.

#### 3.2.2.1 Historical levee failures attributed to animal activity

Animal activity has been mostly associated in literature with failures due to internal erosion (CIRIA, 2013), but a number of other failure mechanisms have been reported in past failures, such as micro-instability (e.g. Taccari 2015) and external erosion (e.g. Burdett 2016).

The following table presents historical failures that have been fully or partly attributed to animal burrows and was assembled mainly based on information that was stored in the Levee Performance Database (accessed in June 2021; see also Özer et al. 2020).

Table 3.3. Summary of reported levee failures that are fully or partly attributed to animal burrows

Year	Country	Location	Failure mechanism	Anomaly
1939	USA	Paradise Cut, California	Internal erosion Breach	Squirrel hole
1949	USA	San Pietro River, Arizona	Piping	Gopher tunnels
1969	USA	Berenda Slough, California	Internal erosion Breach	Rodent hole
1971	USA	Sid White Dam, Near Omak, WA	Seepage (Caused second dam to fail and dumped debris into town of Riverside)	Animal burrows
1980	USA	Lower Jones Tract, California Delta	Seepage	Rodent activities
1986	USA	Yankee Slough, California	Internal erosion Breach	Animal burrows
1992	USA	Water's Edge Dama North of Cincinnati, Ohio	Water flow through animal burrows	Animal burrows
1997	USA	Visalia, California	Unknown Breach	Squirrel holes
2002	Germany	Raguhn, Saxony-Anhalt (Kleckewitzer levee)	Internal erosion No breach	Trees direct at the waterside toe
2002	Germany	Niesau, Saxony-Anhalt. (Niesauer levee 2)	Internal erosion Breach	Trees direct at the waterside toe
2003	UK	Corbridge (Wide Haugh II)	Internal erosion External erosion Breach	Rabbit holes
2008	USA	Truckee Canal Embankment, Colorado		Diffused network of muskrat burrows
2008	USA	Truckee Canal, Fernley, Nevada		
2013	Germany	Retzau	Internal erosion Breach	Fallen trees (because of wind)
2014	Italy	San Matteo, Secchia River	Internal erosion Macro-instability	Animal burrows (foxes or other wild animals)

### 3.2.2.2 Modelling failure processes

In order to understand how animal activity leads to manifestation of certain failure mechanisms a thorough analysis of the physical processes that develop on the levee combined with a study of reported past failures that are attributed fully or partly to the presence of animals on the levee was necessary.

Regarding the physical processes, limited studies for the development of numerical models that correlate geometry of animal burrows or other discontinuities induced by animals with initiation and full development

of specific failure mechanisms were found (see e.g. Palladino et al. 2019; Taccari 2015). To this end, there are also limited data that could be used for validation, which made it necessary to develop approaches for utilisation of fundamentally different datasets to extract relevant information, such as the modification of fragility curves relating seepage probability and size of animal burrows based on field observations related to animal activity (Van der Meij et al. 2012; see also Figure 3.36).

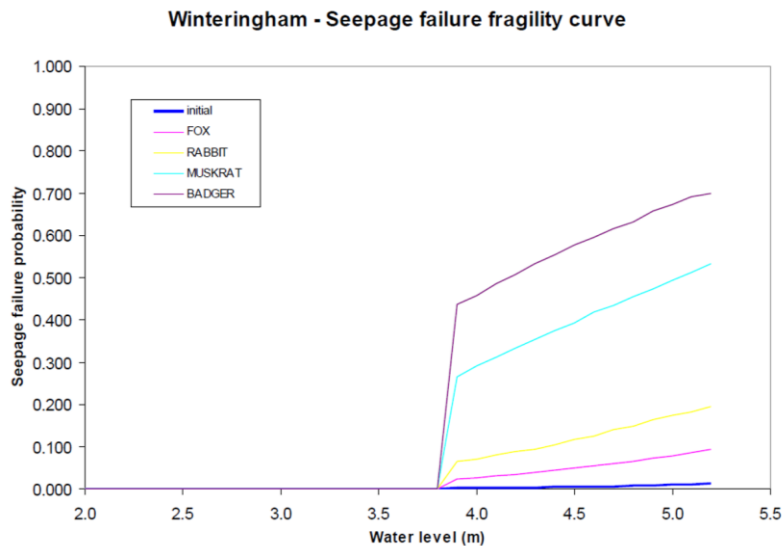


Figure 3.36. Fragility curves correlating water level with the probability of failure due to seepage in the presence of different types of animal burrows on the levee of Winteringham, UK. The curves were modified based on analysis of field observations relating to animal activity (Van der Meij et al. 2013).

For the development of the above fragility curves estimations of sizes of burrows that can be created by different animals were used. Within the domains of ecology and biology there is rich literature on the geometry and characteristics of animal burrows, which could be utilised in further development of numerical, analytical, but also empirical models of failures. Coombes & Viles (2015) developed the following empirical relationship that estimates excavated volumes of badgers with their so-call population dynamic.

$$V = 0.03A - 0.14 \quad (3.1)$$

Where,  $V$  = volume excavated in the subsurface ( $m^3$ ) and  $A$  = surface indicating the extent of 'existing mounds and spoil' ( $m^2$ ), which is defined as follows:

$$A = 8.7\alpha + 1.0X_{yr} + 15.5c - 7.2u - 20.7 \quad (3.2)$$

Where,  $\alpha$  = minimum number of years that the sett exists,  $X_{yr}$  = number of years of residence in the sett,  $c$  = number of cubs in the sett, and  $u$  = number of adult residents in the sett.

### 3.2.3 Preventive and corrective physical countermeasures

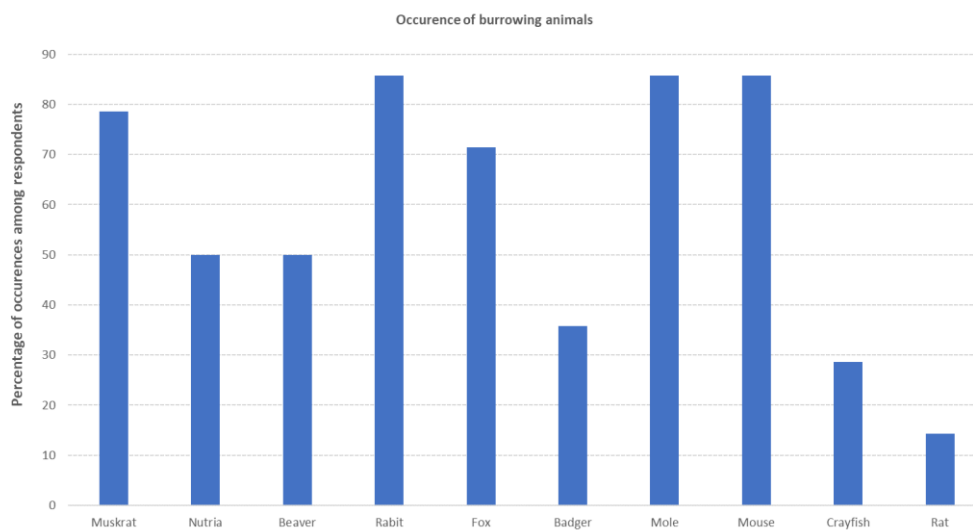
In literature the following preventive and corrective countermeasures are described (Bayoumi & Meguid 2011; CIRIA 2013; US Bureau of Reclamation 2017; Rocque 2001, TCEQ 2006):

- Impenetrable mesh covered by grass
- Pre-cast concrete blocks covered by grass
- Backfilling
- Grouting
- Geosynthetic clay liners
- Cut-off walls (sheet piling or diaphragm walls)
- Excavation & refill
- Top-layer by lime treated soil.

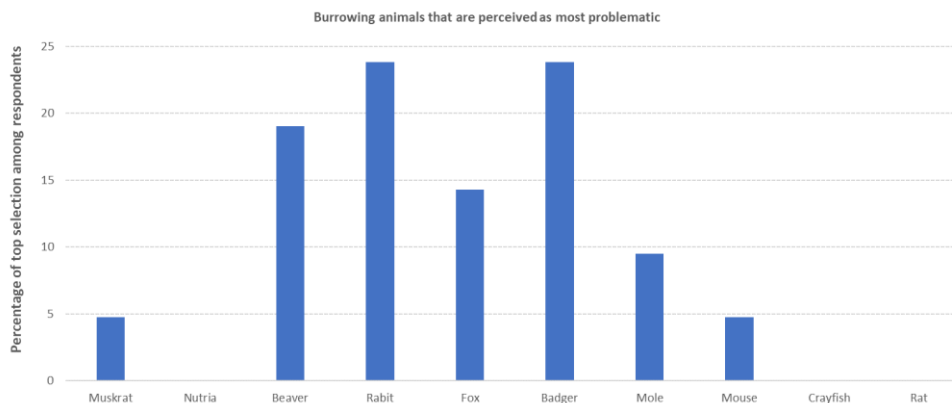
### 3.3 Questionnaire survey

A questionnaire survey was developed to collect information about the state-of-the-art practices on the management of harmful animal activities on levees. The questionnaire was translated in Dutch, English and French with the intention to have it distributed to levee management authorities in the four countries of the Polder2C's consortium. Due to time limitations, the questionnaire was ultimately distributed only to the Dutch Waterboards by HZ in collaboration with STOWA and Deltares. In total 14 responses were received from 9 levee management authorities and Rijkswaterstaat. An overview of the questions included and the responses received has been reported in Van den Berg (2021). The most relevant findings for this study are summarized below:

- Respondents indicated a variety of burrowing animals that induce damages on levees in the areas of their jurisdiction. Muskrats, rabbits, moles, mice and foxes were the most frequent ones. An overview of the responses per animal are shown in figure 3.6.



- Figure 3.6: Percentage of responses per animal to the question 'Which burrowing animals are active in the levees of your area?'.
- Rabbits, badgers, beavers and foxes which are relatively large burrowing animals were selected as the ones causing the most problematic damage (see also figure 3.7).



- Figure 3.7: Percentage of responses per animal to the question 'Which burrowing animals cause the most problematic damages in the levees of your area?'.

- All respondents indicated that animal burrows are detected by means of visual inspections. Sonar and radiographic scanning were also mentioned by one respondent each as techniques that are sporadically used.
- Regarding techniques for monitoring the geometry and extent of detected burrows, the majority of respondents indicated that they measure the depth of burrows with a probe or by excavating the levee section till they reach the burrow.
- All respondents provided a different answer to the question of when they consider an animal burrow in a levee dangerous and that it has to be immediately repaired.
- When it comes to repair techniques for dangerous animal burrows the majority indicated excavation of the burrow and reconstruction of the section and filling the cavity with clay as deep as possible.

### 3.4 Overview of knowledge gaps

Based on literature findings and the responses in the questionnaires, the following overview of current knowledge and relevant knowledge gaps was created.

Table 3.4. Overview of current knowledge and knowledge gaps per topic of interest

Topic	Current knowledge	Knowledge gaps	Activities LLHPP
Failure modes	<ul style="list-style-type: none"> <li>• Internal erosion is the most likely process of failure, but external erosion and slope instability are also possible.</li> <li>• Very limited studies on modelling such processes.</li> </ul>	<ul style="list-style-type: none"> <li>• Equations/models correlating hydraulic conditions, burrow/root geometry and initiation and development of failure.</li> </ul>	<ul style="list-style-type: none"> <li>• Detailed mapping of existing burrows</li> <li>• Forensic analyses of failed sections</li> <li>• Tree uprooting experiments</li> <li>• Fire-hose tests at anomalies</li> </ul>
Detection and measuring techniques	<ul style="list-style-type: none"> <li>• Visual inspection</li> <li>• Gravity survey</li> <li>• Resistivity methods</li> <li>• Seismic reflection</li> <li>• Ground penetration radar</li> </ul>	<ul style="list-style-type: none"> <li>• Comparison of used techniques</li> <li>• Feasibility in evaluating quality of countermeasures</li> <li>• Feasibility in data acquisition during experiments</li> <li>• Identification and feasibility of other (low-cost) techniques.</li> </ul>	<ul style="list-style-type: none"> <li>• Detection in various conditions</li> <li>• Apply various approaches to survey the same anomaly</li> <li>• Apply techniques (e.g. ERT) to monitor anomalies during experiments</li> <li>• Conceive and test (low-cost) techniques</li> </ul>
Countermeasures	<ul style="list-style-type: none"> <li>• Impenetrable mesh</li> <li>• Pre-cast concrete blocks covered by grass</li> <li>• Grouting</li> <li>• Geosynthetic clay liners</li> </ul>	<ul style="list-style-type: none"> <li>• Effectiveness has not been tested in experiments, or known cases of failures.</li> <li>• Applicability in emergency response</li> <li>• Identification and feasibility of other (low-cost) solutions</li> </ul>	<ul style="list-style-type: none"> <li>• Apply countermeasures in LLHPP sections and test them against overflow/overtopping/wave impact</li> </ul>

	<ul style="list-style-type: none"> <li>• Cut-off walls (sheet piling or diaphragm walls)</li> <li>• Excavation &amp; refill</li> </ul>		
--	--	--	--

### 3.5 Action plan for 2021-22

In July 2021 the animal burrows theme group developed a preliminary plan of activities in the living lab. This was based on identified knowledge gaps, and availability of the site as determined by the contractor's work and the preliminary plan of larger-scale experiments by the consortium. The plan is presented in Table 3.5.

Table 3.5. Provisional action plan for experimental season 2021-2022.

Period	Activity
September – October 2021	<ul style="list-style-type: none"> <li>• Detailed mapping of anomalies (visual inspections)</li> <li>• Small-scale tests on multiple locations (grouting &amp; manual excavation, smoke test)</li> <li>• Scanning of pre-selected anomalies (e.g with ERT and GPR)</li> </ul>
November – December 2021	<ul style="list-style-type: none"> <li>• Install countermeasures on pre-selected sections</li> <li>• Large-scale overflow tests on sections with installed countermeasures</li> <li>• Tree uprooting experiment</li> <li>• Test feasibility of anomaly-monitoring during large-scale tests (e.g. with ERT)</li> </ul>
January – March 2022	<ul style="list-style-type: none"> <li>• Repeat mapping of anomalies</li> <li>• Forensic analyses of section failures</li> <li>• Small-scale tests (fire-hose experiments)</li> <li>• Large-scale tests on countermeasures</li> </ul>

Due to limitations originating from the contractor's work and interfaces with other activities in the living lab, some of the activities mentioned in the above table had to be relinquished. The following table provides an overview of activities that were finally executed with dates and location.

Table 3.6. Execution plan for the experimental season 2021-22 and connection with forthcoming chapters.

Activity	Dates	Chapter
Detailed mapping of anomalies (visual inspections)	8/9/21, 24/9/21, 6/10/21	4, 5, 6
Small-scale tests on multiple locations (smoke test)	8/9/21, 7/10/21, 9/10/21	4, 6
Scanning of pre-selected anomalies (GPR)	8/9/21, 7/10/21, 24/11/21	4, 6, 8
Install countermeasures on pre-selected sections	25/11/21	8
Large-scale overflow tests on sections with installed countermeasures	26-29/11/21	8
Tree uprooting experiment	[-]	[-]
Test feasibility of anomaly-monitoring during large-scale tests (e.g. with ERT)	26-29/11/22	8
Repeat mapping of anomalies	[-]	[-]
Forensic analyses of section failures	[-]	[-]
Small-scale tests on burrows (fire-hose experiments)	[-]	[-]

### **3.6 Concluding remarks**

In preparation of the second experimental season of Polder2C's, a conscious effort was made to create an explicit link of activities in the living lab with existing knowledge gaps through a literature review and a survey that was distributed to levee management authorities in the Netherlands. Although the literature review was not exhaustive and the questionnaire survey was only distributed in one country, a preliminary identification of knowledge gaps was possible that guided the work plan development process for the experimental season 2021-2022. communicate it in a way that allows future data users to use the produced results in the right context.

## 4 Survey of small burrows Hedwigepolder (8 September 2021)

### 4.1 Context and objectives

One of the most common discontinuities on levees that are reported by levee guards during visual inspections is animal burrows. Animal burrow systems can vary in size and spatial layout depending on the animal that has created them. Burrows that are created by relatively large animals, such as foxes, rabbits and beavers are easier to detect in a visual inspection and they are considered dangerous for the structural integrity of levees. Burrows that are created by smaller animals, like mice, are more difficult to detect, but they are perceived as less dangerous.

During levee inspection exercises organised by Polder2C's, it became clear that there is no consensus among levee management authorities on the level of risk that various types of burrows pose on a levee. Risk evaluation relies on individual assessments by levee guards and can vary substantially among individuals with different experience, from different authorities or from different countries. Apart from this, it was also noticed that current practices are mostly informed by the experiences of local levee guards that are largely unreported and are not systematically compared to scientific findings.

On 8th September 2021 an animal burrows survey took place in the Living-Lab Hedwige Prosperpolder whose purpose was to collect data in a coordinated manner, hence contribute to future efforts to address the above-mentioned issues. The objectives of the activity are summarised below:

5. Gain insight into the types of animals that are active in the living lab as well as the geometry and spatial distribution of the burrows they create on the levee.
6. Monitor the levee inspection process and derive lessons that can improve the practices of levee guards.
7. Test feasibility and compare results of two methods for evaluation of burrows; the ground penetrating radar and the smoke method.
8. Identify locations with burrows that could be tested later on, in a large-scale overflow experiment.
9. Compare findings from the application of different survey techniques and draw lessons for their future use.

### 4.2 Location and levee geometry

The survey was performed on the levee stretch where overflow experiments were scheduled to take place in the upcoming experimental season, starting in November 2021. This location allowed the identification of burrows that could be tested against overflow. The selected stretch is situated on the Hedwigepolder levee, i.e. the Dutch side of the living lab, and specifically on the southeast of the concrete staircase situated in front of the former farm house of De Cloedt (see also Figure 4.37, left). On the Dutch levee there is an asphalt road at the landside toe of the structure (see also Figure 4.37, right). The team gave priority to the survey of the landside slope as this is the slope that would be tested later against overflow. Although the survey of the waterside slope was considered equally interesting for the rest of the objectives of the study, it was excluded due to time limitations.



Figure 4.37. Left: Map indicating the location of the animal burrows survey on 8th September 2021. Right: Picture of the surveyed levee from the crest.

A typical cross-section at the levee at this location is shown in Figure 4.38. The average landside slope is about 21° or approximately an 8/3 slope (Depreiter et al. 2021).

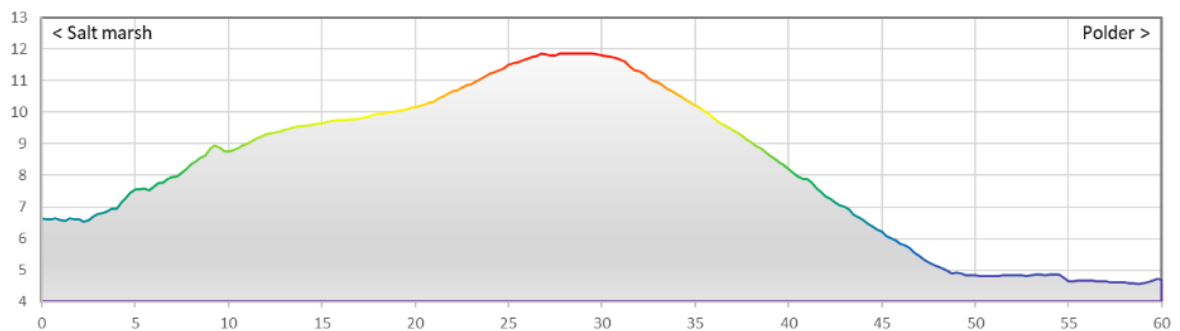


Figure 4.38. Typical cross section at the surveyed location (Source: Depreiter, 2022a)

### 4.3 Work method

The first part of the activity was the mapping of burrows by means of a visual inspection. The group walked the levee and tried to spot as many burrows as possible. All participants used a probe to facilitate this process (see Figure 4.39, left). Burrows that were detected were marked with fluorescent spray and then registered with two techniques; 1) the App2C application and 2) handmade drawings on grid paper (see also Figure 4.39, right). The idea behind this, was to compare both registration techniques in terms of, among others, ease of use and speed.

The survey was performed on the levee stretch where overflow experiments were scheduled to take place in the upcoming experimental season, starting in November 2021. This location allowed the identification of burrows that could be tested against overflow. The selected stretch is situated on the Hedwige polder levee, i.e. the Dutch side of the living lab, and specifically on the southeast of the concrete staircase situated in front of the former farm house of De Cloedt (see also Figure 4.37, left).



Figure 4.39. Left: Detection of burrows with a probe; Right: Paper mapping of burrows

The minimum information that had to be recorded per burrow was its location, its diameter and its depth. The location is automatically registered when App2C is used. For the paper mapping locations were recorded by means of x- and y-distances from preselected reference points, whose coordinates were known from previous surveys of Polder2C's. Reference points were marked on the crest of the levee and x- and y-axes were indicated by laying measuring tapes parallel and perpendicular to the crest respectively, as shown in Figure 4.40.



Figure 4.40. X- and Y-axes for recording distance of burrows from reference points.

The second part of the activity was the application of two non-destructive techniques to survey the geometry of burrows underground; 1) imaging with ground penetrating radar (GPR) and 2) the so-called smoke test. More information about these techniques is given in the following paragraphs. The GPR measurements were performed by ULille and the smoke test by TU Delft. After completion of the paper mapping the team got together to evaluate the results and choose spots for application of the non-destructive techniques. These were spots where a relatively high density of burrows was detected during mapping. In order to allow comparison of the results of the two techniques, they had to be applied on the same location.

The GPR is considered one of the most accurate technique for detection of cavities in levees among rival approaches, like resistivity methods, gravity survey and seismic reflection (Heyer & Stamm, 2019). The GPR emits electromagnetic waves and registers the reflected signals from subsurface elements (see also Di Prinzio et al., 2010). This allows users to detect changes in material, cracks and voids without any intervention on the ground. In this survey two GPR devices were used that scanned the ground with two different frequencies: 2GHz and 400MHz. Higher frequencies allow imaging with higher resolution compared to the imaging achieved in lower frequencies. This provides more details about the geometry of burrows. However, its application in the field is more time-consuming and the processing of data it produces is more laborious.

The smoke test is a technique that a PhD student from the University of Antwerp (Heleen Keirsebelik) developed to show the interconnectedness of burrows by the Chinese mitten crab (see Figure 4.41, left). The complexity of the tunnel systems created by these crabs were also presented by Rudnick et al. (2005), who obtained castings of the tunnel systems (see , right).

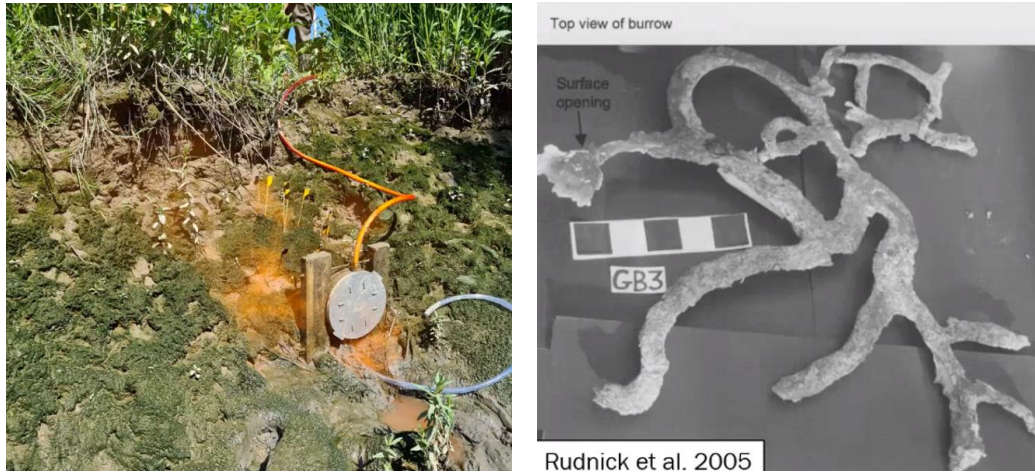


Figure 4.41. Left: using smoke to show interconnectedness in the system of burrows by the Chinese mitten crab. Right: Interconnectedness of burrows by Chinese mitten crabs, from a paper by Rudnick et al. 2005. Both pictures were shown by Heleen Keirsebelik, PhD student UAntwerpen, during webinar EUCOLD presentation, 30-6-2021.

For the purposes of this survey an improvised experimental setup was developed by TU Delft for the performance of a smoke test similar to the one developed by Keiserbelik. The improvised setup consists of a leafblower, a barrel and a tube connected as shown in Figure 4.42. The smoke bomb detonated and placed in the barrel, where the smoke is collected. In this phase, the tube is closed. When enough smoke is gathered inside the barrel, the tube is placed inside the animal burrow, preferably the lowest, as the smoke moves upward. Then the leaf blower, which is attached to the barrel, is turned on, to create enough pressure to blow the smoke through the burrow system. Once smoke comes out of one of the other holes, these are blocked with wet clay. This process is repeated, until no more smoke is detected. The experiment can be repeated for the same burrowing system, but with the tube placed in a different burrow, so that the entire extent of the burrowing system is mapped.

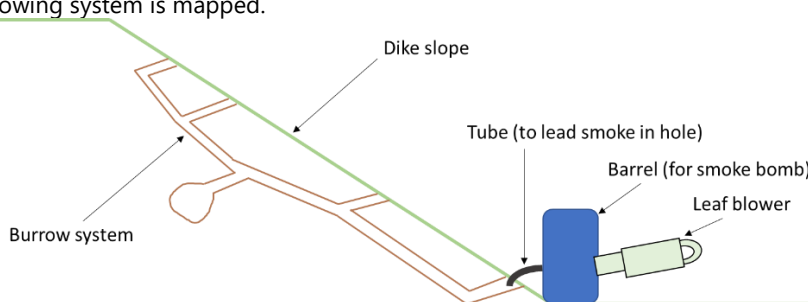


Figure 4.42. Layout of the experimental setup for the smoke test developed by TU Delft.

#### 4.4 Execution and results

In total, 12 people participated in the activity (see also Table 4.6).

Table 4.6. List of participants

Name	Organisation
Vana Tsimopoulou	HZ
Stephan Rikkert	TU Delft
Robert Lanzafame	TU Delft
André Koelewijn	Deltares / STOWA
Frans van den Berg	Deltares
Yasmin Sozer	HZ / RWS

Mario van de Berg	TU Delft
Robert Bentivoglio	TU Delft
Johan Westhuis	Hoogheemraadschap De Stichtse Rijnlanden
Ammar Aljer	U Lille
Sarah NGUYEN Hoang Dung	U Lille
Timothy de Kleyn	U Antwerpen

The equipment that was used is listed in Table 4.7.

Table 4.7. List of equipment

Activity	Equipment	Owner
Detection of burrows	Probes	Polder2C's
	Fluorescent sprays (4)	TU Delft
Digital registration of burrows	Smartphones with App2C installed	All participants
	Cameras (2)	TU Delft / Deltares
Paper mapping of burrows	Grid paper and pencils	TU Delft
	50m-long measuring tapes (6)	HZ / Deltares
	5m-long measuring tapes (2)	HZ
Smoke test	Leafblower	TU Delft
	Barrel	TU Delft
	Smoke bombs (10)	TU Delft
	Hose	TU Delft
	Plastic buckets (2)	TU Delft
GPR scans of burrows	Georadar IDS Opera Duo	U Lille
	Georadar IDS RIS	U Lille

#### 4.4.1 Mapping

Based on the final number of participants, it was deemed realistic to focus on the survey of the landside slope only, and to aim at covering a levee stretch of about 100m from crest to toe. Upon arrival on site the team determined the boundaries of the survey area. The southeast edge of the staircase at the point that the crest meets the landside slope of the levee was selected as a reference point for the paper mapping. The survey boundary was set 80.5m to the southeast of the staircase (see also Figure 4.43). The first 80.5m adjacent to the staircase were reserved for testing various repair strategies and a major intervention had already taken place (see also Figure 4.44). This was an unconventional levee stretch and was considered outside the scope of the survey, so it was excluded.

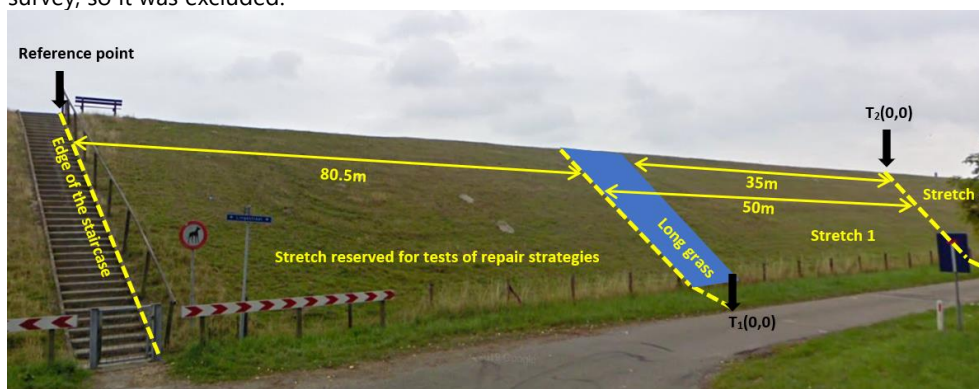


Figure 4.43. Layout of surveyed area. The background picture was taken before construction started in the living lab (source: Google maps, street view).

Beyond that point, two 50m-long levee stretches were set out for mapping, each of them with its own coordinate system. The origins T1 and T2 of the coordinate systems that were set per stretch are shown in Figure 4.43. The yellow indented lines at T1 and T2 indicate the X=0 lines of the coordinate systems. The Y=0 line for the coordinate system of stretch 1 was the edge of the asphalt road at the toe, while the one of stretch 2 is the crest level. The distance from the crest till the edge of the asphalt was approximately 22.5 m, which means that the survey area was  $22.5 \times 100 = 2250$  m<sup>2</sup>. Regarding the condition of the selected section, it is important to note that in a strap of 15m from the beginning of stretch 1 there was long grass (see blue strap in Figure 4.43), while in the remaining 35 m from stretch 1 and the entire area of stretch 2 the grass was freshly mowed.



Figure 4.44. Preparation of sections before application of repair strategies on the southeast side of the concrete staircase in June 2021.

The team was split in two groups. One group surveyed stretch 1 and the other group surveyed stretch 2. On average 4 inspectors were kept busy in every stretch during mapping, but the number of inspectors per stretch varied in the course of the activity between 2 and 6. In each group, about half of the participants used App2C and the other half executed the paper mapping. Some inspectors walked the levee horizontally and others chose to walk vertically, which allowed to look at the levee from various perspectives, increasing the chances to detect burrows. All inspectors walked the entire area, which means that the entire stretch was inspected by 4 pairs of eyes. The team observed that every time a new person inspected an area, new burrows were spotted. A summary of the inspection process and the results per stretch is presented in Table 3.

Table 4.8. Summary of information collected per stretch

	Stretch 1	Stretch 2
Area surveyed	787.5 m <sup>2</sup>	1125 m <sup>2</sup>
No. of inspectors	4	4
Time needed	3.5 hrs	4.5 hrs
No. of burrows detected	61	28
No. of burrows per m <sup>2</sup>	0.08	0.025
No. of burrows per m	1.7	0.56
Range of burrow diameters	1-10 cm	2-12 cm
Range of burrow depths	< 25 cm	6-25 cm
No. of burrows that reach the sand core	0	0

In stretch 1, the team started from the 35m-long levee part with mowed grass, whose area is  $35 \times 22.5 = 787.5$  m<sup>2</sup>. In that part they detected in total 61 burrows, resulting in 0.08 burrows per m<sup>2</sup> or 1.7 burrows per linear m of levee. This part was completed within 3.5 hrs, which was almost twice as much time as it had been initially

expected. For this reason the team decided to only record the exact location of every burrow without keeping a detailed record of the diameter and depth per burrow. By the end of the survey the group confirmed that the diameters of all burrows were in the range 1-10 cm, and their depths did not exceed 25 cm. Considering the time needed and the fact that burrows were difficult to spot even in mowed areas, the team decided not to survey the area with long grass. A casual observation of the transition between the mowed and unmowed area made it clear that it would be very difficult and time consuming to spot burrows with diameters of 10 cm in areas with long grass (see also [Figure 4.45](#)).



Figure 4.45. Left: Landside slope with long grass in the first 15 m of stretch 1. Right: Transition between mowed and mowed grass in stretch 1.

In stretch 2, the group surveyed the entire area, which equals to  $22.5 \times 50 = 1125$  m<sup>2</sup>. They found in total 28 burrows, which is equivalent to 0.025 burrows per m<sup>2</sup> or 0.56 burrows per linear m of levee. In this stretch the team kept detailed records of location but also depth and diameter. Diameters are in the range of 2-12 cm, and depths in the range of 6-25 cm. It took the group 4.5 hrs to complete this survey.

Comparing the two stretches, it is clear that in stretch 1 there is a higher density of burrows, but this is likely a random fact. There were no obvious differences in the physical characteristics of the two stretches that could justify this difference. The vegetation was homogeneous and in both stretches the grass was mowed. The levee geometry and the layers of clay and sand in the subsoil were also uniform, as evidenced by the surveys that were performed in June and July 2020 by the Polder2C's team (Depreiter et al. 2021). The difference in the density of burrows could be partly attributed to the fact that a visual inspection cannot be 100% accurate. Based on previous research, the accuracy of visual inspections can be considered limited as the detection capacity can vary significantly among inspectors (Klerk et al. 2021, Klerk 2022). This finding was also confirmed during this survey, as the inspectors noticed that most burrows were missed the first time that an inspector walked close to them. The more eyes that scanned a spot, the more burrows were found.

The spatial distribution of burrows in stretches 1 and 2 can be seen in [Figure 4.46](#) and [Figure 4.47](#) respectively.

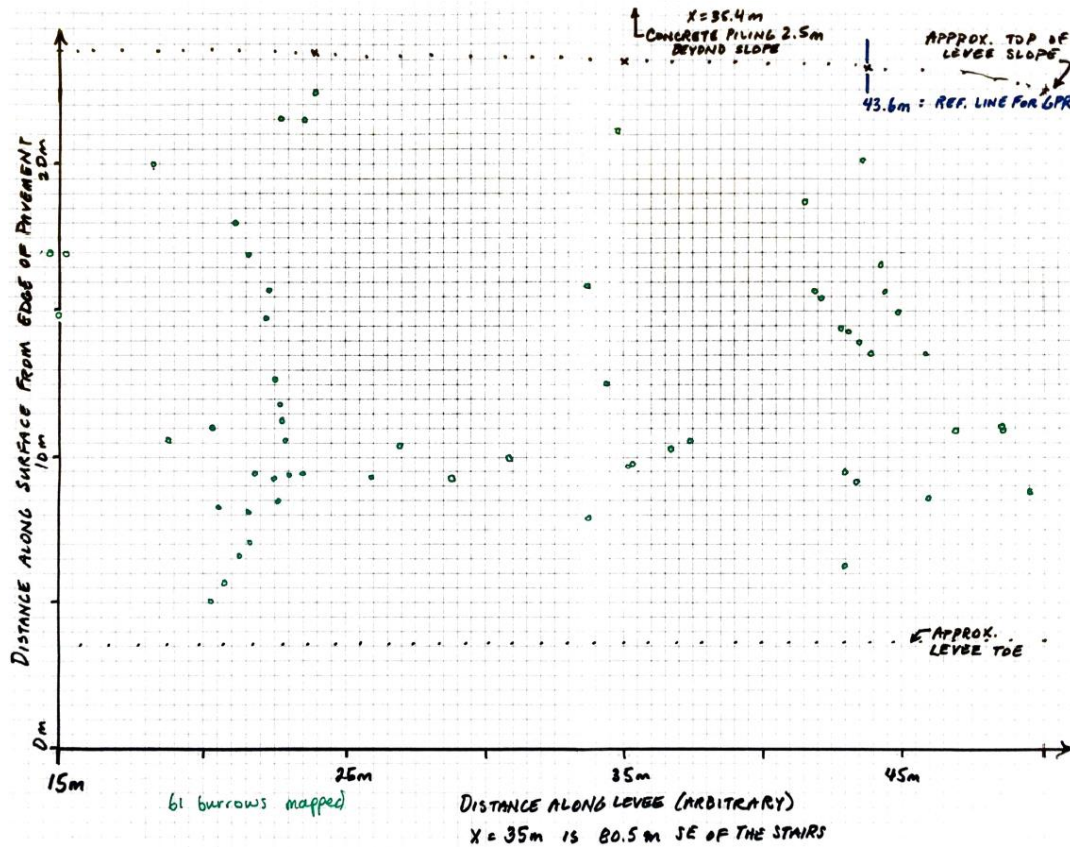


Figure 4.46. Spatial distribution of burrows in stretch 1

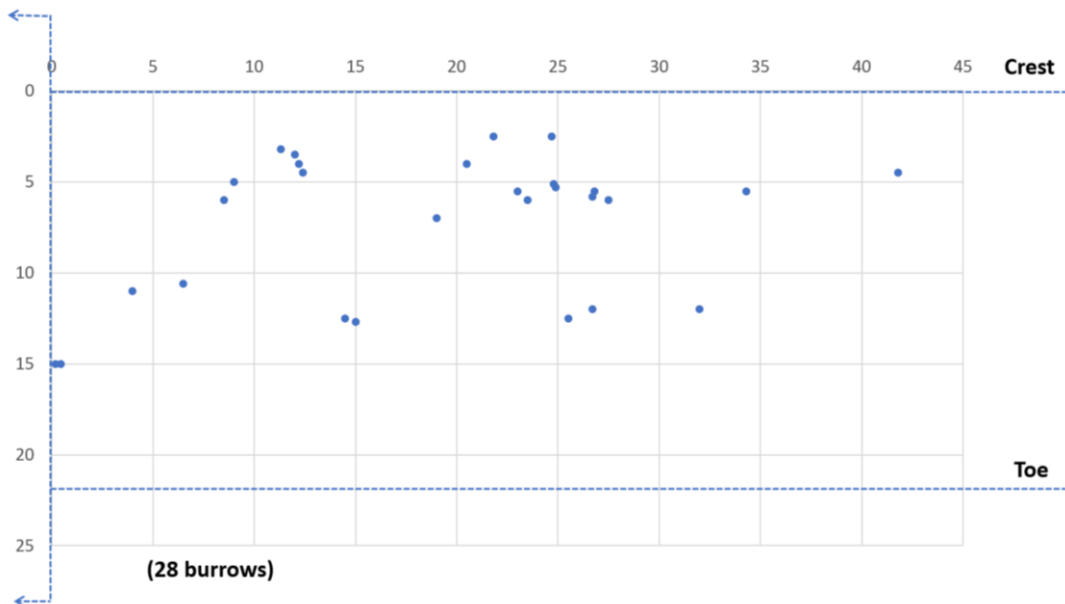


Figure 4.47. Spatial distribution of burrows in stretch 2

These images make it clear that the burrows are not uniformly distributed on the levee slope. There are areas without any burrows and there are areas where burrows are clustered in a relatively small space. Burrows that are concentrated in a small area may be an indication of an underground den of small rodents that can have multiple chambers interconnected with corridors and multiple exit points (see e.g. Avenant & Smith 2002). In stretch 1, apart from clusters, burrows positioned in linear pattern with vertical orientation could also be discerned (see also Figure 4.48). Such linear patterns can be an indication of a linear underground tunnel,

which is characteristic of mole burrow systems (see also Thomas et al. 2013). According to Abel de Boer from Wetterskip Fryslân, who participated in the mole burrow grouting in the living lab in June 2021 and has long experience in the detection of animals on levees, moles build their nests in dry spots, but they create tunnels towards more humid soil, where they can easily find food. This is because warms and other insects are more likely to be found in soil with higher concentration of water. This could be an explanation of the vertical orientation in the linear patterns. It is likely that moles living on a levee build their nests closer to the crest than the toe, where the subsoil can be dryer, but they create tunnels towards the toe, where the soil can be more humid. Based on this analysis it is realistic to assume that burrows that are clustered close to each other and burrows that form a line with orientation crest to toe may be interconnected.

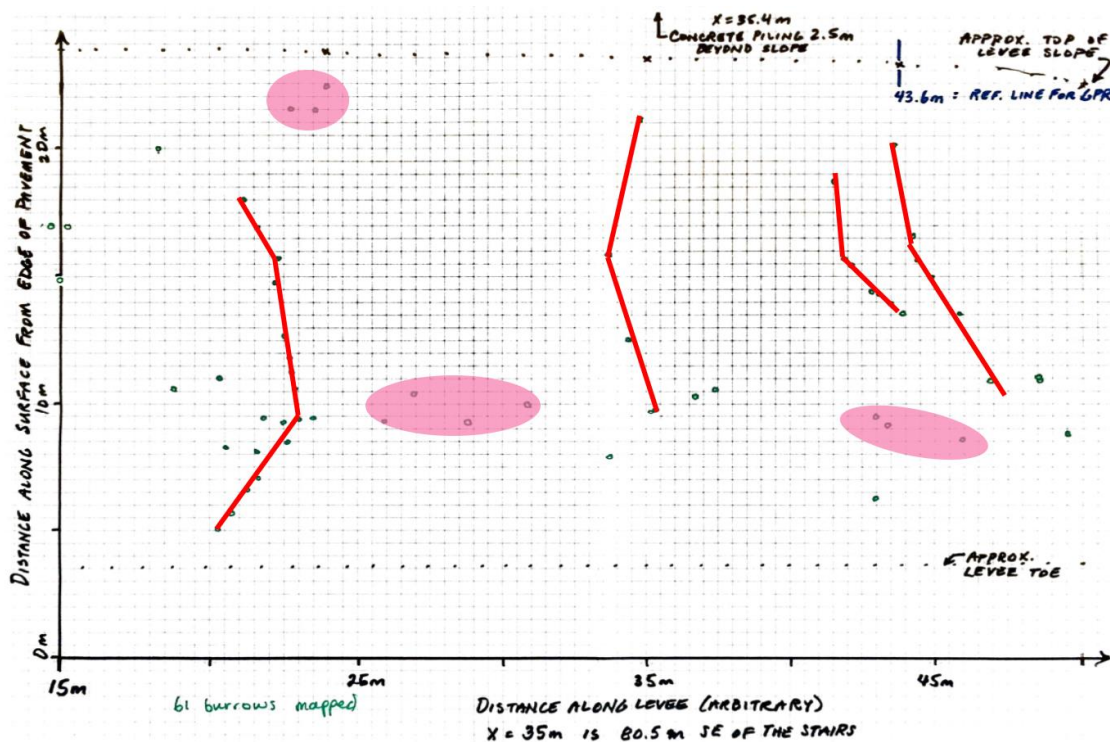


Figure 4.48. Burrows in stretch 1 with linear patterns highlighted (in red) and other clusters encircled (in pink).

#### 4.4.2 Imaging with Ground Penetrating Radar

Due to the limited time that was available, and given that the mapping took longer than was initially expected, the GPR measurements had to start before the mapping of burrows was complete. After about 2hrs of mapping the team got together and chose an area of 3 m x 10 m where a relatively large number of burrows had been detected. This was in the upper half of stretch 1, close to its southeast end, and specifically from X=40.5 m to X=43.5 m and from Y=13.5 m to Y=23.5 m in the coordinate system of stretch 1 (see also Figure 4.49, left).

In order to perform the measurements, a grid was created in the selected area with horizontal and vertical lines with ground distance of 50 cm. The scan was realized by two devices; one with the high-frequency 2GHz and the other with two low frequencies 200MHz and 600MHz. For the high frequency measurements a scan was taken along every line of the grid. With every scan along a horizontal or vertical line of the grid a longitudinal 2D profile or transversal 2D profile was created, respectively. If the quality of the 2D images is good, the 2D-profiles will be extrapolated for the creation of a 3D-illustration of the subsoil, which may provide additional information about the geometry of burrows. The creation of this 3D model is still in preparation. The second device (200 MHz and 600 MHz) was only used to make 3 parallel 5 m transversal transects in the upper part of the section adjacent to the crest. The details of every scan are given in Table 4.9.

Table 4.9. Details of executed GPR measurements

Frequency	Grid size	Precision	Grid location
2 GHz	3m x 10 m	0.5 m	X=40.5-43.5m, Y=13.5-23.5m
400/600 MHz	3 m x 5 m	1 m	X=40.5-43.5m, Y=18.5-23.5m

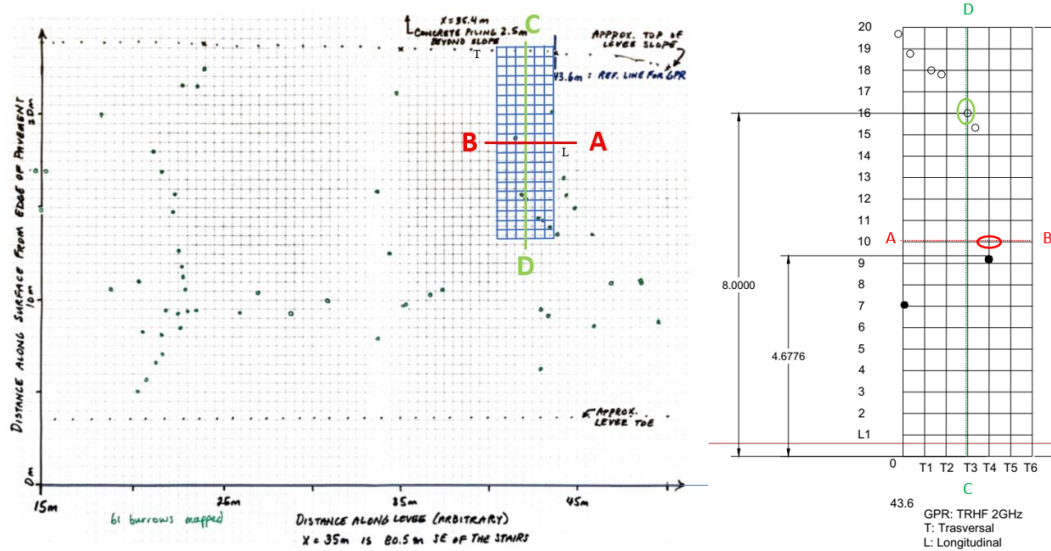


Figure 4.49. Left: Grid indicating the area that was scanned with GPR. Right: Top view of the GPR grid juxtapose with the inspection map, with indications of the positions of burrows and the longitudinal and transversal profiles C-D and A-B, respectively.

In Figure 4.50 the GPR results for the profiles A-B and C-D are shown. In the A-B profile the red circle shows inhomogeneity of up to a depth of about 25 cm from the surface, as the colour of the produced image is different, which shows that the consistency of the soil was different. Since in a distance of about 40 cm from that spot a burrow was detected (Figure 4.49, right), this inhomogeneity is most likely a trace of the underground structure of the burrow system. This inhomogeneity is indicated by a different colour in the produced image. In the C-D profile the green circle shows a similar inhomogeneity up to a depth of 35 cm. This is exactly at the spot where a burrow was detected.

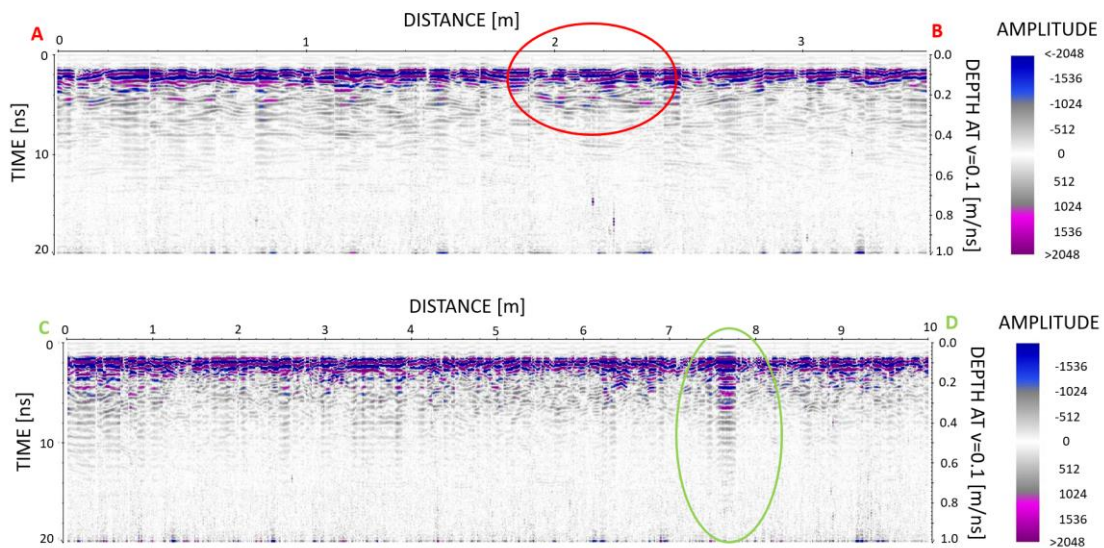


Figure 4.50. GPR scans at the longitudinal profile A-B (top) and at the transversal profile C-D (bottom).

An overview of all 2D results for transversal transects from the 2GHz radar are shown in Figure 4.51. The circles indicate discontinuities that could be attributed to burrows. Further comparison with the results of the visual inspection may provide additional insights.

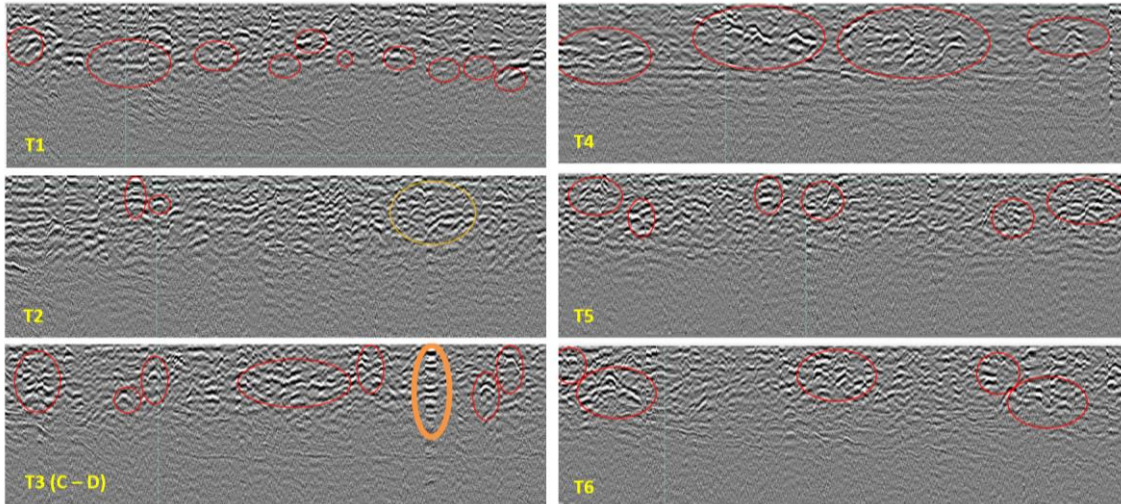


Figure 4.51. Overview of all 2D transversal transects that were scanned in 2GHz. Traces of discontinuities that could be attributed to animal burrows are indicated with circles.

In the following figure a first attempt is made to compare and contrast 2D images collected with GPR and the map of burrows that was created during the visual inspection.

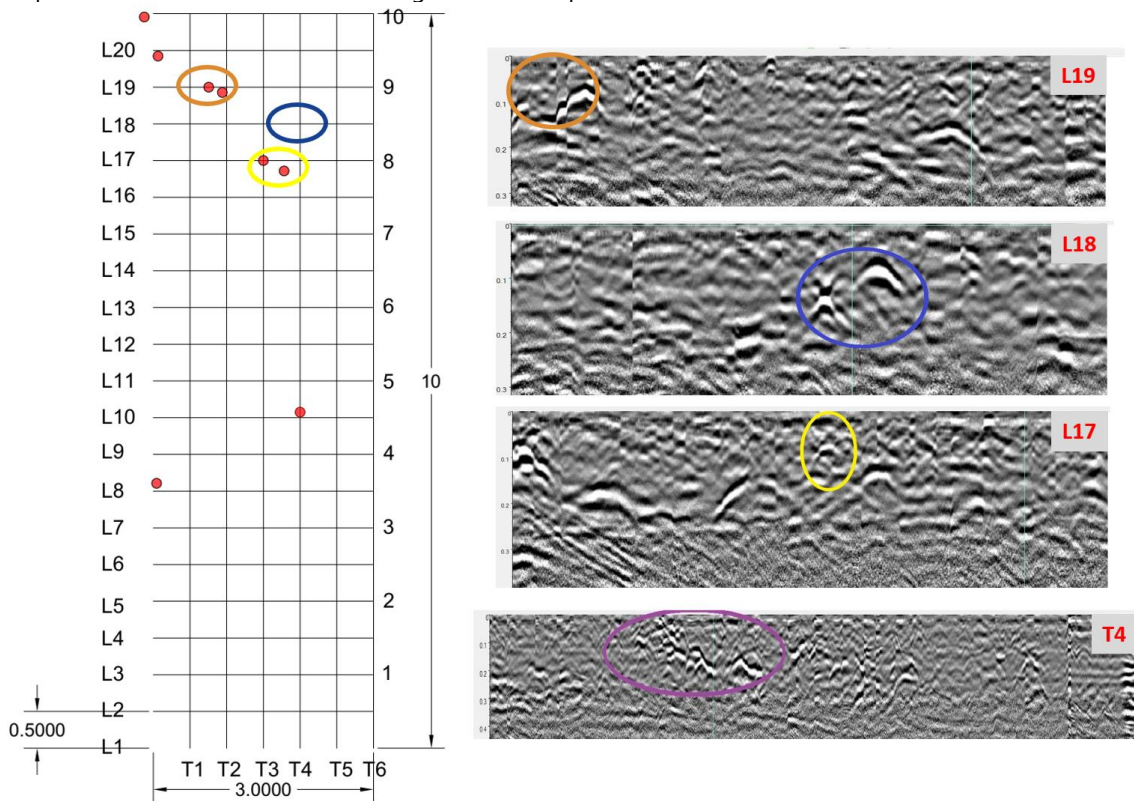


Figure 2.15. Comparison between visual inspections and GPR images.

After comparing between the 2D analysis of the data obtained by the 2G GPR and the visual inspections we can detect cavities in the upper surface near some of the discovered holes (see the yellow, blue and orange circle in transects L17, L18 and L19 respectively). This indicates the continuity of the discovered burrows underground. Around the rest of the burrows that were mapped on this location the GPR did not indicate any important cavity, which reduces their probability to be burrows of a larger network that leads to a den, or perhaps their dimensions are very narrow and cannot be detected. The 2D analysis of the GPR scans in this area shows many possible continued underground cavities (see e.g. the purple circle on transect T4), but no excavation was made in this area to verify if they are indeed a tunnel by a burrowing animal on this spot. A more meticulous analysis in the future may provide more insights. More precise results of the 2GHz GPR could be obtained if the distance between the scanned transects is smaller. This was tried out in subsequent experimentations in the living lab (see also chapters 6 and 8).

The 2GHz antenna is supported with a wheel-encoder to measure the travelled distance. During the measurements the team noticed that the wheel-encoder slipped several times as it moved over the grass layer. As a result the precision of the travelled distance measurement reduced, which made it difficult to handle and scan the surface of pavement. Apart from this, since the measurements were taken on a slope and on the heterogeneous, rough surface of the grass cover, the vertical and horizontal distance error of raw data is expected to be slightly high. This could probably be corrected in the forthcoming processing steps by the use of the 'trace interpolation' function, which can locate and decrease vertical and horizontal distance error.

In addition, a high soil humidity (effect of the weather) can change the propagation velocity and the intensity of electromagnetic waves (by absorbing the electromagnetic energy), and therefore it could affect the quality of recorded data. More specifically, the moisture in the soil can change the reflexion properties of the soil material layer, increase the noise signals and finally confuse a real layer of burrows and other material layer. The velocity of propagation during this measurement was 10 cm/ns while the propagation velocity in other measurements that took place in October and November (see relevant chapters) was from 6.2 to 6.7 cm/ns. There is no information about the level of soil humidity on the day of this survey, but as mentioned before, it was a dry day with high temperatures.

#### 4.4.3 Smoke test

The smoke test was conducted when the mapping of burrows had been completed. Burrows that seemed to be part of a mole system were chosen for this. As an entry point the lowest burrow was selected. Within about 5 s after the team started injecting smoke, the smoke could be seen coming out from the closest burrow in the system (see also [Figure 4.52](#), right). Unfortunately the experiment had to be interrupted, because the experimental setup failed. In particular the hose that connected the barrel with the entry point on the ground was overheated and started melting. The team decided to improve the experimental setup and try out the experiment another day.

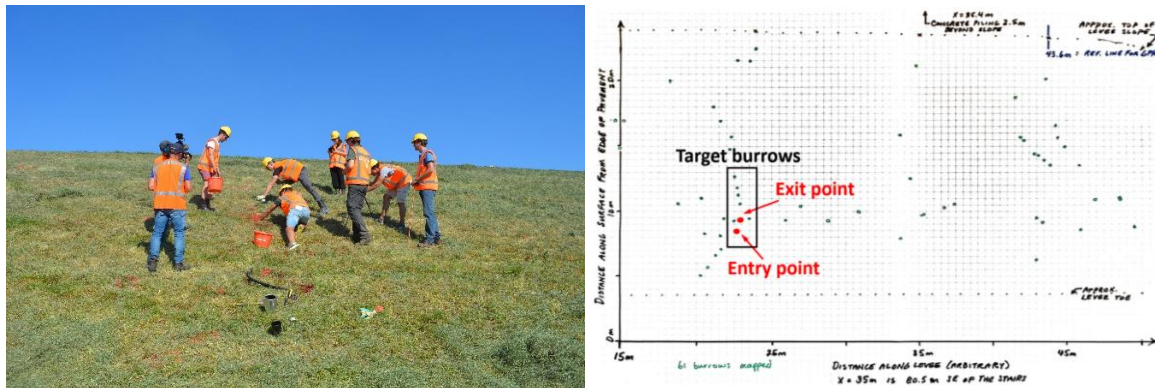


Figure 4.52. Left: Preparation of section for the smoke test. Right: Target area for the smoke test with indication of the entry point, i.e. where smoke was injected, and the exit point, i.e. smoke came out, before failure of the experimental setup.

## 4.5 Concluding remarks

### 4.5.1 Types, geometry and spatial distribution of burrows

1. In the surveyed area the team only detected burrows of diameters up to 12 cm. This size of burrows can only be made by small rodents. This does not exclude the presence of other animals in the living lab. As a matter of fact burrows by larger animals like foxes and rabbits have been witnessed in and around the living lab area (see other relevant chapters in this report).
2. Two spatial patterns of burrows could be discerned in the surveyed area; 1) burrows in a linear setup with orientation in the vertical direction, i.e. crest to toe, and 2) burrows that were clustered close to each other in a relatively small area. The former pattern is very likely made by moles. The latter pattern can be made by mice or other small rodents. The Polder2C's team has witnessed mice in the living lab but no other small rodents. The assumption is made that the burrows that are clustered close together are made by mice. Further research is needed to verify if this is a correct assumption.
3. Regarding the underground geometry of burrows, the team noticed during detection that burrows were almost never perpendicular or vertical to the surface of the levee slope. This shows that the burrows are not by definition on the top of an underground den, but they probably constitute entrances and exits to underground corridors that lead to dens, which may be situated deeper in the body of the levee.
4. The largest burrow depth that was registered during mapping was 25 cm, while the GPR results showed that the scanned burrow system reached a depth of 35 cm. From the results of previous surveys, it is known that the clay layer on the Hedwige levee has a thickness of about 80 – 100 cm. Based on this, it could be assumed that the burrow system in the surveyed area did not reach the sand core of the levee.
5. The smoke test, although it was not successful it provided proof of interconnectedness of two burrows.

### 4.5.2 Burrows detection process

1. Burrows made by small rodents are nearly impossible to detect in sections where the grass is not mowed. In sections that have been mowed detection can still be challenging and time consuming. It is characteristic that during survey of the mowed area, the more times an inspector passed from a given area, the more burrows were spotted.
2. Given the difficulty in detecting small burrows during a visual inspection, the knowledge of expected patterns in the spatial distribution of burrows can be used by inspectors as a rule of thumb. When a mole burrow is detected for example, an inspector can assume that there may be more burrows arranged in a line that connects the crest with the toe. Further research on the spatial distribution of burrows can help in the development of such simple rules of thumb, facilitating levee inspection practice.
3. Burrows made by small rodents are often disregarded in levee inspections, because they are not considered dangerous. Since small burrows may lead to larger dens in the body of a levee, further research

and collection of data about expected animal activity on levees, and evaluation of their severity is needed. Relevant results can inform levee inspection practices in the future.

#### 4.5.3 App2C vs Paper mapping

1. The team had a good experience using App2C to register information about the detected burrows. Inserting information in the app was simple and fast, but data from App2C have not been retrieved yet. However the app had a disadvantage in relation to paper mapping for this specific type of survey; every inspector used her/his own smartphone. The level of accuracy of location data from every smartphone is unknown. This means that although the app can work perfectly in a regular or emergency inspection when larger anomalies need to be reported, it may not give location data of sufficient accuracy for the analysis of spatial patterns of burrows. In this case paper mapping or registration of location data with a high-accuracy GPS device may be more effective.
2. Paper mapping was a simple approach, but in general more time consuming than expected. Measuring X- and Y- distances for every single burrow from a reference point with tapes takes much time, but it can be performed by non-specialised personnel with no equipment costs. This can be an ideal technique for research teams that do not have sophisticated instruments, like a GPS device. It can also be considered as a useful approach for field research that requires an overview of intermediate results during the process. The team could see the patterns of detected burrows at any time during the survey and make intermediate decisions in the course of the day.

#### 4.5.4 Feasibility of non-destructive characterisation techniques (GPR and smoke test)

1. The GPR provided insight into the depth and detailed geometry of burrows under the surface, which is not possible with a visual inspection. Its disadvantage is that its results are not readily available in the field, and the quality of the results depends on weather conditions. If the soil is dry, the images are expected to be of good quality. If the soil is wet, the images may not be of sufficient quality. This survey took place in a period that it had not rained for a while, so the soil was dry. GPR measurements were performed in November on rainy days too (see relevant chapter of this report). A comparison of the results from the two surveys can showcase the quality differences.
2. The 2D transects show clear traces of discontinuities in the first 50 cm below the surface of the levee. These traces can be attributed to underlying burrows. A preliminary comparison and contrast of the GPR images and the results that were obtained from the visual inspection showed that underground cavities can be seen in areas where multiple burrows are clustered together, while in areas where individual burrows were seen no underground cavities were detected. Further comparison and contrast of the images with the results of the paper mapping could enrich these insights.
3. The smoke test indicated interconnectedness between two burrows, but the setup failed during the experiment. The plastic hose was overheated and it started melting. This probably happened because the can that was used to retain the smoke and channel it to the burrow system was too small. This increased its temperature to a level that exceeded the melting point of the hose material.
4. A detailed evaluation of the smoke test can only be made after a new trial with an improved device.

#### 4.5.5 Selection of sections for testing against overflow

Two sections with high concentrations of burrows were selected as candidates for execution of overflow tests on burrows, which are indicated in [Figure 4.53](#). In both sections it was assumed that there were mole burrow systems, which are expected to be extensive in length and probably interconnected. In the upper half of the right-hand side section GPR scans were also made. The team agreed to come back to these spots and make a new trial of the smoke test and more GPR measurements. This would allow a more extensive analysis of the results of overflow tests in this location (see also chapters 6 and 8).

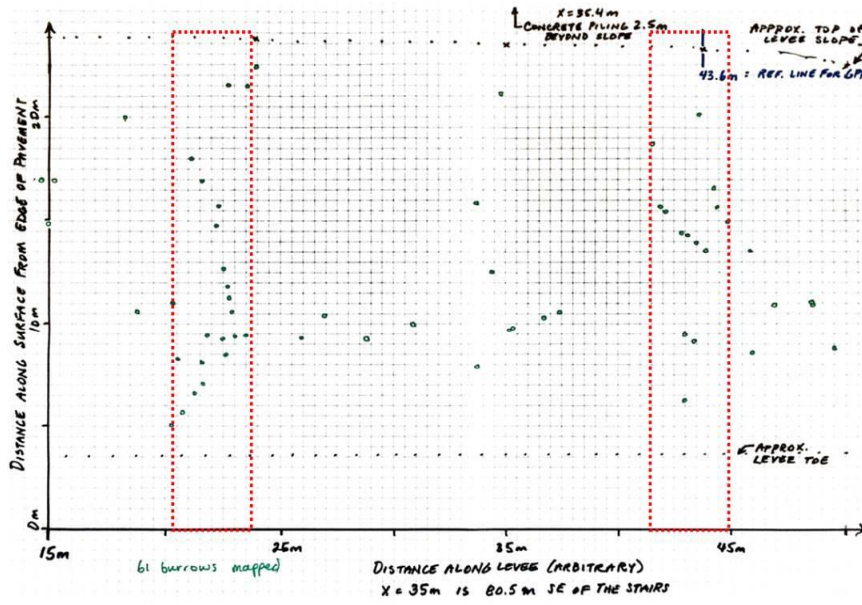


Figure 4.53. Indication of selected sections for the execution of overflow tests on burrows.

## 5 First survey of small burrows Prosperpolder (24 September 2021)

### 5.1 Context and objectives

The animal burrows survey on the Hedwigepolder levee provided various insights into the nature of small animal burrows and the techniques that can be used for their detection and characterisation, as well as clear suggestions of sections where overflow experiments could take place. One limitation of that first survey was that destructive tests could not be considered in the surveyed stretches, because they were reserved for overflow tests. Any other experiment that could damage or alter the reserved sections would influence the test plan of the overflow experiments, and for this reason it was avoided. In order to find a location to perform destructive tests, and more specifically grouting and excavation of a burrow system, another suitable levee section had to be identified.

On September 24th, 2021 a new survey was performed on the Prosperpolder levee. This time the team chose to go to the Belgian side of the living lab, as no other experiments were scheduled there. Apart from that, this could also create an opportunity to identify differences from the survey results on the Hedwige levee that may be the result of differences in the design and maintenance between Dutch and Belgian levees. The objectives of this survey are summarised below:

1. Identify a system of burrows that is suitable for the execution of a grouting and excavation experiment.
2. Validate conclusions of the previous animal burrows survey on the Hedwigepolder levee.
3. Find out if there are any differences between the results of this survey and the previous one that are caused by differences in the design and maintenance regime of the Dutch and Belgian levee.

### 5.2 Location and levee geometry

This survey was performed on the Prosperpolder levee, i.e. on the Belgian side of the living lab, in a distance of approximately 750 m SE of the Dutch-Belgian border (see also [Figure 5.54](#), left). This is section IV of the living lab, where overflow experiments were performed in March 2021. In particular a stretch of 80 m was surveyed on the landside slope starting from the southeast side of the last section that was tested against overflow in March 2021. In that location there is an asphalt road on the crest of the levee and no road at the landside toe that was the case on the Dutch side of the living lab (see [Figure 5.54](#), right).

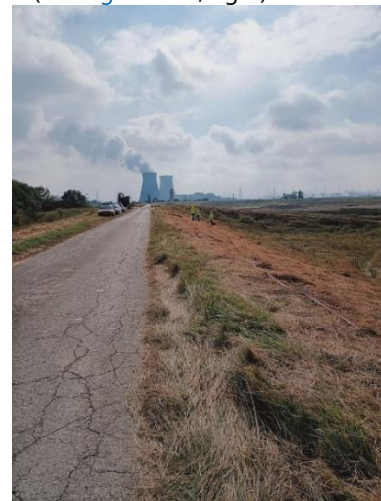


Figure 5.54. Left: Map indicating the location of the animal burrows survey on 24th September 2021. Right: Picture of the surveyed levee from the crest.

The last overflow experiment in March 2021 inflicted serious damage on the test section and it was covered with EPDM to prevent further erosion. The EPDM protection was still on the slope when this survey was performed (see Figure 5.55). Since EPDM is impermeable, the survey team expected that the covered slope would be totally dry, attracting animal activity in its surroundings. This is the reason that they chose to start the survey from that spot.



Figure 5.55. Left: Damage at the last levee section that was tested against overflow in March 2021. Right: EPDM protection covering the same damage, photographed in September 2021.

A typical cross-section of the levee at this location is shown in Figure 5.56. The average landside slope is 17° or approximately a 1:3.3 slope.

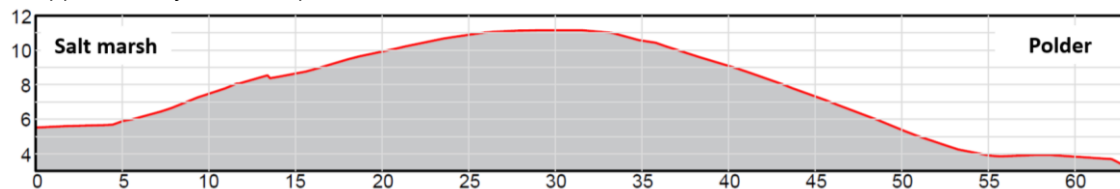


Figure 5.56. Typical cross section at the surveyed location

On the day of the survey only a 12 m-wide zone on the upper part of the landside slope was mowed (see also Figure 5.57). In comparison to the Hedwigepolder levee, vegetation on the prosperpolder levee is in general less homogeneous and contains a variety of species, including bushes with woody roots and trees. At the location of this survey there were no trees, but in the unmowed part of the slope a small number of young bushes could be seen.



Figure 5.57. Left: Impression of the surveyed levee segment illustrating the condition of its vegetation during the survey. Right: Layout of the surveyed area.

### 5.3 Work method

The survey was performed within one day and it was organized by HZ with a small team of participants. Animal burrows were detected by means of a visual inspection. The information was registered using App2C and by paper mapping, following the same procedure that was followed at the survey on the Hedwigepolder levee on 8th September 2021. The team surveyed in detail only the mowed part of a 80m-long levee segment, i.e.  $80\text{m} \times 12\text{m} = 960 \text{ m}^2$  on the upper half of the landside slope. Similarly to the survey on the Hedwigepolder levee, the reference point was selected on the NW boundary of the surveyed area on the level of the crest and at a distance of 1 m from the inner margin of the asphalt road (Figure 5.58, left). The closest fixed point on the levee to the reference point was a monitoring well at a distance of 81 m northwest of the reference point, whose coordinates are known (Figure 5.58, middle).



Figure 5.58. Left and middle: Position of reference point in relation to asphalt road and fixed point on the levee. Right: Fixed point 81 m NW of the reference point.

### 5.4 Execution and results

In total, 4 people participated in the activity (see also Table 5.10).

Table 5.10. List of participants

Name	Organisation
Vana Tsimopoulou	HZ
Yota Mingou	Waterschap Hollandse Delta
Karsten de Pauw	HZ
Lars van de Heuvel	HZ

The equipment that was used is listed in Table 5.11.

Table 5.11. List of equipment

Activity	Equipment	Owner
Detection of burrows	Probes	Polder2C's
	Fluorescent sprays (2)	HZ
	Rakes (2)	WHD
Digital registration of burrows	Smartphones with App2C installed	All participants
Paper mapping of burrows	Grid paper and pencils	HZ
	50m-long measuring tapes (4)	HZ
	5m-long measuring tapes (2)	HZ

In total 60 burrows were detected in an area of 960 m<sup>2</sup>, which is equivalent to 0.0625 burrows per m<sup>2</sup> or 0.75 burrows per linear m of levee. For every burrow details about its diameter, depth and its exact location on the reference system were recorded. The team was active on location for 5 hrs. There was no rain during the survey, but there was strong wind that made paper mapping slightly more difficult in comparison to the survey on the Hedwigepolder levee. This is because the tape that was layed on the crest at Y=0 of the reference area was dislocated several times because of the wind and had to be readjusted. Apart from this, the grass that had been mowed from the levee was still lying on the surface that was being surveyed, making it necessary for the team to remove it in order to detect burrows (see also [Figure 5.59](#)). Despite this difficulty, the time that was spent for completion of the survey and the working speed of the inspectors is comparable to the time and speed recorded in the previous survey on the Hedwigepolder levee.



[Figure 5.59](#). Impression of the surveyed levee segment before (left) and after (right) removal of mowed grass. Regarding the geometry of burrows, their diameters ranged between 2 and 7 cm while their depths between 2 and 30 cm, which are comparable to the dimensions measured on the Hedwigepolder levee. Yet a qualitative difference was observed this time; the clay on the top layer was much more dry and brittle than the clay layer on the Dutch levee, and loose clay could be seen lying around several detected burrows ([Figure 5.60](#)).



Figure 5.60. Loose clay (left) and sand (right) around detected burrows.

Quantitative information collected in this survey is summarised in Table 5.12.

Table 5.12. Summary of collected information

<b>Area surveyed</b>	<b>960 m<sup>2</sup></b>
No. of inspectors	4
Time needed	5 hrs
No. of burrows detected	60
No. of burrows per m <sup>2</sup>	0.0625
No. of burrows per m	0.75
Range of burrow diameters	2-7 cm
Range of burrow depths	2 - 30 cm
No. of burrows that reach the sand core	1

Comparing to the values collected in the survey of the Dutch levee, the most prominent difference is that in the Prosperpolder levee a burrow was detected with sand spread around it, which is evidence that the burrow reached the sand core of the structure (see also Figure 5.60, left). The maximum depth measured in the Prosperpolder levee is also slightly larger than that in the Hedwigepolder levee. For a more detailed comparison, the frequency of encountering burrows of a certain size needs to be considered. This is illustrated in Figure 5.61, where the exceedance frequencies of given diameters and depths of burrows on the Hedwigepolder levee and the Prosperpolder levee are contrasted. For the Hedwigepolder levee only burrows from stretch 2 are presented in the plot, because in stretch 1 detailed information on diameters and depths was not collected. The graphs show that burrows of the Dutch levee had in general larger diameters and depths.

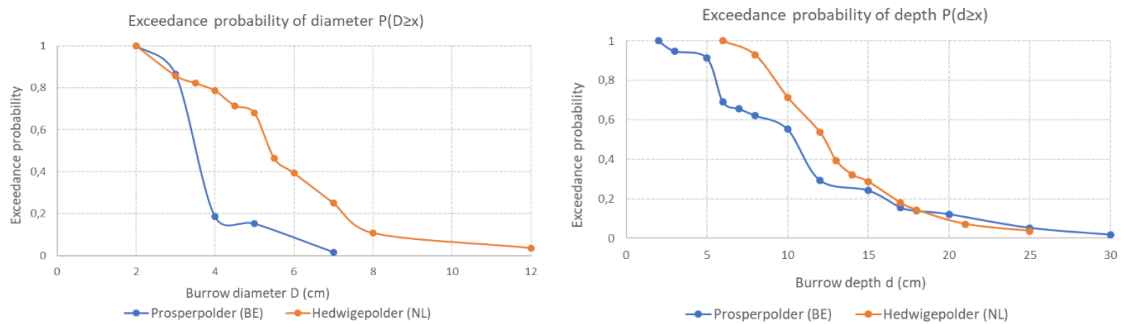


Figure 5.61. Contrast of exceedance probabilities of burrow diameters (left) and burrow depths (right) in the Hedwigepolder and the Prosperpolder levee.

The spatial distribution of the surveyed burrows is shown in Figure 5.62.

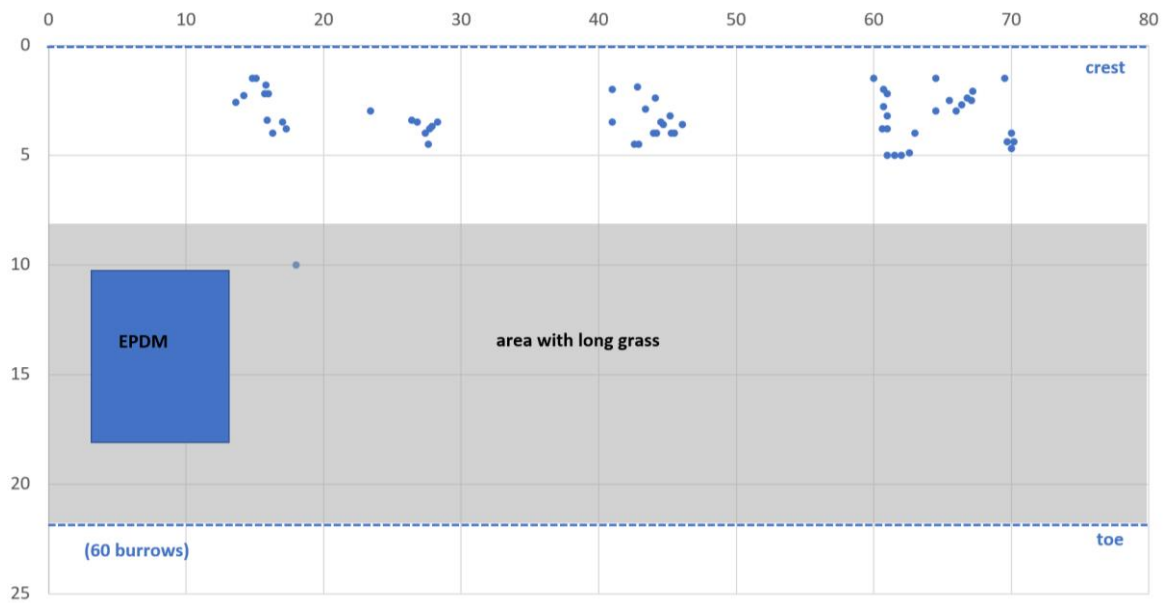


Figure 5.62. Spatial distribution of burrows in the surveyed levee segment.

Clusters of burrows, similar to those identified in the Hedwigepolder levee, can be clearly discerned there. Unlike the Hedwigepolder levee, linear patterns that characterise mole systems are not present. The burrow shown in the grey area was the only one detected in the unmowed part of the slope. The team looked at that area because much loose clay was spread around the cluster of burrows above that point, which could be attributed to an extensive burrow system under the surface; hence the team tried to see if there were any traces of a linear pattern. Although it would normally be unlikely to detect a small burrow in an area with long grass, the burrow was probably detected because there was loose sand around it, whose light colour was easier to see among the vegetation, as visible in Figure 5.63.



Figure 5.63. Left: Animal burrow with sand spread in the unmowed part of the levee slope; Right: Impression of vegetation surrounding the burrow. In the background the EPDM cover can be seen.

## 5.5 Concluding remarks

### 5.5.1 Selection of location for further animal burrows testing

Based on the outcome of this survey, a 6-8 m wide section adjacent to the EPDM cover on the SE side was selected for further investigation (Figure 5.64). This is the section that contains the burrow with sand at its periphery, which makes it clear that the local burrow system reaches the sand core of the levee.

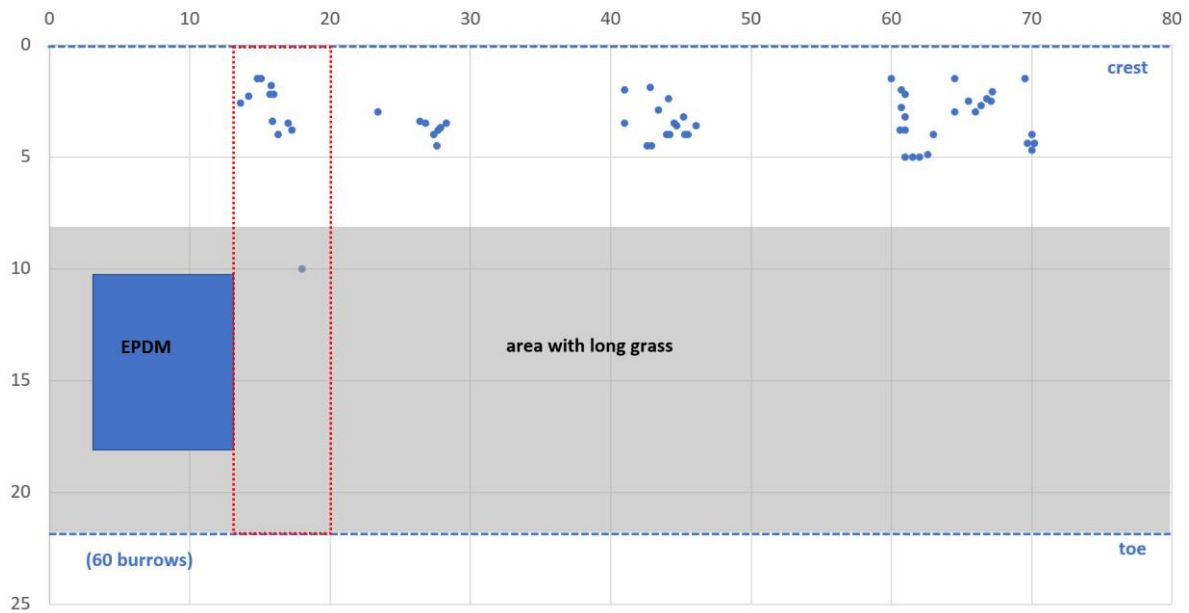


Figure 5.64. Red rectangle: area selected for further investigation.

#### 5.5.2 Comparison to results of the survey in the Hedwigepolder levee

1. Regarding the size of burrows, while on the Hedwigepolder levee burrows are on average slightly larger and deeper than on the Prosperpolder levee, the maximum burrow depth was detected on the Prosperpolder levee. It is also characteristic that on the Belgian levee a burrow was detected with sand at its periphery, which shows that the local burrow system penetrated the sandcore of the structure.
2. Regarding the spatial distribution of burrows, the density of detected burrows is comparable to that found in the previous inspection. Clusters of burrows, similar to those identified in the Hedwigepolder levee, could be clearly discerned. Unlike the Hedwigepolder levee, linear patterns that characterise mole systems were not identified. This may be due to the fact that on the lower half of the section there was long grass that did not allow a detailed visual inspection.
3. Regarding the visual inspection process, the speed of the inspection is comparable with that on the Hedwigepolder levee. It is worth mentioning that a burrow with sand at its periphery was detected on the part of the section with long grass. This shows that it is possible to detect burrows with distinct characteristics even in areas with longer grass.
4. A qualitative difference was observed between the Dutch and the Belgian levee that should not be disregarded in the comparison of results; the clay on the top layer on the Prosperpolder (i.e. Belgian) levee was much more dry and brittle than the clay layer on the Dutch levee. Apart from the soil consistency, the vegetation was also slightly different between the two locations, as on the Belgian levee more diverse vegetation was present, with more bushy plants with harder roots. A comparison and contrast of soil and vegetation data in the two locations could provide useful information for the definition of possible correlations between soil properties, vegetation and types of burrows.
5. It is known among the Polder2C's partners that there is a difference in the thickness of the clay layer between the Dutch and the Belgian levee. On the Dutch levee, the clay layer is 80-100 cm, while on the Belgian levee it is 30-50 cm (Depreiter et al. 2021). This allows making the hypothesis that rodent burrowing that reaches the sandcore is more likely in the Belgian levee than on the Dutch levee. This hypothesis is supported by the fact that a burrow with sand was found on the Prosperpolder levee and not on the Hedwigepolder levee, but it cannot be safely generalised. Further data collection in this direction is need.

## 6 Second survey of small burrows Prosperpolder (6 – 7 October 2021)

### 6.1 Context and objectives

Based on the survey results of the 24th of September, a section was selected on the Prosperpolder levee for a more detailed survey that would allow a new round of applications of non-destructive detection techniques, with collection of data that could be later compared to the results of a grouting experiment that was due on the same section on the 9th of October. This detailed survey was performed on the 6th and 7th of October 2021 and its objectives can be summarised as follows:

1. Repeat the smoke experiment with a new, improved experimental set-up and evaluate its feasibility and quality of its results.
2. Validate and expand conclusions about the feasibility, advantages and disadvantages of three survey techniques; visual inspection, ground penetrating radar imaging and the smoke experiment.
3. Establish the extent that deviations in the results between this survey and the one performed on the Hedwigepolder levee can be attributed to differences in physical characteristics and maintenance regimes between the Dutch and the Belgian levee.

### 6.2 Location and levee geometry

The main location for this activity is the same as in the previous survey and the exact area of focus is the section indicated in [Figure 5.64](#). An exception was made for the smoke test though, which was applied both at this location and the location of the mole system that was selected for testing against overflow on the Hedwigepolder levee (see also [Figure 4.53](#), burrows in the left hand side red square). The condition of the grass at the sections was the same as on the days that the sections were previously surveyed, i.e. 8th and 24th of September, respectively. The geometry of the sections can be seen in [Figure 4.38](#) and [Figure 5.56](#), respectively.

### 6.3 Work method

The survey started with paper mapping of the section with registration of information about diameters and depths of all burrows. As a reference point the upper left corner of the section was selected, in line with previously performed paper mappings. The reference point was directly adjacent to the EPDM protection. Subsequently the section was scanned with the ground penetrating radar using two different frequencies. The entire section was scanned in a low frequency, while two areas of higher interest were scanned in a higher frequency too.

In the end the smoke experiment was also executed with an improved set-up. In relation to the previous set-up, two key improvements were made (see also [Figure 6.65](#)); 1) The plastic hose was replaced by a rubber hose, and 2) the aluminium can was replaced by a larger metal barrel. The purpose of these improvements was prevent failure of the hose due to overheating, which was the case in the first trial of this experiment.



Figure 6.65. Improved setup for the smoke experiment.

#### 6.4 Execution and results

In total, 8 people participated in the activity (see also Table 6.13).

Table 6.13. List of participants

Name	Organisation
Vana Tsimopoulou	HZ
Stephan Rikkert	TU Delft
Robert Lanzafame	TU Delft
André Koelewijn	Deltares / STOWA
Xiaobing Wang	TU Delft
Mario van de Berg	TU Delft
Ammar Aljer	U Lille
Sarah NGUYEN Hoang Dung	U Lille

6.5 The equipment that was used is listed in Table 6.14.

Table 6.14. List of equipment

Activity	Equipment	Owner
Detection of burrows	Probes	Polder2C's
	Fluorescent sprays (4)	HZ
	Rakes (2)	HZ
	Pruners (3)	HZ
Paper mapping of burrows	Grid paper and pencils	HZ
	50m-long measuring tapes (6)	HZ
	5m-long measuring tapes (2)	HZ
Smoke test	Leafblower	TU Delft
	Barrel	TU Delft
	Smoke bombs (4)	TU Delft
	Hose	TU Delft
	Plastic buckets (2)	TU Delft
GPR scans of burrows	Georadar IDS Opera Duo	U Lille
	Georadar IDS RIS	U Lille

### 6.5.1 Paper mapping

Paper mapping was performed with a visual inspection. A 5m-wide section was inspected by 5 people from crest to toe. In order to make it possible to detect as many burrows as possible, the team had to mow and remove the grass on the day of the survey manually with gardening tools (Figure 6.66 left). Then the burrows were detected with probes and were marked with fluorescent sprays (right).



Figure 6.66. Left: The visual inspection team mowing and removing long grass before detection of burrows. Right: Detected burrows marked with fluorescent spray.

The total surveyed area is  $5 \times 21 = 105$  m<sup>2</sup>. In that area the team detected 64 burrows, resulting in 0.61 burrows per m<sup>2</sup> or 12.8 burrows per linear m of levee, which is considerably higher density than the density of detected burrows in the previous two surveys. This detection was completed within 1 hr (Table 6.15). The diameters of burrows were in the range of 1.5-6 cm, which is comparable to the range of burrow diameters in previous surveys. Their measured depths were between 5 and 39 cm, numbers that are also comparable with the numbers on the previous surveys. Yet the deepest burrow in this case is 9 cm deeper than the deepest burrow that was previously detected.

Table 6.15. Summary of collected information

<b>Area surveyed</b>	<b>105 m<sup>2</sup></b>
No. of inspectors	5
Time needed	1 hr
No. of burrows detected	64
No. of burrows per m <sup>2</sup>	0.61
No. of burrows per m	12.8
Range of burrow diameters	1.5-6 cm
Range of burrow depths	5 - 39 cm
No. of burrows that reach the sand core	1

The exceedance probabilities of diameter and depth occurrences are presented in Figure 6.67 (right). On the left hand side of the same figure, the spatial distribution of detected burrows is illustrated. It is clear in this illustration that burrows appear in clusters. Some areas on the grid seem to be densely populated by burrows, while other areas are clean. Regarding the linear patterns that were detected during the survey in the Hedwigepolder levee, it is difficult to identify them on the grid because of the high density of burrows. The linearity in the underground systems could only be verified with the grouting experiments that were performed later on the same section (see forthcoming relevant chapters).

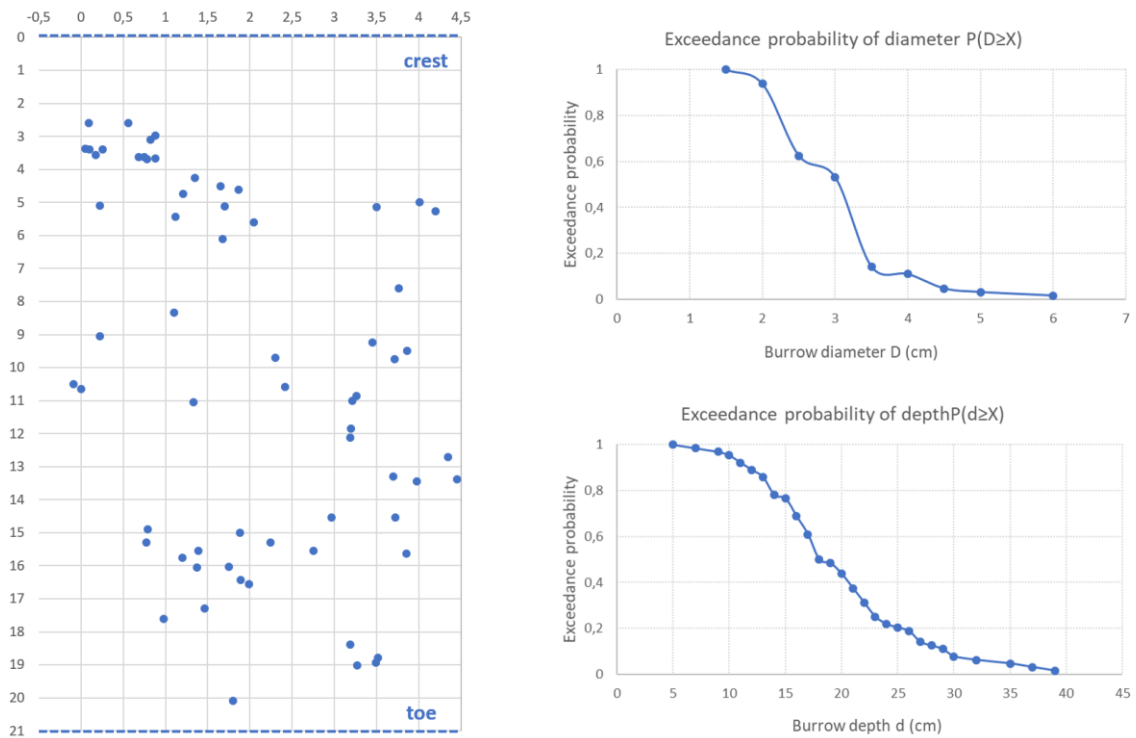


Figure 6.67. Left: Spatial distribution of detected burrows. Right: Exceedance probability of measured burrow diameters (top) and depths (bottom).

### 6.5.2 Imaging with Ground Penetrating Radar

The GPR measurements were taken in two frequencies; 2GHz and 400 MHz. Two zones with a relatively high density of burrows were scanned in 2 GHz frequency, while the entire section was scanned in the lower frequency (see also Table 6.16). The zones that were scanned in a higher frequency are shown in Figure 6.68 (left).

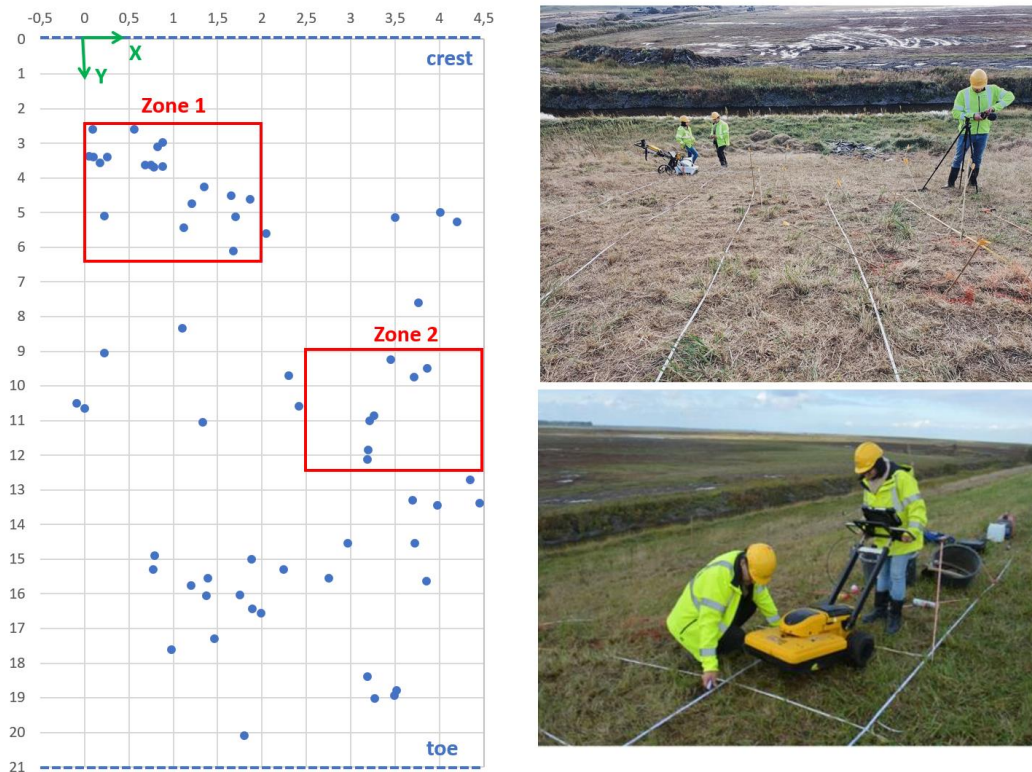


Figure 6.68. Left: Image indicating the reference point of the GPR grid (0,0) and the areas that were scanned in high frequency (i.e. Zone 1 and Zone 2). Right: Data collection with Ground Penetrating Radar.

Table 6.16. Details of executed GPR measurements

Grid location	Frequency	Grid size	Precision
Entire section	400 MHz	5 m x 21 m	1 m
Zone 1	2 GHz	2 m x 4 m	0.1 m
Zone 2	2 GHz	2 m x 3.5 m	0.1 m

For the zones that were scanned in high frequency, vertical transects were extracted in the X- and Y-direction with a distance of 10 cm from each other. Horizontal transects were extracted up to a depth of 50 cm from the surface, see Figure 6.69. These transects reveal the occurrence of cavities whose presence appears to be more prominent in the depth zone of 30-50 cm below the surface, illustrated at the three bottom transects of Figure 6.5. The depths of the burrows that were detected at this area by means of visual inspections were all in the range of 10-30 cm, which shows that similarly to the previous GPR survey on the Hedwigepolder levee (described in chapter 4), the depths that were measured with probes during the visual inspection were smaller than the ones detected with GPR.

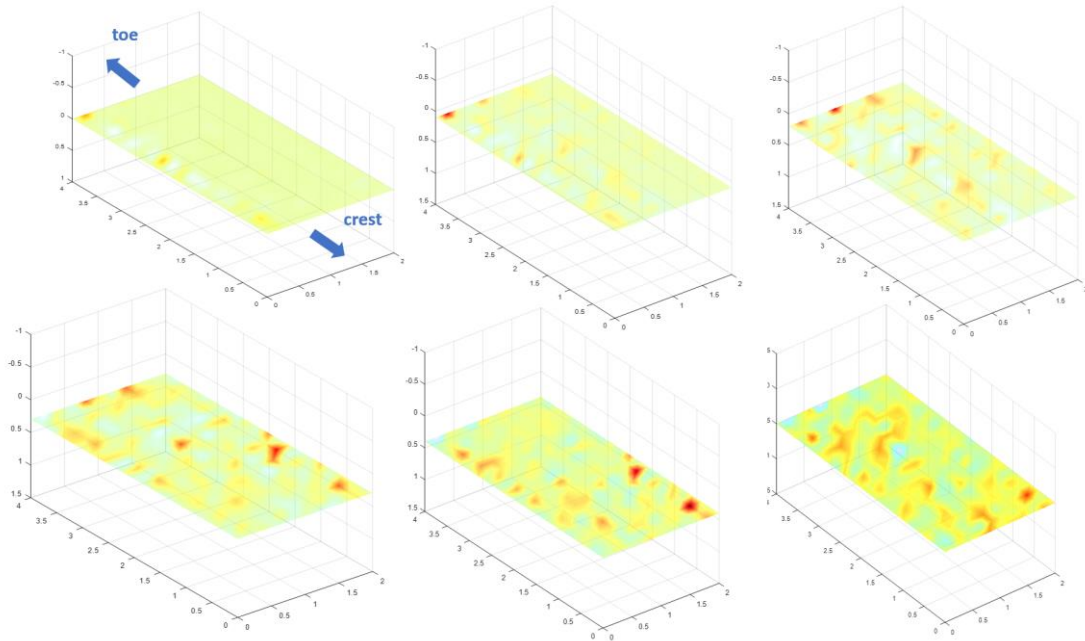


Figure 6.69. Horizontal transects in Zone 1 presented individually, starting from the level of the surface (Z=0, top left transect) to a level of 0.5 m depth (Z=0.5, bottom right transect).

After completion of the activity, a 3D image of the first 50 cm of the levee subsoil was created, by interpolating this dense network of images (Figure 6.70 - Figure 6.72). The red lines indicate areas occupied by air, which are discontinuities that could be attributed to animal activity. A casual observation of the cavities illustrated in red colour in the figures below and the density of burrows detected in zone 1 (see figure 6.4, left) make it clear that a dense system of cavities is located under an area where a cluster of small burrows was visible in the surface.

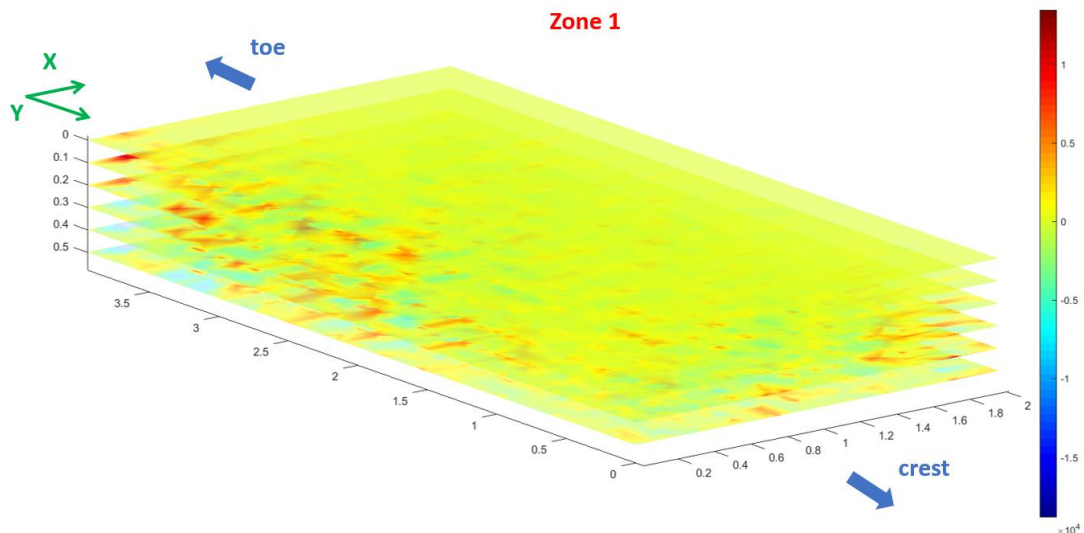


Figure 6.70. Composition of horizontal transects in Zone 1.

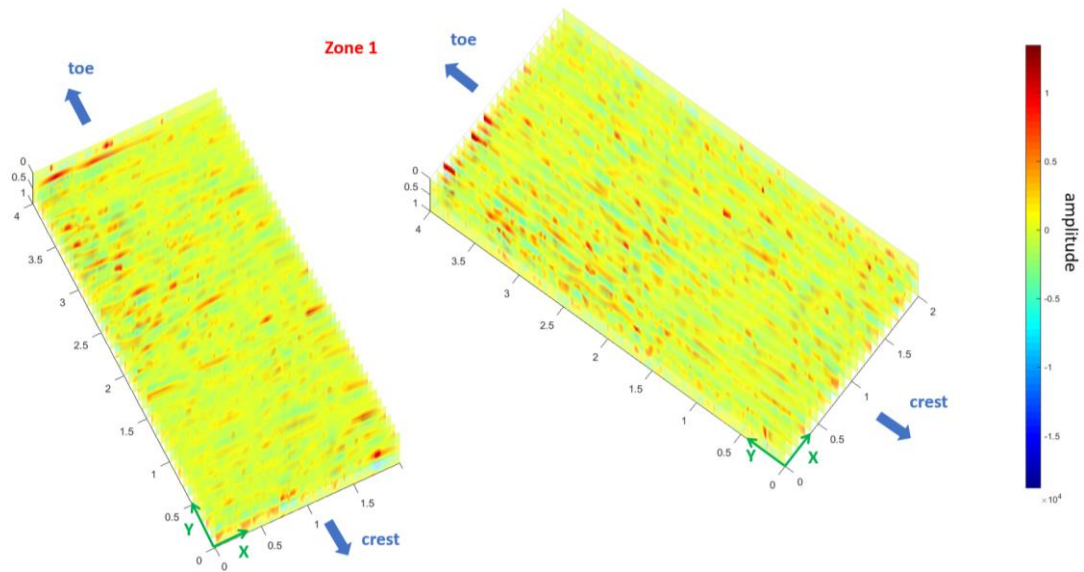


Figure 6.71. Composition of vertical transects in Zone 1 in X-direction (left) and Y-direction (right).

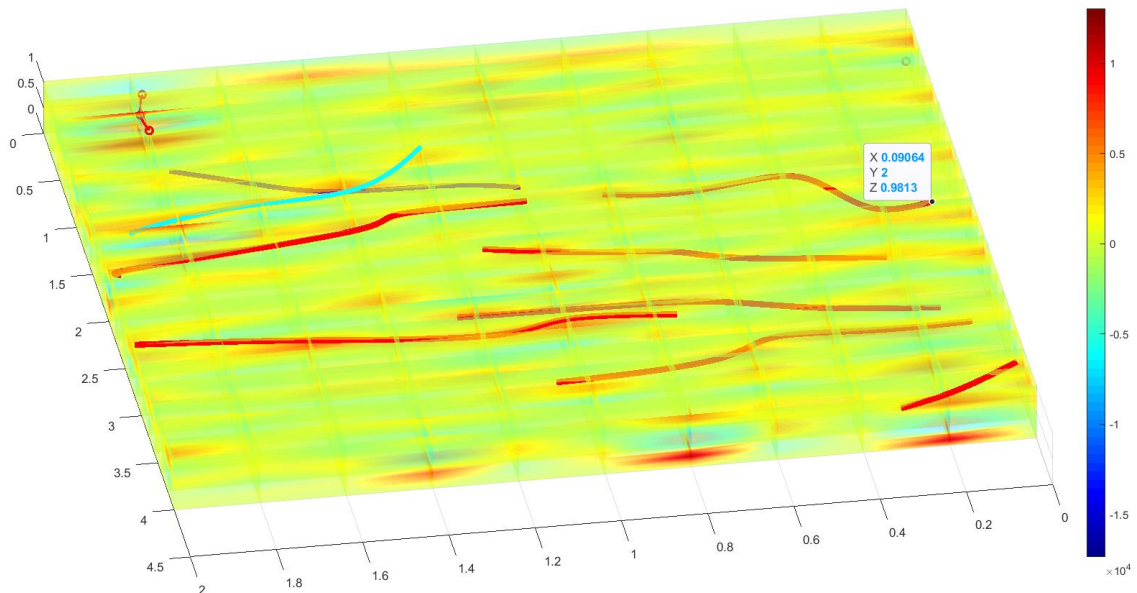


Figure 6.72. 3D image of the first 50 cm of levee subsoil, created by interpolation of horizontal and vertical transects in Zone 1.

### 6.5.3 Smoke test

The smoke test was first attempted at the cluster of burrows in zone 1 (Figure 6.68, left) without success. The injected smoke did not appear to be exiting the ground from other burrows. A second attempt was made at the cluster of burrows that was the closest to the toe (Y=14-18 m), with a successful result. Smoke was injected in one of the lowest burrows in the cluster (X=0.98 m, Y=17.6 m). Every time that smoke appeared coming out from a burrow, the burrow was covered with wet clay to block the exit and redirect smoke to other exit points in the system (Figure 6.73).

Smoke was witnessed exiting from 17 neighbouring burrows in total (see Figure 6.74). It is characteristic that in this trial of the smoke test, a number of burrows were spotted that had not been detected during the visual inspection. Apart from this, all newly detected burrows as well as a small number of exit points were located lower on the section than the entry point. This contradicts the initial expectation that burrows at higher points

than the entry points can be detected with this technique. Although it may still be more likely to detect burrows at higher locations with the smoke test, it is incorrect to assume that this is the only way to execute the test successfully.



Figure 6.73. Left and middle: Application of wet clay on burrows where smoke was witnessed. Right: Two burrows covered with wet clay.

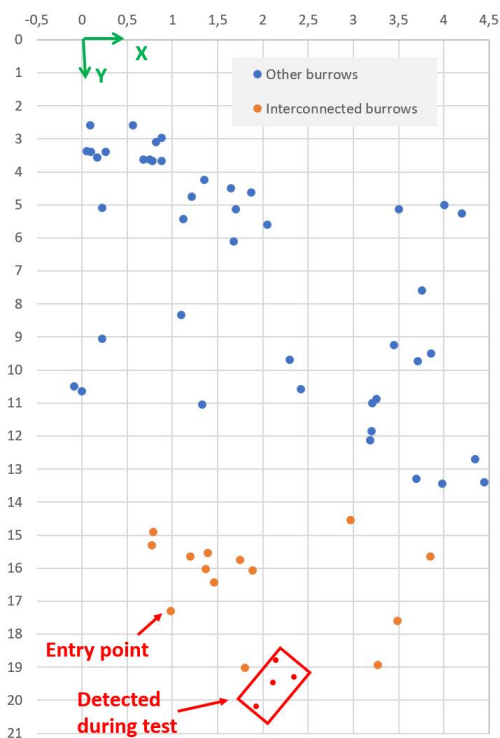


Figure 6.74. Left: Image indicating which burrows proved to be interconnected based on the outcome of the smoke test. Right: Execution of the smoke test (top) and evidence of red smoke exiting the burrows in the red rectangles (bottom).

Afterwards the team moved to the Dutch side of the living lab to repeat the smoke test on the section that had been selected for an overflow experiment with burrows, at the area where an animal burrows survey was executed on the 8th of September 2021. This was the left-hand side section of [Figure 4.53](#) (see also Depreiter, D. 2021). The smoke test indicated 8 interconnected burrows at this location ([Figure 6.75](#)).

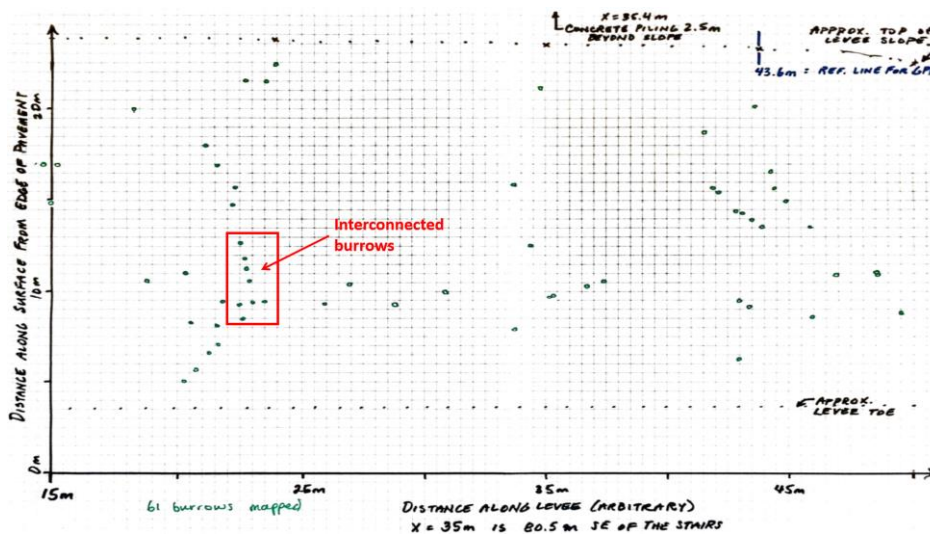


Figure 6.75. Smoke test result on the section where overflow testing with burrows had been planned to take place in November 2021.

### 6.6 EPDM influence on the density of burrows

The survey was performed at this specific location with the premise that the impermeable EPDM sheet that protected the adjacent section for more than 6 months may have caused excessively dry conditions at the soil that covered, inducing at that specific spot and its surroundings increased animal activity. The density of detected burrows during this survey in a 5m-wide section right next to the EPDM protection was considerably higher than the densities measured in previous surveys, which is a fact that supports the initial premise. During the survey, the team removed the EPDM sheet to inspect the soil underneath (Figure 6.76, left). The soil was indeed excessively dry, and it is characteristic that traces of increased animal activity were found. Upon removal the team witnessed an ant colony on the top of the soil that tried to find refuge elsewhere as soon as they were exposed to the open air. An area of about 50 x 50 cm was covered by ant eggs, that within 2min were transferred elsewhere by worker ants. Besides ants, the team witnessed a mouse running away. On the soil surface small holes could be seen that were connected by up to 1cm-wide channels in a high frequency (Figure 6.76, right). Based on the shape and frequency of those patterns, the hypothesis was developed that the patterns could have been burrow systems of small rodents that were excavated at the interface soil and the EPDM sheet. A rival hypothesis is that the patterns were just cracks that were created by the lack of water in the soil. To this end, further research is needed.



Figure 6.76. Left: Removal of EPDM protection. Middle: Impression of soil appearance after removal of the EPDM sheet. Right: Holes and channels on the soil surface that was covered with the EPDM sheet.

The team could not establish whether the EPDM protection played a role in the increased density of burrows that was discovered during this survey.

## 6.7 Concluding remarks

### 6.7.1 Smoke test

1. The smoke test worked well with the improved setup and illustrative results were provided in two locations. Further testing in other locations and in different weather can provide insight into the conditions under which the technique is most effective.
2. Although the smoke test worked well in the cluster of burrows close to the toe, it did not work in the cluster of burrows close to the crest (see Zone 1 in figure 29). Zone 1 was used to perform a grouting experiment the day after (see also next chapter) which proved that the burrows in that spot were interconnected. This shows that there are probably factors that can affect the result of the smoke test. Based on the available information, a possible explanation for this deviation in the outcome between the two tested clusters is the water content in the soil. The day that this survey took place there was heavy rain in the morning that later stopped and the sun came out. The temperature was about 20°C. During the heavy rain the upper part of the section was mowed while the lower half still had very long and dense vegetation, which may have prevented water from infiltrating the ground.
3. Although the new setup works well, the size of the barrel makes the installation less easy to transport. This would probably make it inconvenient for testing in regular levee inspections. It would be therefore beneficial to consider replacing it with a smaller container. Since the plastic hose was also replaced with a rubber hose, it is possible that a smaller barrel can still prevent overheating of the installation.
4. During the successful trial of the test on the Prosperpolder levee, a number of burrows were spotted that had not been detected during the visual inspection. This illustrates how the smoke test can be complementary to visual inspections.
5. During the successful trial of the test on the Prosperpolder levee, a number of exit points were located lower on the section than the entry point. This contradicts the initial expectation that only burrows at higher points than the entry points can be detected with this technique.
6. Further research and feedback from biology experts is necessary in order to ascertain how the technique can be used in a manner that is safe for the animals.

### 6.7.2 Ground Penetrating Radar

1. A dense network of horizontal and vertical transects was collected, whose interpolation led to a reasonably accurate 3D illustration of the first 50 cm of soil from the surface of the levee. The level of precision that was chosen for the data collection made it possible to successfully discern discontinuities that could be attributed to animals. To this end further comparison and contrast of identified patterns with the collected visual inspection data and the results of the forthcoming grouting experiment is needed. Yet the data GPR images reveal a dense network of cavities in an area where a relatively dense cluster of burrows had been identified with a visual inspection, pointing to the fact that areas that small burrows are clustered together can be easily erodible.
2. The GPR does not allow the production of an equally detailed image of the subsoil in depths beyond the first 50 cm from the surface. Images of larger depths can only be extracted in lower GPR frequencies. The entire section was also scanned in lower frequency, but the results have not been analysed so far. An analysis of information collected in lower frequency can show to which extent traces of burrows can be discerned in the images.
3. The weather was sunny at the time that the measurements were taken, but it had rained heavily earlier on the same day. Although the quality of GPR images is influenced by water content on the ground, the extracted images were of satisfactory quality.

### 6.7.3 Spatial distribution and geometry of burrows

1. The diameters and depths of burrows measured during the visual inspection are comparable to the diameters and depths that were collected in the two previous surveys on the Hedwigepolder and the Prosperpolder levee, but the density of burrows was much higher in this location.
2. The high density of burrows is the outcome of increased animal activity that could be due to the presence of EPDM protection right next to the surveyed section. Although there are facts that support this theory, no real evidence of causality was found in the field. Further research is needed to ascertain this relation.

## 7 Grouting experiments on the Prosperpolder levee (October 2021 & February 2022)

*This chapter partly reproduces content that was previously published by Johannes Idsinga in the framework of his minor thesis in TU Delft (Idsinga, 2022). The content has been reproduced with the author's consent.*

### 7.1 Context and objectives

On the 6<sup>th</sup> and 7<sup>th</sup> of October non-destructive monitoring techniques were applied on a levee section in Prosperpolder, which revealed a dense system of animal burrows that also proved to be partly interconnected. In order to inspect the exact geometry and dimensions of the underground system, two clusters of burrows on that same section were grouted with concrete and later excavated on the 9<sup>th</sup> of October 2021 and on the 8<sup>th</sup> of February 2022. The objective of this activity was to compare its results with the results of the previously applied techniques, i.e. GPR imaging, paper mapping and the smoke test.

### 7.2 Location and levee geometry

The location was the same as in the previous survey (see chapter 6).

### 7.3 Work method

By pouring a small-grained grout with slightly excess water into burrow holes and excavating this when the grout has solidified, the exact course of burrow system can be identified, which is the main goal of these experiments, carried out on the 7<sup>th</sup> of October 2021. Furthermore, the excavated burrow system can serve as a reference to assess the accuracy of the other detection methods. For instance, in case the GPR scan shows a certain burrow tunnel at one location, the excavated grout could confirm this and say something about the discrepancy in size or location of the tunnel in comparison to the GPR scan.

The burrow holes that were previously marked and identified on the same coordinate grid as used to make the GPR scans, were filled with a total of 20 liters of grout, spread over the 63 burrow holes that were found on this 4 meter wide stretch of the levee. Figure 7.77, left, shows the process of filling a burrow hole with the grout mixture and Figure 7.77, right, indicates the final result, after all burrow holes have been filled up.



Figure 7.77. Left: Filling a burrow hole with grout. Right: Numerous grout-filled burrow holes on the coordinate grid.

## 7.4 Execution and results

### 7.4.1 Initial excavations

During a small session of the winter school on October 9<sup>th</sup>, where students of the HZ University of Applied Sciences could get familiar with the living lab and participate in activities on the effect of animal burrows on the erosion resistance of levees, a few of the grouted burrow holes were excavated (Figure 7.78). The groups used garden tools to dig in the vicinity of the marked burrow holes to aim and follow the grouted system as accurate as possible. Excavations took place close to the levee crest, and specifically at Zone 1 of the GPR scan that was performed the day before (see also figure 6.4., No GPS measurements were taken to allow the extraction of detailed information about the exact shape and orientation of the excavated burrow system. However casual measurements of the depth in which concrete was found showed that the concrete was found in the of range of 25-50 cm depth from the surface. This is very much aligned with the depths where cavities could be seen in the results of the GPR measurements at the same location, which was in the depth zone of 30-50 cm from the surface (see figure 6.5). Most of the concrete appeared to be shaping one piece, which shows that most burrows in this zone were interconnected and were probably leading to the same den. Unlike the grout that was excavated at the location of the rock bags installation in June 2021 (see also figure 1.2b), the grout at this location did not have a linear shape, but rather an indented shape, which shows that a different type of animal created this burrow system. While the one excavated in June was attributed to a mole, this one was attributed to mice. Comparing this irregular shape of the grout and the coloured shapes that illustrate cavities in the GPR transect at a depth of 45 cm in figure 6.5, it is clear that irregularities of the cavity shape is captured well by the GPR scan.



Figure 7.78. Excavations during the winter school session on October 9<sup>th</sup> 2021

### 7.4.2 Second experiment session (8<sup>th</sup> and 9<sup>th</sup> of February 2022)

This batch of experiments was again carried out by a team from TU Delft, HZ University of Applied Sciences and Deltares. The following subsections describe the procedure of the experiments that took place those two days.

Similar to the excavations on October 9<sup>th</sup>, garden equipment was used to excavate a large part of the grouted burrow system, which was grouted during the first batch of experiments on October 7<sup>th</sup>. On the 8<sup>th</sup> of February, a group of approximately 10 people started digging out the grout around the marked burrow entrances. The unpredictable nature of the burrows made it relatively hard to accurately follow the burrow system through the soil and the fact that the grout became highly brittle and sometimes hard to distinguish from the soil with the naked eye, caused damages to the grouted burrows. In practice, grouted burrow parts were often found piece by piece and in most cases the trail was lost after a while. On the second day, the 9<sup>th</sup> of February, a smaller group of 6 people continued following the traces from the previous day and eventually, in 2 areas of the levee, intact burrow tunnels were found. One of which is located towards the toe of the levee, and connected to a large chunk of grouted material on top of the levee surface, this was a location where a lot of grout poured out during the grouting of the holes on October 7<sup>th</sup>. The tunnels that were found were relatively long, in the order of a few meters and consisted of branches, making up a tunnel system with a diameter of a

few centimetres, characteristically made by moles. Images of this burrow system can be seen in Figure 7.79. The excavated burrows that are visible in the left-hand side image are connected to those visible in right hand side image of the same figure. It is important to note that in this excavation it was clear that the grout had reached the sand core of the levee.

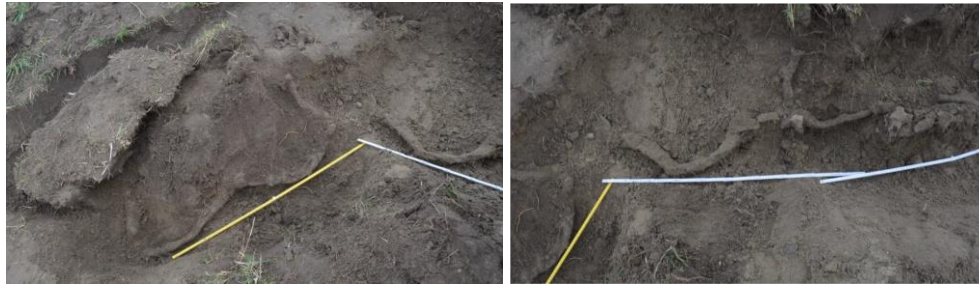


Figure 7.79. Part of the excavated mole burrows.

Further up the slope, towards the crest, a small system of dense tunnels was found, assumed to be connected by small chambers which is characteristically made by mice (Figure 7.80). The mole burrow system was later scanned by the LiDAR and the location of interesting points on the grouted system was measured using RTK-GPS scanning.



Figure 7.80. Excavated mice burrow system.

#### 7.4.3 RTK-GPS scans

As previously mentioned, the coordinates of points of interest of the excavated burrow systems were scanned using Real Time Kinematic (RTK) measurements. RTK measurements use phase delays of signals between satellites to accurately determine the location of the rover. It returns the x, y and z coordinates in the Dutch Rijksdriehoek coordinate system. The accuracy of the RTK locations are in the order of 1 – 2 centimeters (Utiugova, 2021).

Apart from the excavated burrow systems, the coordinates of some of the grouted burrow holes were scanned before the excavations took place. The aim of the RTK measurements is to determine the exact locations and thereby to facilitate the mapping of the different datasets as well as to assess the accuracy of manual inspection and mapping of the burrow holes on the levee slope.

In some instances, the points of interest that were measured by the RTK were photographed and the measurements were given a name, so that the RTK measurements could be linked with the LiDAR scans. The analysis afterwards turned out to be more complicated than foreseen, yet at several locations points before and after excavation were rather close, and an estimation of the excavation depth was easily possible.

All point measured, except those near the crest, are shown in Figure 7.81. The labels indicate the height above the Dutch reference datum (NAP) in mm.

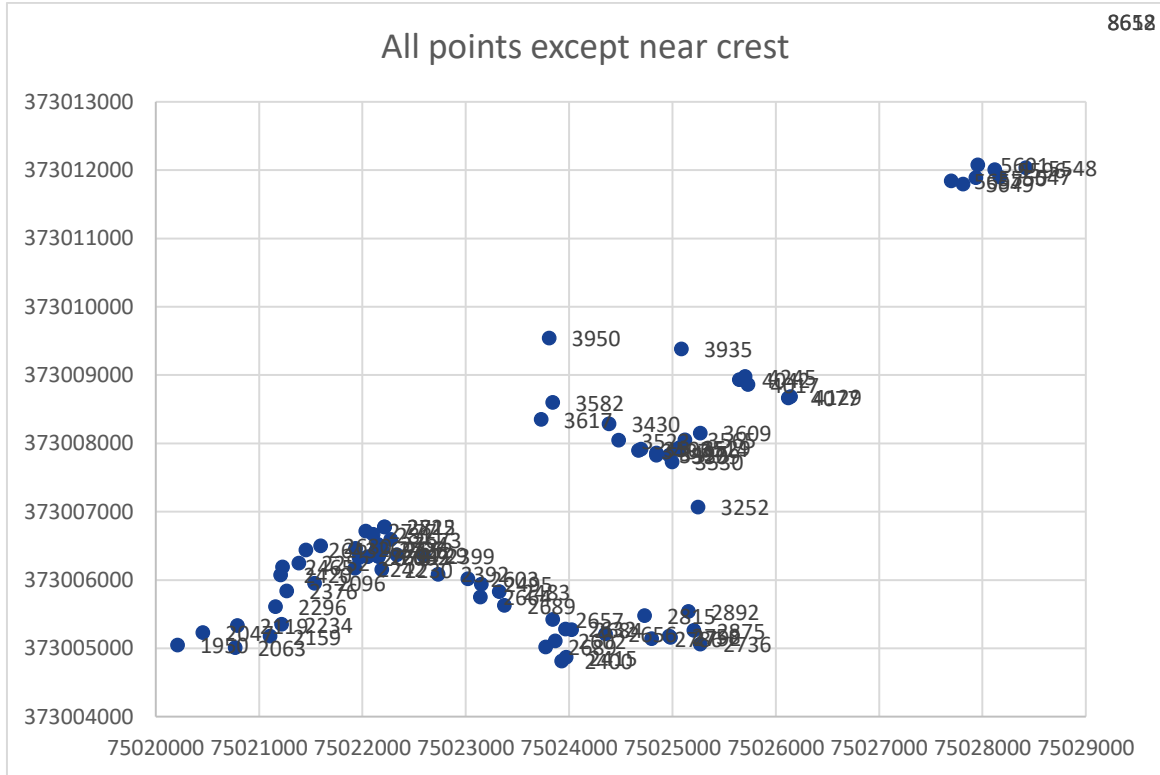


Figure 7.81 All RTK measurements except the points near to the crest.

Figure 7.82 shows a zoomed plot of the points in the middle of the previous figure. The label '4245', rather on the right of this figure, refers to the main point of entry of the animal burrow that consumed a lot of grout while pouring the grout. The two points close to this point have been measured after excavation and these are over 20 cm lower.

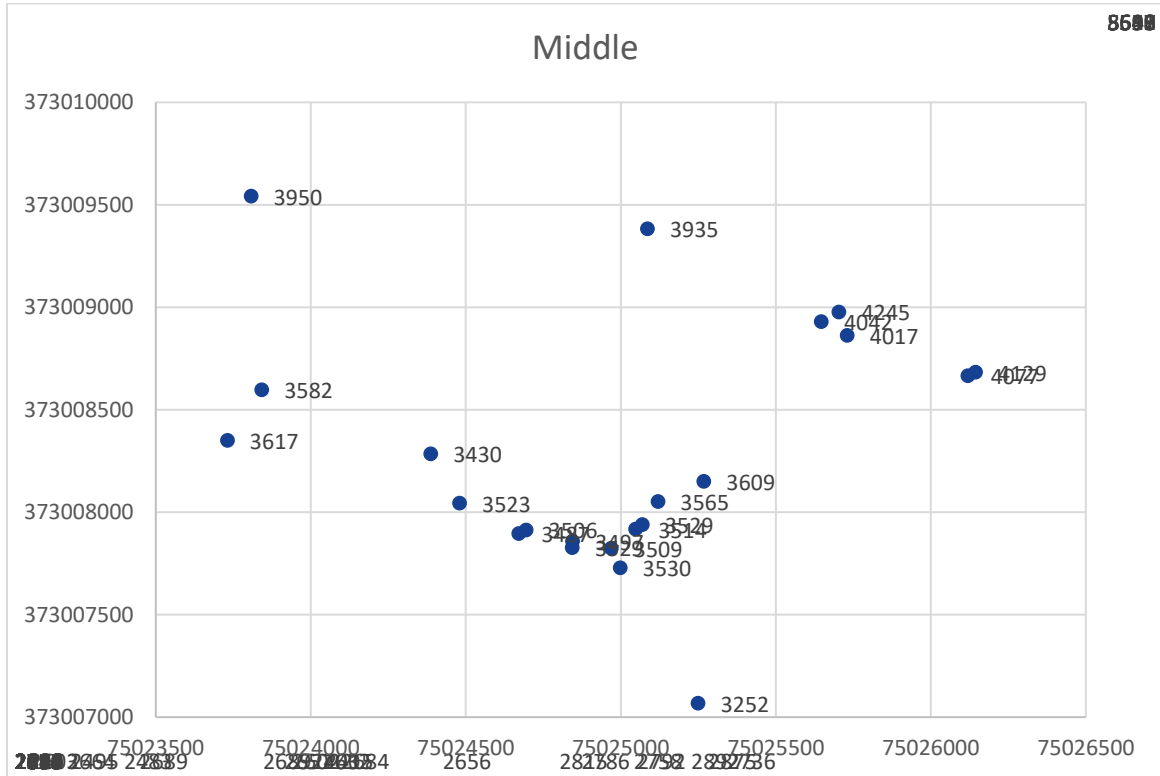


Figure 7.82 RTK measurements in the middle of the excavated area.

Similarly, Figure 7.83 shows the points in the lower left corner. To the right, the pairs of points are related to an intermediate excavation phase and the final depth. No initial level was measured here, as there was no burrow exit here. By reconstructing the slope, the total excavation depth can be estimated. In short, further analysis of this data still seems possible.

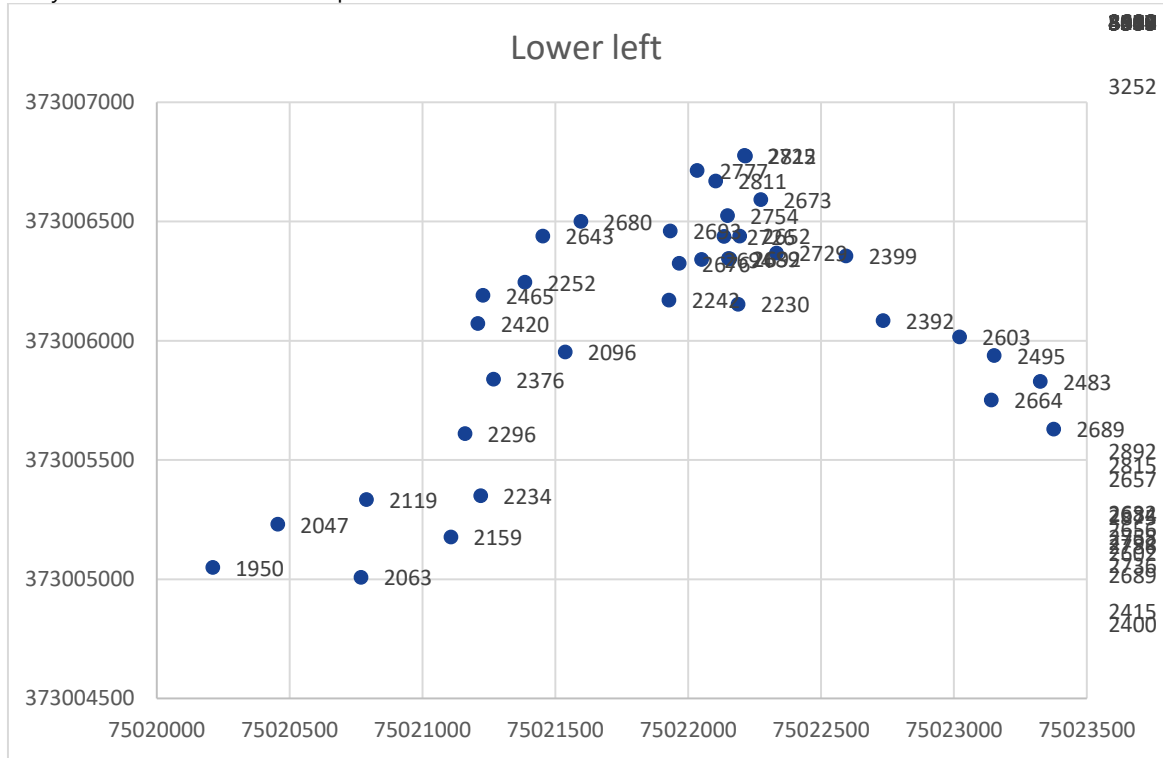


Figure 7.83 RTK measurements in the lower left part of the excavated area.

In Figure 7.84, the locations of the RTK points are compared with the grouting and smoke experiment data.

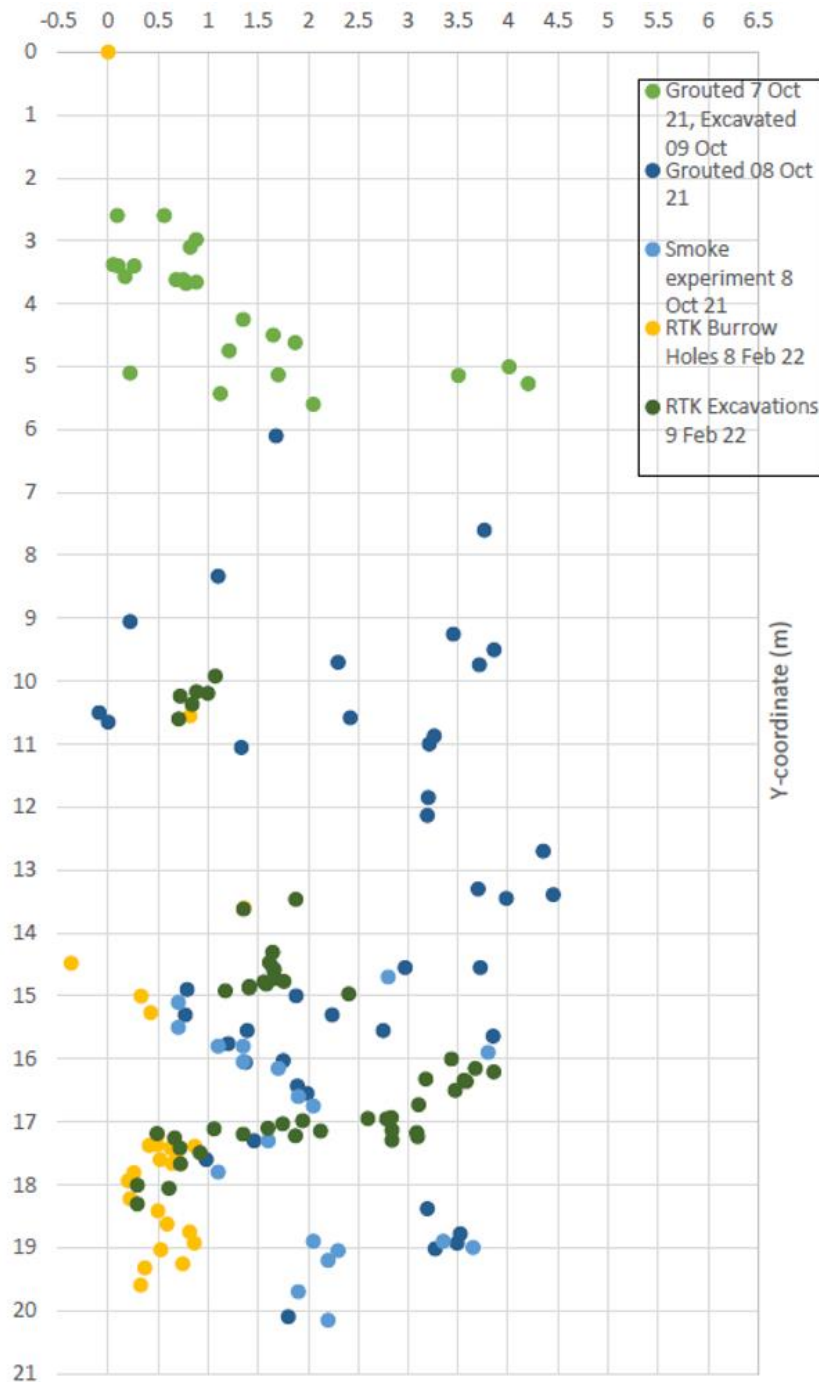


Figure 7.84. Combining the RTK data points with the grouting and smoke experiment data.

#### 7.4.4 LiDAR scans

Light Detection and Ranging (LiDAR) scanners use lasers to evaluate distances and depth. Every laser scan creates one point and all of these millions of points combine into an accurate 3-dimensional image of the excavated burrow systems. In total, 4 different scans were made using the LiDAR scanner built into the iPad. The goals of these scans is to facilitate the mapping of the excavated areas.

Several LiDAR scans have been made on the 9<sup>th</sup> of February and the software CloudCompare is used to process these scans. Figure 7.9 (right, top) shows the full excavations that have been carried out that day with the RTK data points added on top. The RTK coordinates are aligned to the LiDAR scans by taking 3 datapoints from which the location is most accurately known from pictures taken during the excavation on Feb 9th and using the registration tool called 'Align (point pairs picking)'. For this procedure, the points labelled Robert 1, Robert

2 and Robert 9 were used as they were most easily recognisable on the LiDAR scan. The grouted burrow system is best visible in the stretch of data points which are labelled 'Robert 1' till 'Robert 11', as shown in Figure 7.85 (right, bottom).

Post-processing and analysis of these scans are made using the open-source software CloudCompare, the full scan of the total excavated area consists of approximately 7.5 million data points.

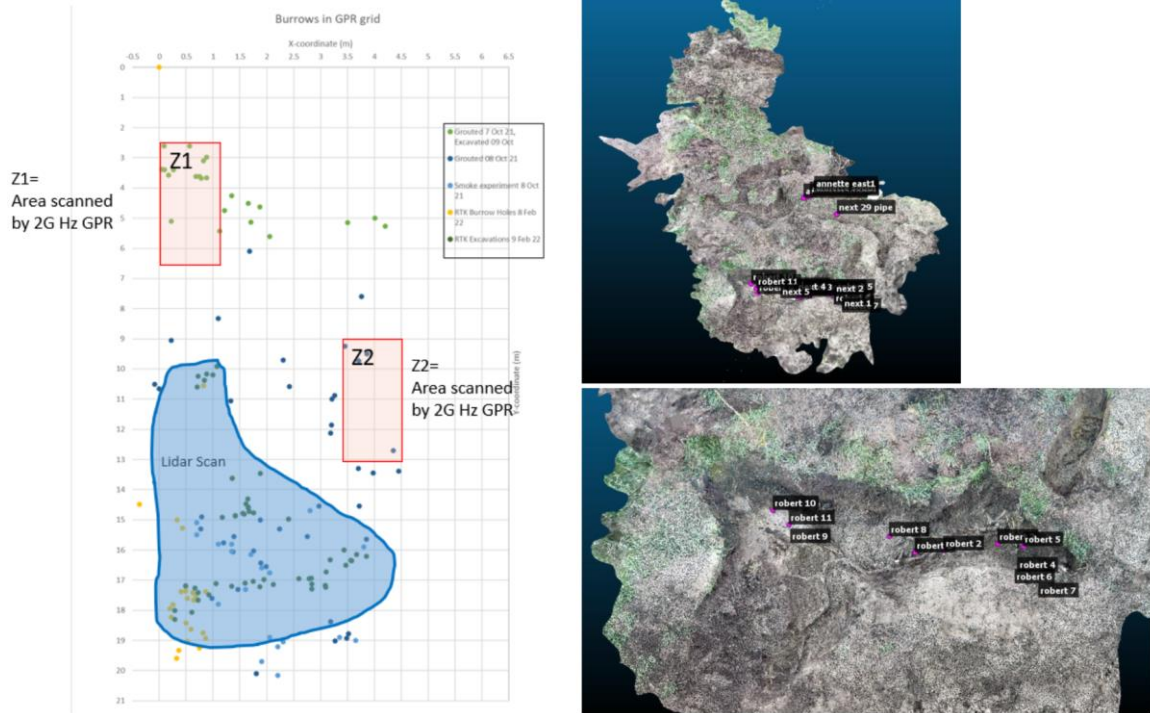


Figure 7.85. Left: Full map of all data points, highlighting the areas scanned by GPR in red and LiDAR in blue. Right: LiDAR scan of the full excavated area (top) and LiDAR scan of most detailed stretch of excavated burrow (bottom).

### 7.5 Concluding remarks

This chapter presents data collected through grouting clusters of small burrows that were previously surveyed with visual inspections, the smoke test and GPR. A preliminary comparison was made between the grout that was excavated in Zone 1 and the GPR images that were collected there. The comparison shows that the depths in which the grout was found, are very much in line with the depths where cavities were registered by the GPR signal. It is also evident that the GPR has approximated well the indented shape of the grout. This is an indication that GPR is a suitable technique to detect the depth and approximate shape of cavities created by small animals like mice and moles. A more systematic comparison of the results obtained by the various techniques is recommended.

## 8 Overflow experiments on section with animal burrows (Nov-Dec 2021)

### 8.1 Context and objectives

During the execution of overflow experiments in November and December 2021 insights were collected about the influence and management of animal burrows. One section with an underground system of mole tunnels was tested aiming at filling in previously identified knowledge gaps on the topic, but findings were also collected in a less coordinated manner during other overflow experiments. The entire series of overflow experiments took place at the Hedwigepolder levee, at the same location where the survey of small burrows had taken place on 8 September 2021 (see also chapter 4). It is important to note that the activities that were undertaken during the overflow experiments could provide insights into a small fraction of the knowledge gaps that had been previously identified on the topic. Due to planning limitations, only one levee section could be dedicated exclusively to questions on this topic, the aforementioned section with the mole tunnel. For this reason the team tried to increase the experimental output by creatively combining activities in a manner that allowed to collect insights into various questions. The learning objectives of those activities are summarized below:

1. Observe if and how animal burrows influence surface erosion during overflow.
2. Test feasibility of electric resistivity tomography (ERT) as a technique for monitoring the influence of overflow in subsurface erosion during testing.
3. If ERT proves feasible, monitor internal erosion patterns through observation of the evolution in the geometry of burrows during overflow.
4. Test feasibility and effectiveness of a low-cost technique for temporary protection of the mole system with the use of road plates.

Apart from the abovementioned primary objectives, a number of additional activities were undertaken with the following additional objectives:

5. Compare the results of the ERT scans with GPR scans at the same location.
6. Refine the test installation of the smoke experiment.
7. Observe erosion patterns around an artificial burrow.

The above objectives were pursued during three different overflow tests, which have already been introduced in the Polder2C's overflow test plan for the winter 21-22 (Depreiter 2021) and are described in more detail in the fact sheets of overflow tests. These sections are referred to as N-OF09, N-OF03 and N-OF04. The table below indicates which objectives were pursued in each experiment.

It should be noted that an overflow test was also performed on a section where a large rabbit hole was detected. This test is not included in this report, but its results are presented in detail in Depreiter et al. 2022b.

Table 8.1. Overview of levee sections tested against overflow where objectives related to animal burrows were pursued.

Overflow test code	Date	Brief description	Objectives
N-OF09	26-29/11/22	Section with mole burrow system	2, 3, 4, 5, 6
N-OF03	7-8/12/22	Reference section	7
N-OF04	16-17/12/22	Second reference section	1

## 8.2 Locations and levee geometry

The locations of the three sections are shown in the figure below (left). All three sections are on the Hedwige polder levee. Section N-OF09 is within the area where animal burrows were surveyed earlier and where an extensive system of mole burrows had been detected on 8<sup>th</sup> September 2021 (see also chapter 4). The existence and the extent of the mole system was verified on the 6<sup>th</sup> of October with the smoke experiment (see also chapter 6, Figure 6.74 and Figure 6.75).

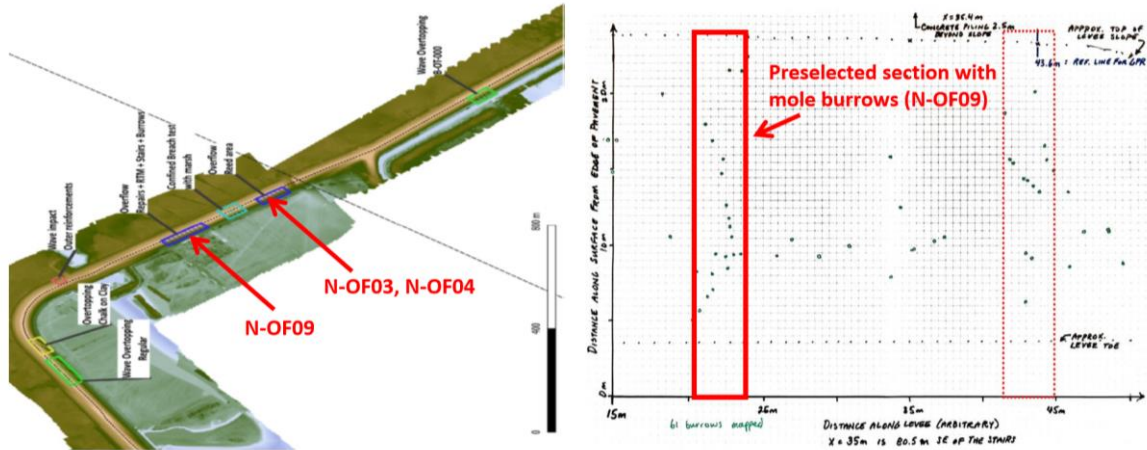


Figure 8.1. Left: Digital terrain model of the area where overflow experiments took place in November-December 2021 with the locations of the burrows test sections indicated. Right: Animal burrows map at the location of test section N-OF09.

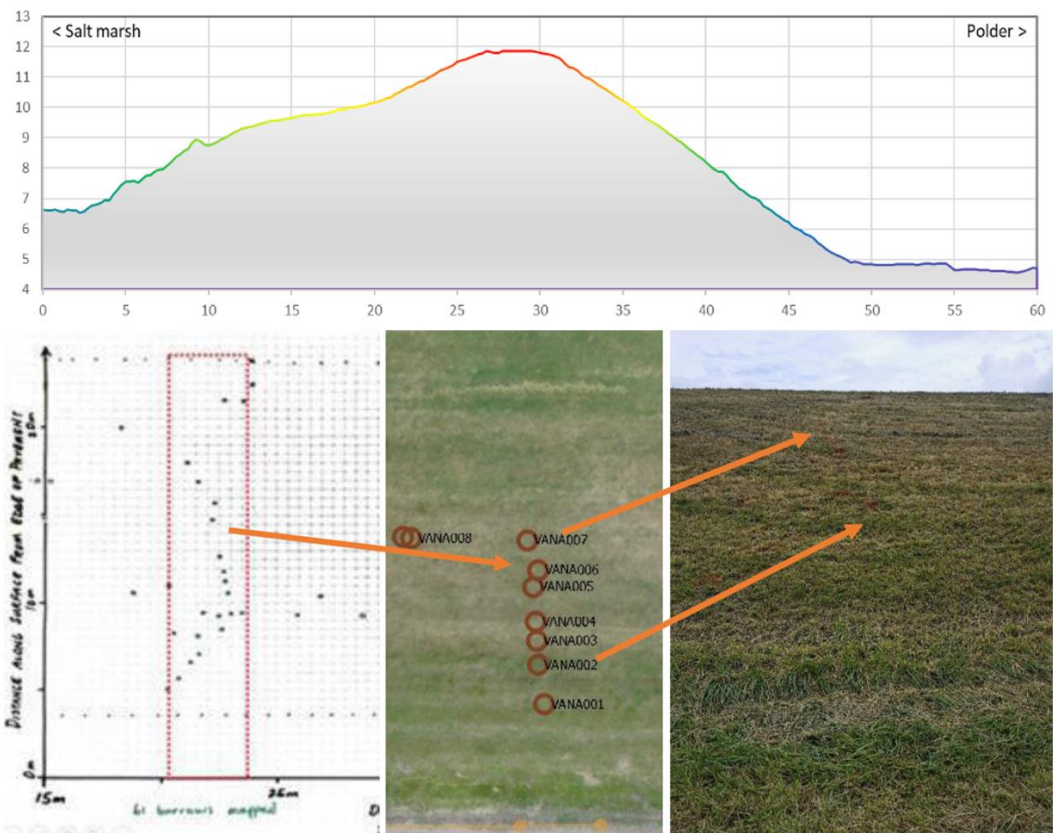


Figure 8.2. Top: Cross section at the location. Bottom: Animal burrows map at the same location with the selected burrows section highlighted.

### 8.3 Activities in section with mole burrows (N-OF09)

Three key activities took place on this section; 1) GPR scanning of the mole tunnels before the overflow test, 2) Installation of ERT cables and monitoring of subsurface erosion during the overflow test, 3) Installation of temporary protection with road plates and monitoring of its performance during the overflow test.

#### 8.3.1 Preparatory work

The first step in the preparation of activities in section N-OF09 was to choose the exact borders of the 2m-wide test section. Four areas of interest were defined, based on the burrows that had been detected and monitored in that location (see also figure 8.3):

- Area 1: Cluster of burrows that seems to be disconnected from burrows in areas 2 and 3.
- Area 2: Burrows that seem to be part of the mole pathway. The smoke test that was performed here did not prove interconnectedness with the rest of the burrows in area.
- Area 3: Cluster of interconnected burrows. Their interconnectedness was proven with the smoke test.
- Area 4: Burrows outside the test section that seem to be part of the mole pathway.

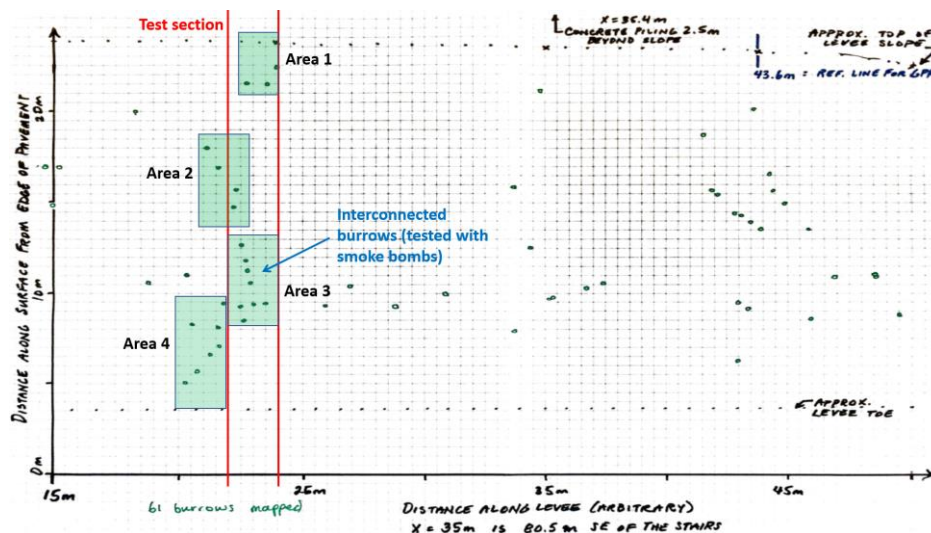


Figure 8.3. Top: Borders of test section N-OF09 and areas of interest that were defined in the process of positioning the test section.

The exact location of the test section, which is also shown in figure 8.3 was chosen in a way that as many detected burrows as possible would be within the section, and at the same time the entire cluster of interconnected burrows, i.e. area 3, would be inside the section too. A large number of burrows provided more opportunities to observe erosion patterns in their vicinity during the overflow experiment, while the interconnected cluster of burrows provided the opportunity to test an area that the team assumed to be weaker than an area without discontinuities, based on the experiences with overflow tests B-04 and B-11, that presumably failed because of animal burrows (Depreiter et al., 2022b).

The next step was to choose the parts of the test section where ERT monitoring would be applied, and where the road plates would be placed. For both of them area 3 was considered the most interesting because its burrows were interconnected. The length of the ERT cables allowed to extend monitoring to the burrows of area 2 as well. The road plates protection could also be extended to the burrows of area 2 as they appear to be relatively close to those of area 3 and conveniently situated for application of the plates (see also section 8.3.4). Regarding the GPR scanning, area 3 was scanned in a high frequency to allow comparison with the ERT

results, while the entire section was scanned in a lower frequency. An overview of the activities performed per area is given in the table below.

Table 8.2: Overview of activities per area of interest.

	Test section	GPR scanning	ERT monitoring	Road plates
Area 1	x	x		
Area 2	x (1/2)	x	x	x
Area 3	x	x	x	x
Area 4				

The people that participated in each one of the activities are presented in table 8.3.

Table 8.3. List of participants

Activity	Name	Organisation
GPR scanning	Ammar Aljer	U Lille
	(Sarah) Hoang Dung NGUYEN	U Lille
	Abdelhakim Ramzi	U Lille
	Lhamidi Khalil	U Lille
ERT monitoring	Vana Tsimopoulou	HZ
	André Koelewijn	STOWA / Deltares
	Roeland Nieboer	HZ / Deltares
	Edvard Ahlrichs	HZ / Deltares
Road plates installation	Vana Tsimopoulou	HZ
	André Koelewijn	STOWA / Deltares
	Annette Kieftenburg	Waterschap Brabantse Delta
	Johan Merckx	Waterschap Brabantse Delta

### 8.3.2 GPR scanning

GPR scanning was the first activity on the section as the measurements had to take place before commencement of the overflow test, which could possibly influence the geometry of the underlying system of burrows. It took place on November 24<sup>th</sup> 2022, one day before installation of the overflow generator and it was performed by the University of Lille using the same equipment that was used in previous GPR measurements (see also chapters 4 and 6). First Area 4 was scanned in a high frequency (2GHz) to allow for a comparison with the ERT results. The area was divided in four zones that were scanned separately (see also figure 8.4). Subsequently almost the entire area of the test section was scanned (19m x 2.5m) twice in lower frequencies (400MHz and 600MHz) to provide additional information about the general patterns of soil discontinuities at larger depths than those that the high-frequency scanner can capture.

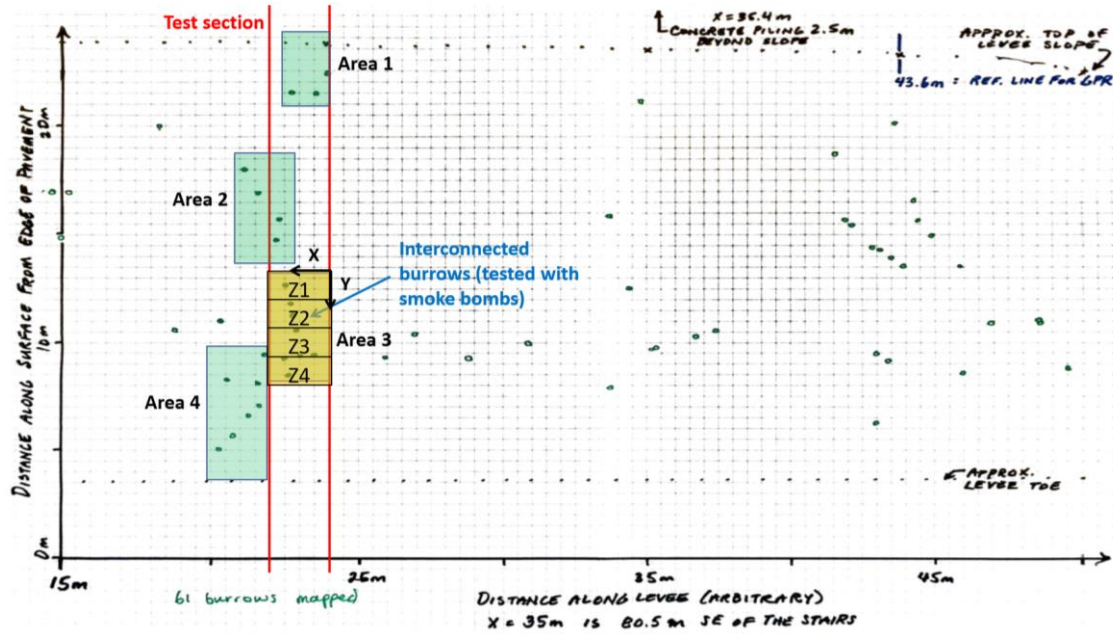


Figure 8.4. Illustration of the four zones (Z1-Z4) where high-frequency GPR measurements were taken. The high frequency measurements in area 3 resulted in the production of horizontal and vertical transects spaced by 0.1m. Indicative results from zones Z1 and Z3 are illustrated in the figures below.

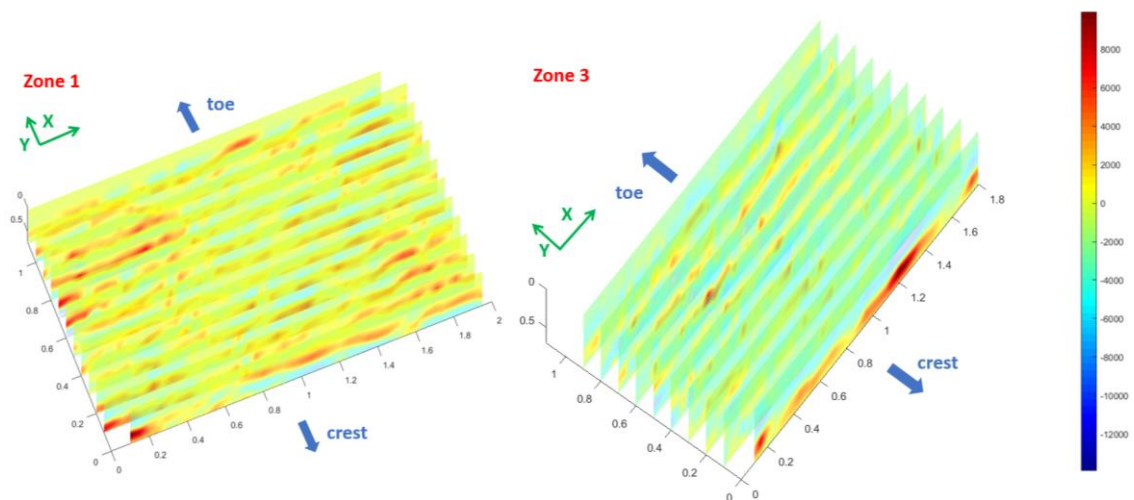


Figure 8.5: Vertical transects in zones Z1 and Z3 in X-direction.

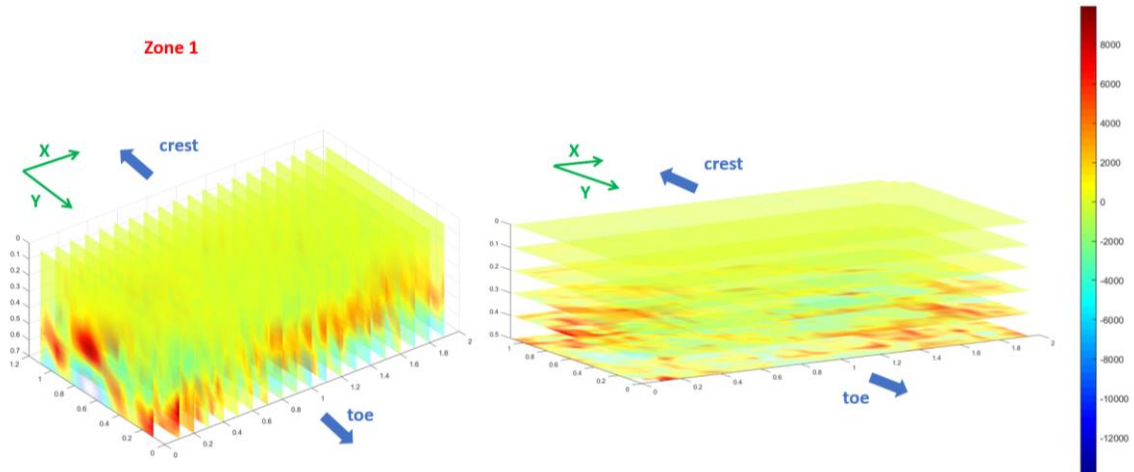


Figure 8.6. Left: Vertical transects in zone Z1 in Y-direction. Right: Horizontal transects in zone Z1.

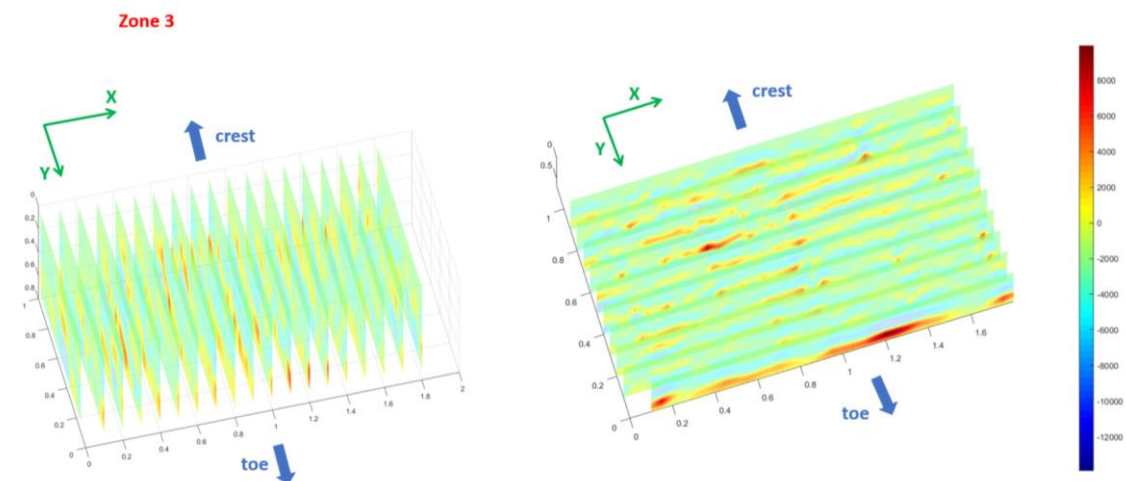


Figure 8.7. Left: Vertical transects in zone Z3 in Y-direction. Right: Horizontal transects in zone Z3.

The transects show clearly the presence of discontinuities, which are illustrated with red colour. In the figures below it can be seen that some of those discontinuities are matching well the presence of burrows on the surface. For example in the lowest horizontal transect of zone Z3 (figure 8.7, right), a red line is visible that extends almost in the entire width of the test section, in a depth of about 0.5m. Along this line three burrows had been detected (see also figure 8.4) that the smoke test showed that they are interconnected. This means that the red area in the transect probably illustrates the existence of a mole tunnel in a depth of about 0.5 m. However there are also discontinuities in the GPR results that cannot be correlated to the detected burrows. See for example the vertical transects in Y-direction of zone Z1 (figure 8.5, left). In those transects various red areas can be observed, while in that location only one burrow was detected that was interconnected with a burrows lower in the levee. It is unclear if such discontinuities are related to the subsurface burrow system. In the final assessment of the GPR results it should be taken into account that on the day of the measurements the weather and soil conditions were not ideal for GPR. It was a rainy day and the soil was not dry. Possible errors stemming from the weather and soil conditions need to be factored in. The accuracy of the GPR results depends on scan conditions, soil characteristics, properties of devices and analysis techniques. A more detailed analysis of the results will probably provide interesting insights. GPR use for the detection of burrows in levees is not really widely used, which means that its usability can be improved via a study like this.

### 8.3.3 ERT monitoring

After installation of the overflow generator on section N-OF09, the ERT monitoring system was set up. The installation, data collection, post-processing of data and their preliminary assessment have been extensively reported by Deltares (Karaoulis, 2021). Here a brief summary only is presented.

Two cables of electrodes were installed along the flume and parallel to each other, one as a main receptor and the second for back-up. The main receptor was installed under the road plates that covered the left-hand side half of area 3 (see also section 8.3.4). The back-up was installed on the right-hand side of area 3. Every cable contained 81 electrodes that were placed with 10cm-spacings.



Figure 8.8. Left: Construction of the flume on section N-OF08 before installation of the ERT cables. Right: Installation of the ERT cables.

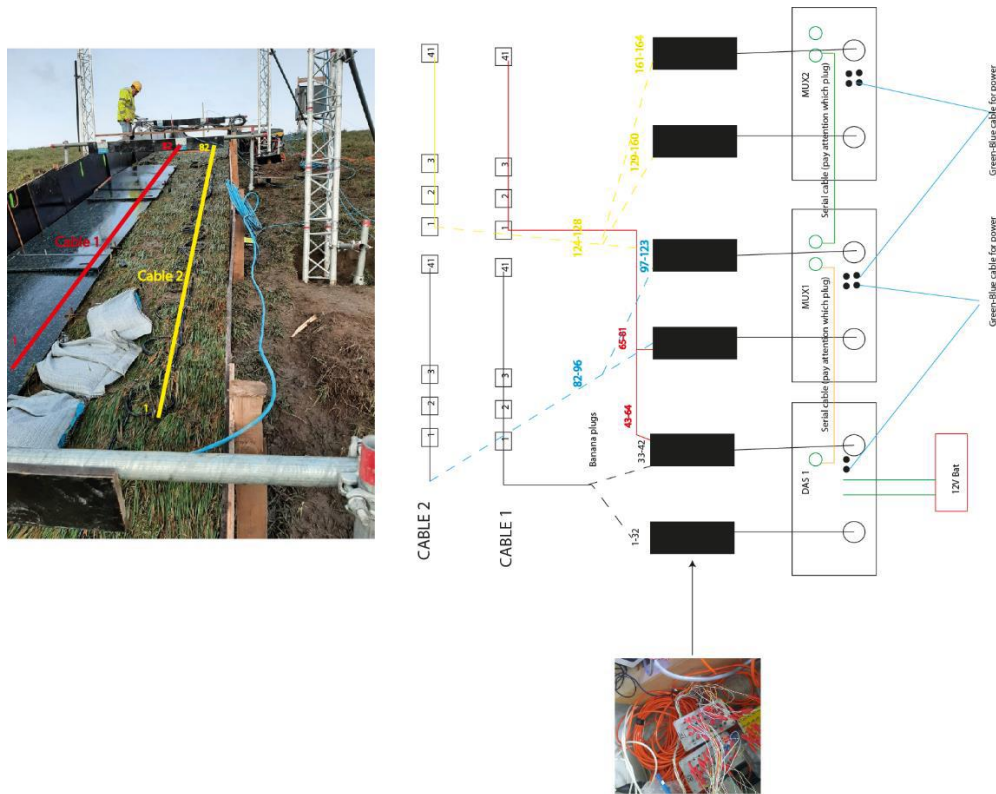


Figure 8.9. Detailed sketch of the ERT unit used to measure and the pin locations.

Five data sets were collected. The first one was a static, reference dataset before the experiment started. The other four are time series that correspond to four different flow rates that were tested. An overview of the flow rates for which ERT data were collected is presented in the table below.

Table 8.3. Overview of flow rates per ERT measurement

Measurement	Flow rate (m3/min)
1	No flow (calibration)
2	5.6
3	5.8
4	9
5	12

Four types of phenomena were recorded during the overflow test; 1) Existing air gaps (i.e. mole tunnels) in the subsurface being filled with water; 2) Development of new discontinuities (i.e. gaps filled with air or water in the subsurface); 3) Collapsing of existing tunnels; 4) Tunnels starting to connect with each other. The results are shown in the figures below. Before starting with data processing, an evaluation of data quality was undertaken, filtering out erroneous data. After completion of the field measurements, a so-called geophysical inversion process was conducted to determine the subsurface resistivity configuration that gave rise to the measured data at the surface.

Results are presented as ratio images. Each ratio image is produced during and after the overflow experiment (every 3min or every 6 min, depending on the protocol used), and show which areas of the scanned volume

change over time: the ratio results indicate new (air filled) holes by a high ratio (red colour). Lower values indicate saturation (amongst others, water filled holes). The results of the ratio images are presented below per measurement.

Basis 08:30 Flow of 5.6m<sup>3</sup>/min

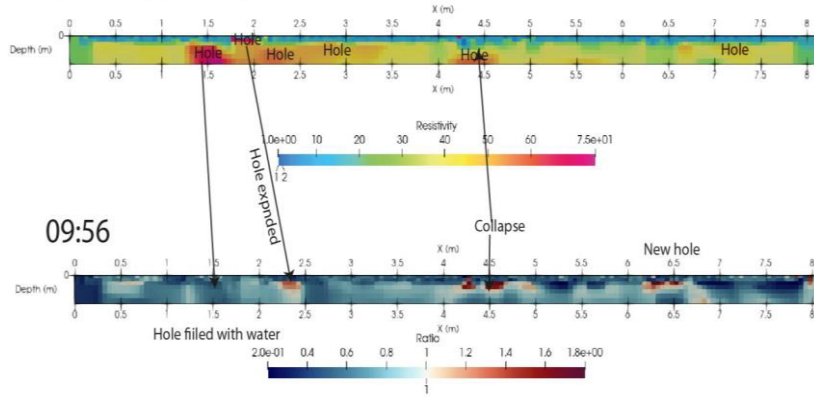


Figure 8.10. Measurement 2 from cable 1. Top figure shows the resistivity structure of the subsurface, where with high resistivities values (red) we expect the presence of multiple holes. The ratio images show that we have water infiltration in the top 25cm of soil.

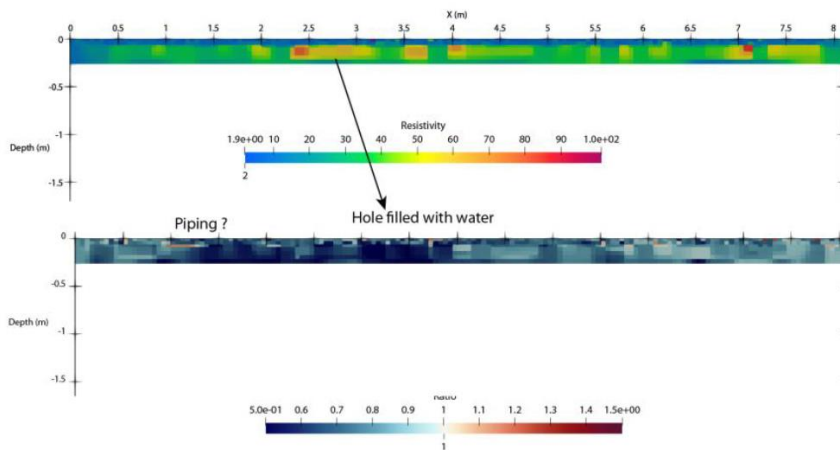


Figure 8.11. Measurement 2 from cable 2. Only small new holes were detected, and the water infiltration can be seen in the whole section.

Basis 10:04 Flow of 5.8m<sup>3</sup>/min

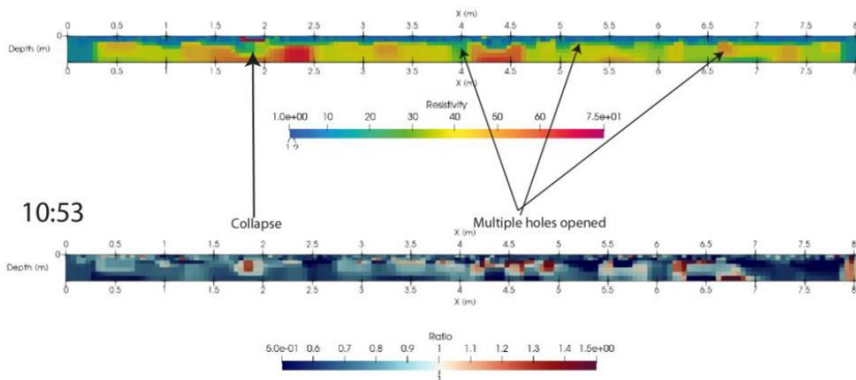


Figure 8.12. Measurement 3 from cable 1. Similar results with measurement 2. There are areas (on horizontal x-axis 4 to 6m) where we observe extended creation of new holes.

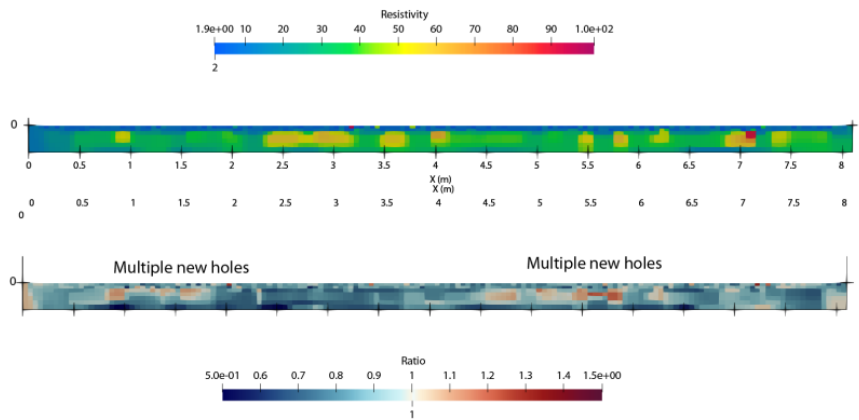


Figure 8.13. Measurement 3 from cable 2. Compared to measurement 2, the creation of multiple new holes can be observed.

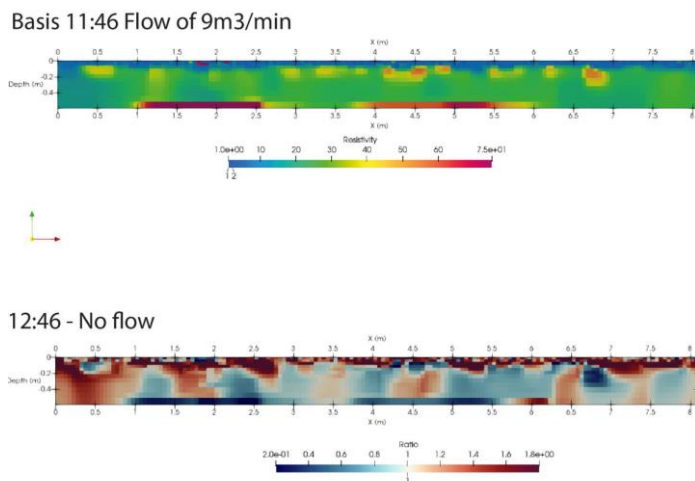


Figure 8.14. Measurement 4 from cable 1. Many more new holes can be observed that extend deeper than in measurements with lower flow rates. There are sections where the new holes are connected (i.e on the horizontal axis 0-1m). Overall the ratio images show many more red spots, indicating that the soil shows a higher activity.

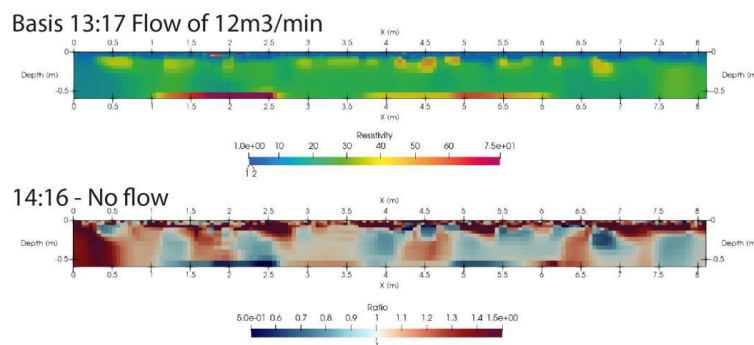


Figure 8.15. Measurement 5 from cable 1. The result here is very similar to measurement 4. No new holes created, but the existing ones are enlarged and show more connectivity (i.e. along x-axis 2-3.5m). It seems that

once “enough” holes are present in the subsurface, then no new holes are created but they start to connect to each other.

The obtained results indicate a correlation between flow rate and rate of observed changes in the subsurface. The detailed recording of the development of the four abovementioned phenomena (existing air gaps, filling gaps with water, collapsing and enlargement of burrows) over time and space provide datasets that can be used to model internal erosion processes during overflow.

The measured changes as evidenced by the collected data are well above noise level, hence can be considered reliable. This provides confidence that the method is suitable for monitoring subsurface changes during overflow levee experiments.

Further validation of the collected results is necessary by comparison with the static data collected with GPR. A more detailed analysis of the GPR results is necessary in order to make this comparison. Any attempt to apply this method in the future requires attention to the presence of metal objects in the experimental set-up. The metal frames that were used for the sensors and cameras of the overflow experiment did not influence the results at this instance, nor did the metal pins to attach the synthetic road plates (see §8.3.4). But larger metal objects in the flume could have influenced the quality or results.

#### 8.3.4 Temporary protection with road plates

Before commencement of the overflow experiment a temporary protection of the interconnected mole burrows of area 3 and the additional burrows of area 2 was installed. Road plates (figure 8.16) combined with metal pins (figure 8.17) and bicycle inner tubes were used to create a low-cost assembly of a temporary barrier for the protection of levee sections with mole burrows, in anticipation of high water and overflow.



Figure 8.16: Synthetic road plates that were used for the assembly of the temporary protection of the mole burrows.



Figure 8.17: Metal pin types that were combined to attach the road plates on the soil

Three road plates of (3x1) m were placed in the flume in a linear set-up adjacent to the flume wall. The plates were installed in such a way that most detected burrows within the flume were covered by them. In order to minimize the passage of water under the plates, metal pins were used at their periphery to attach them to the ground. Furthermore, the plates were placed so that they overlapped with each other by about 50 cm, with the lowest plate being fully attached to the ground, the second overlapping with the first, and the third overlapping with the second. At the overlapping areas, the elastic tubes were placed on the top and pinned on the ground to provide additional resistance to the uplifting forces of the water. At the edges of the overlapping areas and at the upper edge of the assembly, synthetic sandbags were placed and pinned on the ground to provide extra protection against water passage under the plates.

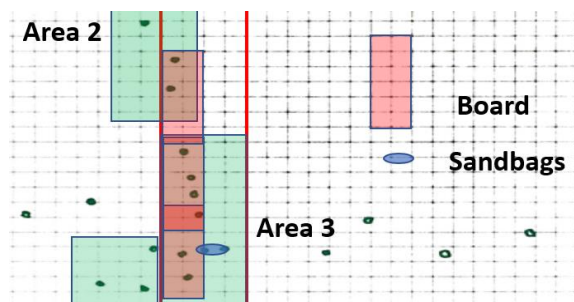


Figure 8.18. Top view layout of the solution.



Figure 8.19: Temporary protection with road plates before commencement and during the overflow test.

The installation was completed in 15 min by a team of 3 people. This makes it a very practical solution for emergency interventions, especially when compared to other interventions tested in the living lab (see e.g. EPDM or levee challenge repairs). The installation appears to have worked well, as no erosion was detected after completion of the experiment on the covered area. Yet the sandbags did not provide any essential protection as they were washed away by the water flow very early in the experiment. The pins and bicycle tubes remained intact. The same plates and pins were also used in several other overflow experiments to protect scour holes at the transition between grass and asphalt at the toe, and their performance there was always satisfactory. This provides confidence about the suitability of this method to protect larger burrows and other discontinuities too.

Further testing of this solution at locations with larger burrows and other discontinuities but also under different loads (e.g. overtopping) is necessary for its final benchmarking.

#### 8.3.5 Smoke experiment

After completion of the overflow experiment and removal of the road plates, the smoke test was performed on burrows of this section once again in an improved version. This time only a smoke bomb and leafblower was used, but the leafblower was larger than the one in the previous trial. The smoke bomb was placed directly at the entrance of the burrow and the smoke was blown inwards with the leafblower. With a larger leafblower the pressure of the air was increased, which led to instant passage of air from the subsurface cavities. Air started exiting from a number of burrows almost instantly (figure 8.20).



Figure 8.20: Application of the smoke test on mole burrows in section N-OF09.

The only disadvantage this time was that there was no provision made to seal the exit points of the smoke, which would have possibly allowed to identify more exit points. Wet clay that was also used in the previous trials of the smoke test could be a solution. An improved alternative could be the use of glass tiles instead of clay. This solution was tried in May 2022 by Karsten de Pauw during his graduation internship at Hoogheemraadschap van Rijnland and it worked well. (see also [relevant video](#)).

#### 8.4 Observation of artificially created burrows in section N-OF03

N-OF03 was a reference section without any particular discontinuities or irregularities. Four vertical bore holes were created on the section with a hand drill to introduce a discontinuity that partially resembles an animal burrow. Two of the holes were introduced close to the toe and the other two about halfway between the toe and the crest. This took place after about 4hrs of overflow, when the first traces of surface erosion had appeared on the section. The experiment continued for another two hours, and no noticeable changes around the bore holes were observed. This observation is in line with observations in previous attempts to create an artificial burrow during an overflow experiment in the Hedwige-Prosperpolder and other locations in the Netherlands.

#### 8.5 Surface erosion patterns on reference section with mice burrows N-OF04

Prior to the test, the section did not appear to have any noticeable discontinuities, such as damage by machinery, irregular vegetation patterns or large animal burrows. Through a thorough visual inspection before commencement of the test a number of small burrows were detected within and adjacent to the test section. Their depths were in the range of 8-12 cm and their diameters in the range of 3-5 cm, while none of them seemed to have penetrated beyond the clay layer. Their geometry and spatial distribution resembled mice burrows.

During the test, surface erosion and burrows were monitored every 2 test blocks of flow, each lasting about 1 hrs. Surface erosion started with the uprooting of grass and exposure of small patches of clay with diameters in the order of 2-3 cm, which gradually expanded and connected with adjacent patches of clay. This is a common pattern that has been observed in all overflow tests in the living lab. Most of the mice burrows in the test section were within the first patches that formed, which shows that the burrows may have played a role in the early formation of surface erosion.

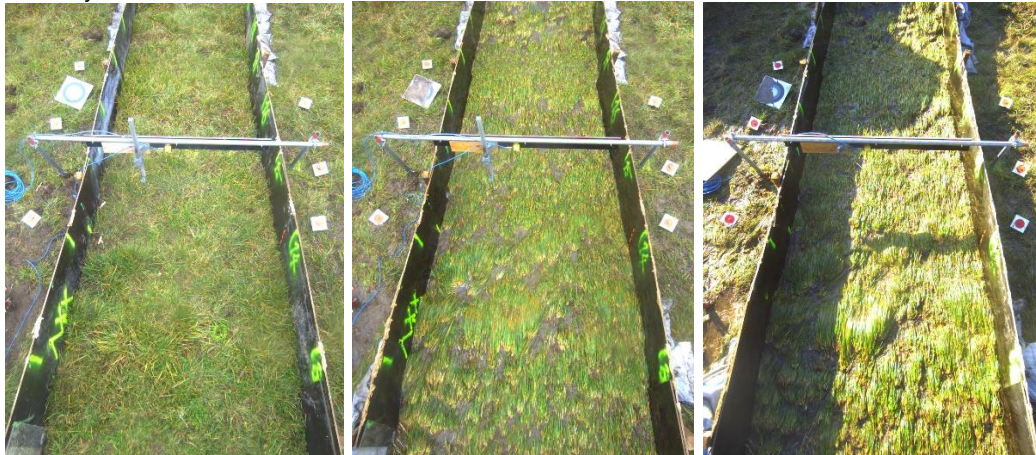


Figure 8.21. Progression of surface erosion around a small burrow in the test flume. Left: Picture before initiation of the test. A mouse burrow is marked with fluorescent spray on the grass. Middle: Picture halfway in the test. Right: Picture after completion of the test.

Similar observations in other overflow tests are needed to validate this finding. Regarding the depth of erosion, in every monitoring cycle the patches in the area of the toe were noticeably deeper than the rest, while a relatively deeper patch started forming, at the point of transition between the EPDM protection and the bare levee surface (figure 8.22). A third point of interest regarding erosion depth was the transition between asphalt and soil at the downstream side of the road. At that spot a scour hole with a diameter of about 30 cm and a depth of about 45 cm was formed after 4 hours of flow.

After the test, the most significant damages could be observed at the transition between EPDM and bare soil on the crest (erosion depth 1-2 cm in an area approx. 20 x 80 cm), at the toe (erosion depth 5-10 cm in an area approx. 10 x 80 cm) and at the downstream transition between asphalt and soil (erosion depth 45-50 cm in an area approx. 30 x 30 cm).



Figure 8.22. Transition between EPDM and soil close to the cress of the test section before (left) and after (right) the test.

## 8.6 Concluding remarks

This chapter presents the results of activities that were performed on sections with small burrows during the overflow experiments. Most activities took place on section N-OF09, where a system of mole burrows had been detected.

First a GPR scan was performed. A preliminary analysis of the results shows clearly the existence of cavities on the location that the mole system had been detected, but discontinuities are also visible on scanned areas with no detected burrows. The fact that the measurements were taken on a very wet day may have influenced the accuracy of the results, but it is also likely that cavities did exist without having an exit within the scanned area. The section was subsequently tested against overflow. During the test an ERT monitoring system of the levee subsurface was installed and data about the subsoil condition throughout the test were successfully connected. It is the first time that monitoring of the levee subsoil is achieved during an overflow experiment. The results provide information that can be useful for the development and validation of internal erosion models.

Apart from the ERT monitoring system a temporary protection of the mole burrows was applied with a composition of road plates, pins and bicycle inner tubes. The installation performed well in this test but further testing in different conditions is recommended.

Visual observations made on sections where burrows had been detected led to the conclusion that those burrows can points where surface erosion is initiated during overflow, as they constitute relatively weaker areas of the surface.

A more in depth analysis of the GPR results is recommended to allow a detailed comparison with the ERT findings.

## References

- Avenant, N.L., Smith, V.R. The microenvironment of house mice on Marion Island (sub-Antarctic). *Polar Biol* 26, 129–141 (2003). <https://doi.org/10.1007/s00300-002-0464-x>
- Cobos-Roa, D. A. (2015). *Transient Seepage Through Levees and the Influence of Roots and Animal Burrows*. University of California, Berkeley. url: <https://escholarship.org/content/qt56w38938/qt56w38938.pdf>
- Depreiter, D., Peeters, P., Vanhille, W., Muylaert, S., De Backer G., Koelewijn, A. & Van Calster, W. (2021) Survey overview report. Polder2C's
- Depreiter D. 2021. Polder2C's Overflow test plan - Winter 2021
- Depreiter, D. et al., 2022a. Polder2C's Overflow test summary report.
- Depreiter, D., Vercruyssen, J., Verelst, K., Zomer, W., Koelewijn, A., Tsimopoulou, V. & Peeters, P. (2022b), Continuous Overflow tests on Belgian levees, Polder2C's
- Di Prinzio, M., Bittelli, M., Castellarin, A., & Pisa, P. R. (2010). Application of GPR to the monitoring of river embankments. *Journal of Applied Geophysics*, 71(2-3), 53-61.
- Van Duin, M. & Berghuijs, J. D. (2007). The safety chain as a strategy for thinking and acting. (In) *Fire Brigade Studies into Organisation and Practice*. (Eds) Helsloot, I., Muller, E. M. & Berghuijs, J. D. Kluwer, Dordrecht, 2007, pp. 509–528.
- Federal Emergency Management Agency. *A Nation Prepared. Federal Emergency Management Agency Strategic Plan 2003–2008*. FEMA, Washington, DC, 2003.
- Heyer, T. & Stamm J. (2019) *Burrowing Activity of Muskrats, Nutrias and Beavers on River Levees – Damages, Consequences and Mitigation Measures*. (Eds) Ching, J., Li, D.K. & Zhang, J. 7<sup>th</sup> International Symposium on Geotechnical Safety and Risk. Taipei
- Holscher, R. & Zomer, W. (2021) Field research on burrows and discontinuities in embankments. Fact finding field research in the Hedwige-Prosperpolder. STOWA Report no: 2021-52
- Klerk, W. J., Kanning, W., Kok, M., Bronsveld, J. & Wolfert A.R.M. (2021) Accuracy of visual inspection of flood defences, *Structure and Infrastructure Engineering*, DOI: 10.1080/15732479.2021.2001543
- Klerk, W. J., Decisions on life-cycle reliability of flood defence systems, PhD thesis, TU Delft, 2022, [doi.org/10.4233/uuid:877bed45-d775-40bb-bde2-d2322cb334f0](https://doi.org/10.4233/uuid:877bed45-d775-40bb-bde2-d2322cb334f0)
- Koelewijn A., Kieftenburg A. & Husken L. (2020) Graverij door dieren: Invloed op de veiligheid van waterkeringen. 11205235-003-ZWS-0001. Deltares
- Koelewijn, A. (2021). Waargenomen invloed van mollengangen op dijkveiligheid, Polder2C's report, 5 May 2021, 39 pp.
- Loke, 2010. M.H. Loke, Res2Dinv version 3.59 for Windows XP/Vista/7, Rapid 2-D resistivity & IP inversion using the least-squares method, *Geoelectrical imaging 2D & 3D*, Geotomo Software, Penang, 2010.

Ministry of Interior of the Netherlands. Integrated Safety Report 1993. BZ, The Hague, 1993 (in Dutch).

Özer, I.E., Van Damme, M., Jonkman, S.N. (2019) Towards an International Levee Performance Database (ILPD) and Its Use for Macro-Scale Analysis of Levee Breaches and Failures. *Water*. 2019; 12 (1):119.

Revil, A., Karaoulis, M., Johnson, T. & Kemna, A. (2012) Review: Some low-frequency electrical methods for subsurface characterization and monitoring in hydrogeology. *Hydrogeology Journal* (2012) 20: 617–658

Rocque Jr., A.J. (2001) Guidelines for Inspection and Maintenance of Dams. Connecticut Department of Environmental Protection. Available at [http://www.ct.gov/dep/lib/dep/water\\_inland/dams/guidelinesforinspectionandmaintenanceofdams.pdf](http://www.ct.gov/dep/lib/dep/water_inland/dams/guidelinesforinspectionandmaintenanceofdams.pdf). Accessed September 23, 2010

Rudnick, D. A., Chan, V., & Resh, V. H. (2005). Morphology and impacts of the burrows of the Chinese mitten crab, *Eriocheir sinensis* H. Milne Edwards (Decapoda, Grapsoidea), in south San Francisco Bay, California, USA. *Crustaceana*, 787-807.

Texas Commission on Environment Quality (2006) Guidelines for operation and maintenance of dams in Texas, pp. 65–72

Ten Brinke, W. B. M., Saeijs, G. E. M., Helsloot, I. & Van Alphen, J. (2014) Safety chain approach in flood risk management. *Proceedings of the Institution of Civil Engineers Municipal Engineer* 161 June 2008 Issue ME2 Pages 93–102 doi: 10.1680/muen.2008.161.2.93

Thomas, H.G., Scantlebury, M., Swanepoel, D. et al. Seasonal changes in burrow geometry of the common mole rat (Rodentia: Bathyergidae). *Naturwissenschaften* 100, 1023–1030 (2013). <https://doi.org/10.1007/s00114-013-1105-7>

Tweede Kamer (2010) Motie stemming 23 nov. Retrieved from <https://www.tweedekamer.nl/>

Van den Berg, F. (2021) Graverij door dieren; Een kwantitatieve analyse en overzicht huidige kennis. 11206793-002-ZWS-0002. Deltares

Van der Meij, R., Tourment, R., Maurel, P. & Morris, M. (2012) Combining information for urban levee assessment. Report number: WP03-01-12-24. Deliverable 3.3 of [FloodProBe project](#).

Van der Steen, H. (2018). Muskrat and Bisam Control in the Netherlands, Duderstadt, Germany (in German)